Spectral index of thermally induced electromagnetic fluctuations

Thesis
submitted to the
University Of Chile
in partial fulfillment of the requirements
for the degree of
Master of Sciences with mention in Physics
Faculty of Sciences

by

Valentina Andrea Acuña Villaflor

July, 2024

Thesis Advisors: **Dr. Juan Alejandro Valdivia**
Dr. Benjamín Toledo

FACULTY OF SCIENCES

UNIVERSITY OF CHILE

APPROVAL REPORT

MASTER THESIS

The Graduate School of the Faculty of Sciences is informed that the Master's Thesis presented by the candidate

Valentina Andrea Acuña Villaflor

has been approved by the Thesis Evaluation Committee as a requirement for the Master's degree, in the Private Thesis Defense examination given on 8th of July, 2024.

Thesis Advisors

Dr. Juan Alejandro Valdivia _____

Dr. Benjamín Toledo _____

Thesis Evaluation Committee

Dr. Marina Stepanova _____

Dr. Mario Riquelme _____

Biography

I am the the firstborn daughter of Lorena and the older sister of María-José. I was born and raised in La Serena, and from a young age, I had a passion for space. This passion was clearly fueled by my mother, who filled me with books about stars. What better city to indulge this enthusiasm than one with clear skies and observatories? I attended a school in La Serena and chose the scientific-mathematical elective, although I didn't yet understand how beautiful it is to explain the world with mathematics. I participated in Physics Olympiads. They took me to the La Silla Observatory, I visited laboratories at USACH, listened to many scientists, and transitioned from wanting to study Astronomy to wanting to study Physics. I always focused my attention on science and trying to understand everything. In my home, always full of cats, I was able to further develop these interests. My mother is a Biologist, and I was always interested in her insect collections, her huge books, her work tools, and more. I don't think I ever decided to study Physics; it naturally evolved from all those interests. I left La Serena to study a Bachelor's degree in Physics at the University of Chile. Tremendous women have accompanied me throughout my life, starting with my foundational pillars, my mother and sister, followed by my scientific family that inspired me to traverse this path with strength. I hope that what lies ahead is filled with people and experiences of this caliber.

Acknowledgments

I want to thank my advisors Alejandro Valdivia and Benjamín Toledo for all the long and extensive conversations, for supporting me in completing this work, for motivating me, and for expertly guiding the research. I also want to thank Roberto Navarro for all the insight that helped to take this work to an end.

I want to thank the "Postgraduate among Friends" group for all their support, companionship, laughter, and good lunches. Particularly to the postgraduate girls, Matilde, Gabriela, Javiera, Belén, and Valentina, for being role models, for giving me affection, support, and for being the great women they are. Especially, I want to thank Matilde for sharing her wisdom since the beginning of my career, for always guiding me, and for ensuring that I never lacked her advice and companionship. Also, Gabriela, whose expressions of support, unconditional care, office companionship, relaxation after workdays, and incredible presence always made everything better. Finally, Valentina, who accompanied me through every part of the process, an irreplaceable friend who was always present, who listened to and accompanied me in every aspect of my personal and academic life, providing support and advice that helped me move forward.

Most importantly, I want to thank my family; without them, I wouldn't be here. I want to thank my mother, Lorena, and my sister, María-José, who always understood and accompanied me, who always motivated me to keep going, and who I am sure will continue to encourage me to achieve every goal I set for myself. Even though we were apart for most of the year, I always felt their presence by my side. Thank you.

Finally, I want to thank the ANID/Fondecyt 1190703 project and CEFEX.

Contents

Chapter 1

Introduction

1.1 Context

The term *plasma* originally referred to a liquid component of blood that lacks blood cells but contains suspended constituents. This concept served as inspiration for physicist Irving Langmuir in 1914, who adopted it to describe an ionized gas. Although the earliest observations of what we now know as *plasma* date back to 1879, when William Crookes termed it "radiant matter", it was Langmuir's pioneering work in 1924 that significantly propelled the field of study. In his experiments investigating electric discharges in mercury vapor, Langmuir developed the Langmuir probe, which allowed to measure the densities and velocity distributions of ions present in the gas. Furthermore, they observed the discharge structures formed by these ions, although they did not have a name for them. Langmuir noted that the equilibrium part of the discharge acted as a substrate carrying particles with specific characteristics, such as high-speed electrons, along with ions and gas impurities. This phenomenon reminded him of how blood plasma transports particles in the blood, leading to the proposal to call these uniform discharges *plasma* Mott-Smith (1971).

Following Langmuir's pioneering studies, plasma research experienced a notable growth. Various studies were conducted addressing the different contexts in which plasmas can manifest. The discovery of a region in the atmosphere capable of reflecting and absorbing radio waves, known as the ionosphere, occurred with the invention of radio. In 1947, Edward V. Appleton was awarded the Nobel Prize for his confirmation of the existence of the ionosphere in 1927, a region with large-scale ionization in the Earth's atmosphere. This finding led to investigations into the propagation of radio waves in the ionosphere, revealing a diversity of waves propagating in this environment.

In this same context, the question arose about the presence of this state of matter in other parts of the cosmos, given that it had already been observed in experiments around Earth. Many astrophysicists recognized that a significant portion of the universe is composed of plasma, thus emphasizing the importance of observations in this field. Over the years, the cosmic environment has been explored through the visualization of the electromagnetic spectrum, revealing emissions in specific regions such as X-rays and gamma rays. These emissions, for the most part, originate from magnetized cosmic plasmas, making the study of astrophysical processes generating these emissions a fundamental area of development. Information about plasma in the universe can be obtained through in-situ measurements in the magnetosphere, as the fundamental properties of a plasma can be extrapolated to other regions Alfvén (1987).

Before the space age, scientists theorized about the possibility of charged particles being trapped around the Earth's magnetic field. This theory was confirmed in 1958

when space scientist James Van Allen and his research group at the University of Iowa discovered the radiation belts that are now known as the Van Allen belts. This group used multiple satellites to study these belts and published their results in 1959 Van Allen and Frank (1959). From studies conducted in the theory of plasmas trapped by magnetic fields and ionospheric physics, the theory of wave propagation in plasmas was developed.

From the early discoveries, fundamental theories emerged to study plasmas. In 1942, Hannes Alfvén published his influential theory that anticipated the field of Magnetohydrodynamics (MHD), where he demonstrated the existence of hydromagnetic waves in a plasma Alfvén (1942). In this work, Alfvén presents the plasma state as a current-conducting fluid. In the presence of a constant magnetic field, electromagnetic fields could be generated, which in turn could induce electric currents in the medium. Furthermore, he emphasizes that this phenomenon can be studied using the equations of electrodynamics along with the equations of hydrodynamics. In this description, only the macroscopic quantities of the system are considered, such as density, temperature, electric and magnetic fields, and the equations governing the evolution of the plasma in space and time. Therefore, it is not necessary to know the information about the individual characteristics of each particle. This representation is known as the macroscopic or fluid description of a plasma, referred to it as *fluid theory*.

On the other hand, if we aim to conduct a microscopic analysis of this system, we turn to the formulation of *kinetic theory*. This approach seeks to understand the behavior of a distribution of particles in the plasma, considering aspects such as their

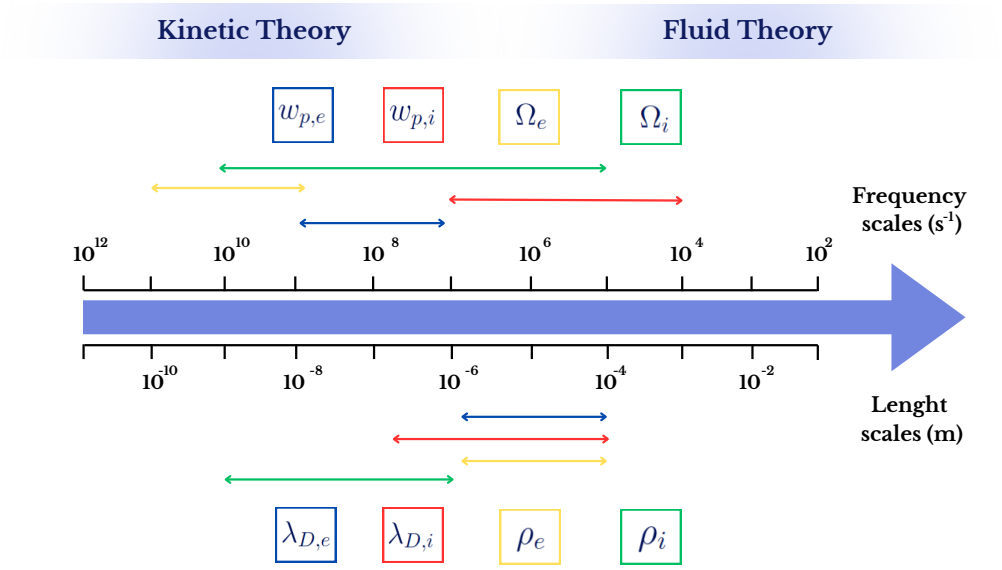

Figure 1.1: Relevant frequency scales for plasma description.

velocities and energy distributions. Kinetic theory provides a detailed perspective at microscopic level, complementing the macroscopic description offered by MHD and allowing for a more comprehensive understanding of plasmas in various contexts. The description to be used, whether kinetic or fluid description of a plasma, is framed by different frequency ranges relevant for the system in question, as depicted in Figure 1.1 (frequencies are defined in Table 1.1).

In fluid theory, the motion of the particles, usually described by the Velocity Distribution Function (VDF), are well represented by the local average bulk motion of the particles and the evolution of the VDF is well represented by the changes in the average bulk motion, and possibly the temperature through the width of the VDF. Similarly, spatial scales in standard single fluid theory, must be considerably larger than the Debye length and the ion gyrofrequency (w_{ci}), as depicted in Figure

1.1. This scale is where the long-range electrostatic potentials of each particle are screened by other particles of opposite charge in the plasma. This is the validity range for single fluid theory.

Table 1.1: Frequency definitions. Here, n_e and n_i are the electron and ion density, respectively. m_e and m_i are the electron and ion masses, respectively. e is the electron charge, B is the magnitude of the background magnetic field, c is the speed of light, and Z the atomic number.

Frequency	Definition
w_{pe}	$\left(\frac{4\pi n_e e^2}{m_e}\right)^{1/2}$
w_{pi}	$\left(\frac{4\pi n_i Z^2 e^2}{m_i}\right)^{1/2}$
w_{ce}	$\frac{eB}{m_e c}$
w_{ci}	$\frac{ZeB}{m_i c}$

Magnetohydrodynamic single fluid theory (MHD) is already a simplification of multifluid theory in which the evolution of a single fluid, representing the motion of the local center of mass of the different species. However, some aspects excluded in MHD are crucial for the processes that will be described in this work. Therefore, we need the formulation of kinetic theory.

Hence, physical quantities derived from the fluid description do not represent the complete information of the system in the phase space of the particle distribution, particularly, when the evolution of the VDF cannot be simply described by the dynamics of the mean velocity and its width. For systems where these processes are relevant, a more detailed description is required to understand plasma dynamics.

This can be achieved using an exact microscopic analysis, but this involves solving Newton's law for a large set of particles interacting with each other, thus, impractical. In this sense, microscopic theory gave way to kinetic theory, which uses statistical and probabilistic concepts about an ensemble of particles. By taking a statistical average of microscopic information, the kinetic equations of the system can be obtained. Examples of microscopic description usually start with the Klimontovich or Liouville equations. It is possible to construct a Hierarchy of approximations to these equations, that start in its simplest form as the Vlasov equation that considers no fluctuations, but provide a structure to derive successive improvements to consider the left out physics such as the Boltzmann, Landau, and Lenard-Balescu equations, the way in which these formalisms are obtained are shown in Figure 1.2.

In this work, we will use the Vlasov formalism to find the dispersion relations that will provide us information about the types of waves that are allowed to propagate in a electron-proton plasma, with conditions similar to the solar wind, or the magnetosphere. In general, waves can propagate parallel or oblique to the background magnetic field, in this case we consider waves propagating parallel to it. The Vlasov-Maxwell equations, as a representation of the plasma dynamics, corresponds to the lowest description of a Hierarchy that starts with the Klimontovich or Liouville equations, where the fluctuations have been disregarded, so that they represent the dynamics of an ensemble averaged distribution function under ensemble averaged fields. Starting from the Klimontovich equation, if we consider a decomposition of the microscopic fields into ensemble averaged electromagnetic fields plus fluctuations

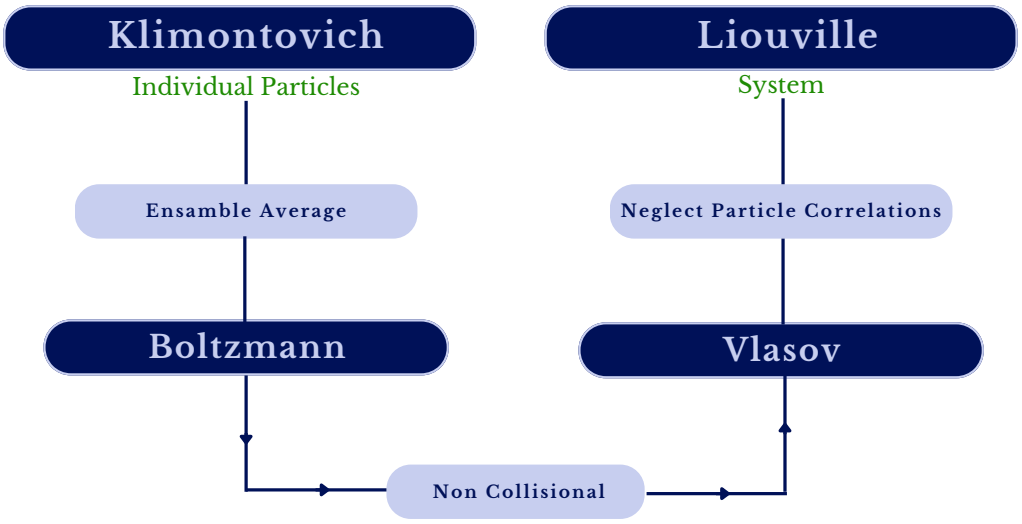

Figure 1.2: Kinetic plasma theory. Vlasov is at the bottom of the hierarchy (no fluctuations), and then additional physics is included as the Hierarchy progresses.

of these, we obtain the Boltzmann-like Transport Equation, where fluctuations and particle correlations can be considered.

The aforementioned equation includes an additional term respect to the Vlasov equation, that resembles the collisional term of the Boltzmann equation, but that in this case corresponds to correlations between particles and field fluctuations. Here we have assumed that the collision frequency between particles is much smaller than the plasma frequency w_p, to define what is called, *collisionless plasmas*. Of course, they can be added into the formalism if necessary. To neglect the effective collisional term described above, to arrive to the Vlasov equation, we assume that the average distance between particles is smaller than the Debye length, this is a general consideration for a system to be considered a plasma. Charge particles from a thermal

distribution move randomly, producing naturally electromagnetic fields that account for the fluctuations in the plasma that are included in the additional terms in the equation for the particle distribution function. Thus considering a mean electromagnetic field and a deviation from the mean field due to interactions between charged particles, it is possible to show that variations in entropy due to collisions are much slower than variations due to microscopic quantities, thus omitting this additional term. Therefore, when these additional terms are omitted, we obtain the Vlasov equation. The system of Vlasov equations together with Maxwell's equations provide an important description of plasma dynamics. Its linear approximation allows to derive the dispersion relation of the allowed waves of the system, by uniquely relating plasma frequencies and wavenumber. As we include correlations and fluctuations, we break this unique relation, and obtain a continuous spectra as we will discuss below.

The Vlasov formalism does not predict the existence of electromagnetic fluctuations in plasmas, nonetheless, these have been observed in various environments through observations and simulations Bale et al. (2009); Tu and Marsch (1993); Marsch and Tu (1990), to name a few. These fluctuations, that do not follow a dispersion relation, represent variations in magnetic and electric fields, as well as in the densities of charged particles in these regions of space. Fluctuations in the density of charged particles, such as electrons and protons, are also common in the solar wind, magnetosphere, and other plasma environments. These fluctuations can contribute to the turbulence in the solar wind and can affect the propagation of electromag-

netic waves. The existence of electromagnetic fluctuations in the solar wind has been studied through various formalisms, including non-linear theory, quasi-linear theory, and linear theory. However, none of these approaches have provided a satisfactory explanation for the presence of these fluctuations in such environments.

For example, it is possible to organize the observations of the solar wind in the so called beta-anisotropy diagram, where β is the ratio between the parallel kinetic energy density of the protons divided by background magnetic field energy density and the anisotropy is the ratio between the perpendicular and parallel temperature of protons Bale et al. (2009). Within this diagram, there is a quasi-stable region where observations are present, which is the region where the system evolves into a dynamical quasi-stability state, and seems to stay there for a long time. Additionally, in this work it is also shown that finite level of electromagnetic fluctuations are observed in this region, despite the fact that linear kinetic theory predicts that within this region the system is linearly stable and no electromagnetic fluctuations should be observed. Therefore, researchers have proposed that these fluctuations could be part of the turbulent cascade from MHD scales; or very unstable parcels of plasma that evolve into the quasi-stable region, although hybrid simulations do not support such argument; or inherent fluctuations produced by the thermal motion of particles, balanced by dissipation, described by the Fluctuation-Dissipation theorem. This has been confirmed by hybrid simulations; or combinations of them. We will study the contribution of the thermally induced electromagnetic fluctuations in the quasi-stable region of the beta-anisotropy diagram, and the spectra that they could generate.

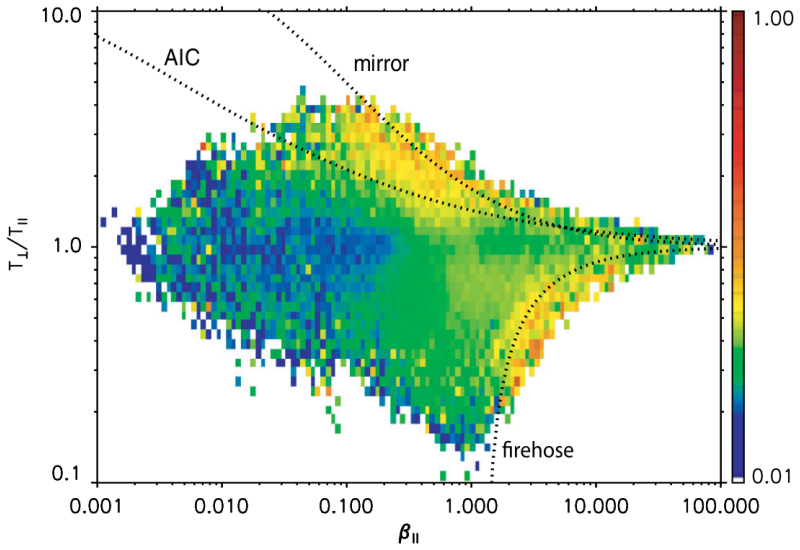

Figure 1.3: Magnitude of magnetic fluctuations $|\delta B|$ averaged into bins of $T_\perp/T_\parallel$ vs $\beta_\parallel$, Figure obtained from Bale et al. (2009).

Furthermore, observations in the solar wind seem to be constrained by instability thresholds, as shown in Figure 1.3. Thus, suggesting that kinetic physics at the microscales, regulates the macroscales of the system Schlickeiser et al. (2011); Kasper et al. (2002); Hellinger et al. (2006); Bale et al. (2009). Inside this region, that seems to be bounded by instability thresholds, the quasi-stability region shows finite electromagnetic fluctuations. There is an issue regarding the physical origin of electromagnetic fluctuations in the absence of plasma instabilities, since the regions with low temperature anisotropy should not present fluctuations, but we observe them regardless. One potential explanation is remnant solar wind turbulence, believed to originate from the Sun's surface region but observed pervasively throughout the solar wind. Another possible source could be the spontaneous emission of low-frequency electromagnetic fluctuations by thermal plasmas. Such mechanism was proposed by

Navarro et al. (2014); Vinas et al. (2014); Viñas et al. (2015); Araneda et al. (2012), and it is the formalism studied in this work. As mentioned above, we propose that these fluctuations are originated due to induced electromagnetic fluctuations coming from thermal motion of particles within the plasma Weibel (1959).

To theoretically analyze the fluctuations that naturally arise in a magnetized plasma, we will use the set of Klimontovich-Maxwell equations to derive the spectrum of electromagnetic fluctuations, under the theoretical derivation developed by Schlickeiser and Yoon (2012) and Schlickeiser et al. (2015) for the case of unmagnetized and relativistic plasma and magnetized plasma respectively, and the Fluctuation-Dissipation theorem used in the context analyzed by Navarro et al. (2014).

Particularly, the Fluctuation-Dissipation theorem states that the response of a system to a external linear perturbation is expressed in terms of the fluctuations of the system close to thermal equilibrium Kubo (1966). This theorem was demonstrated by Callen and Welton (1951). In this context, according to the Fluctuation-Dissipation theorem, there is a dynamical balance between the emission and absorption of fluctuations, meaning that due to the thermal motion of particles present in the plasma, the production of electromagnetic fluctuations can be predicted. This is the foundation used in Navarro et al. (2014) to explain the phenomenon of fluctuations in magnetized plasmas, under quasi-stable conditions. This was proposed in other studies such as Vinas et al. (2014); Viñas et al. (2015); Araneda et al. (2012). On the other hand, the analysis derived in Schlickeiser et al. (2015) begins by describing quantities that fluctuate in space from the particle correlation function

between particles in a magnetic field, which can be directly related to electromagnetic fluctuations. The way in which these quantities are defined should include information about the correlation between particles and electromagnetic fields in the system. This formalism provides us with a good description of electromagnetic fluctuations in plasmas.

In what follows, we will first describe the Vlasov equation and the Klimontovich equation, since it will be useful when analyzing fluctuation theories. This is a first consideration for both formalisms since to explain electromagnetic fluctuations we will incorporate the Fluctuation-Dissipation theorem and the system of Klimontovich-Maxwell equations. We will focus our attention in induced electromagnetic fluctuations, which are included in both theories. In this context we will differentiate the different physical implications of both proposed formalisms. Below, we will define the environment where electromagnetic fluctuations have been observed to define the different theoretical frameworks that will be studied. Therefore, as the solar wind originates from the Sun, we will first focus on defining the characteristics of the Sun before addressing the context of study.

1.2 Structure of the Sun

The Sun has a radius of approximately $700,000$ kilometers. Additionally, it has a mass of 2×10^{30} kilograms, a volume of 1.5×10^{18} cubic meters, and an average density of 1.4 grams per cubic centimeter. It is composed approximately of 90% Hydrogen, 10% Helium, and 0.1% of other elements such as Carbon, Nitrogen, Oxygen, etc. The Sun interior is divided into: The core, the radiative zone, and the convective zone. Within the solar atmosphere are the photosphere, the chromosphere, and the corona. Finally, the heliosphere is located in the outermost zone of the Sun.

The **core** extends from the center of the Sun to approximately 25% of its radius. This is where Helium is produced from Hydrogen. The temperature inside decreases radially so rapidly that it allows the formation of radiative and convective zones. The **radiative zone** has temperatures decreasing from 7 to 2 million Kelvin as we increase the radius. Because the temperature gradient is smaller than that predicted by adiabatic theory, the dynamics of this zone are governed by radiation rather than thermal convection. The **convective zone** extends from about 0.7 solar radii to near its surface. Since this zone is not hot enough, it does not allow the transmission of energy through radiation, but rather the energy is carried to the surface by plasma motion, as conduction is not able to transmit the energy to the surface.

The visible part of the Sun is called the **photosphere**, located in the outermost part of the convective zone. In this layer, photons generated are able to escape the solar atmosphere, producing the visible light of the Sun and solar radiation. This layer of the Sun is mainly composed of Hydrogen and Helium. Above the

photosphere is the **chromosphere**, a transition region characterized by an increase in temperature.

The **corona** is the outermost part of the Sun's atmosphere and lies above the chromosphere. It extends millions of kilometers into space and is visible during a total solar eclipse as a white halo. The corona is characterized by its high temperatures, ranging from 1 to 3 million Kelvin, which is much hotter than the surface of the Sun. This temperature difference is a subject of ongoing research, and it is thought to be due to processes such as magnetic reconnection and wave heating. The corona is also the source of the solar wind that fills the heliosphere.

The region of the **heliosphere** is the outermost part of the solar atmosphere. It is mainly composed of solar wind, a flow of charged particles consisting mainly of electrons, protons, and alpha particles with traces of other ions. This region is defined by the distance at which the solar wind becomes super-Alfvénic, which occurs at 0.1 AU or 20 solar radii.

1.3 Solar Wind

The solar wind is a flow of charged particles originating from the solar atmosphere, particularly from the solar corona. This plasma is composed of roughly equal numbers of electrons and ions, with protons (95%) predominating among the ions, 4% helium ions, and 1% other heavier particles. Additionally, it contains a mix of heavy ions such as carbon, nitrogen, oxygen, among other elements.

The solar wind varies in density, temperature, and velocity over time and at different solar latitudes. The particles present in the solar wind plasma are able to

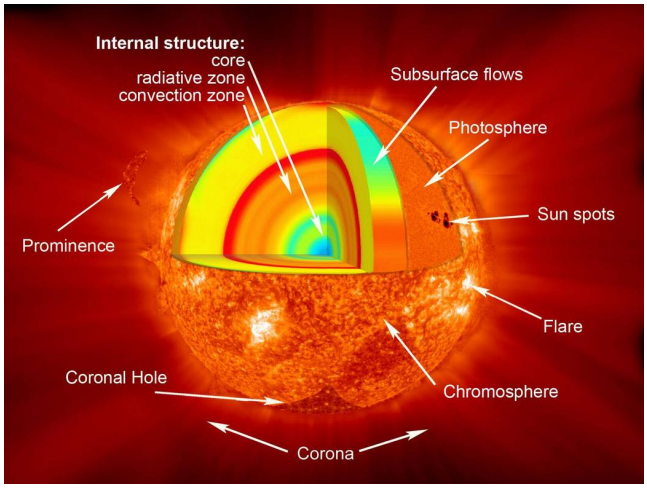

Figure 1.4: General structure of the Sun described in its interior and exterior zones. `https://www.nasa.gov/image-detail/sun/`.

escape solar gravity, among other things, due to the temperature gradient from the Sun. The solar wind, is not constant, but varies in time. In addition, under certain conditions, the sun produces coronal mass ejections (CMEs), from solar flares that are able to produce large events that ejects plasma and fields into space. The boundary separating the solar corona from the solar wind is the **Alfvén Surface**, defined as the region where the Alfvén speed of the coronal plasma and the speed of the large-scale solar wind are equal. This is a natural boundary that marks the causal disconnect of individual plasma packets and magnetic flux from the Sun itself. The Alfvén point or Alfvén surface is the place where the radial motion of the accelerated solar wind passes the radial Alfvén speed, and thus any displacement of material cannot carry information back to the corona by Alfvén waves. Therefore, it is the natural outer boundary of the solar corona and the inner boundary of interplanetary space.

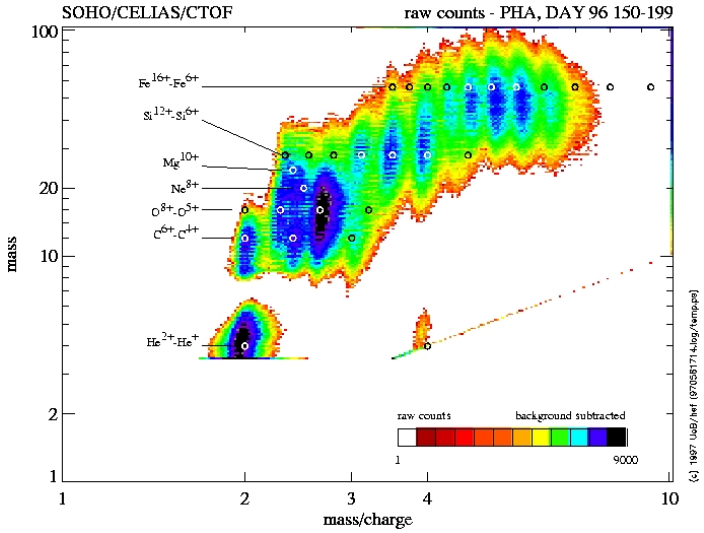

Figure 1.5: The CELIAS/CTOF sensor on SOHO determines for each charged particle entering the sensor its mass, charge, and energy. Here a compilation of all PHA (Particle Hit Analyzer) data for the period between DOY 150 and DOY 199 of 1996 is shown. Clearly, prominent minor ions such as Carbon, Oxygen, Silicon, and Iron can be easily identified, along with their respective charges. Even less abundant minor ions, such as Neon (Ne) or Magnesium (Mg), can be identified. `http://www2.physik.uni-kiel.de/SOHO-CELIAS/data.html`

The magnetic field exerts a pressure similar to that of the gas thermal pressure, indicating that magnetic effects could be as important as the pressure effects exerted by the solar wind, this takes a role when choosing important parameters to analyze different phenomena in the solar wind. In the vicinity of Earth's orbit, the solar wind exhibits approximate speeds, densities, and magnetic field intensities of $470\,\mathrm{km\,s^{-1}}$, $9\,\mathrm{cm^{-3}}$, and $6.6\,\mathrm{nT}$, respectively.

During solar minima, fast flows prevail with speeds between $500\,\mathrm{km\,s^{-1}}$ and $800\,\mathrm{km\,s^{-1}}$ (fast solar wind), whose composition is similar to that of the photosphere

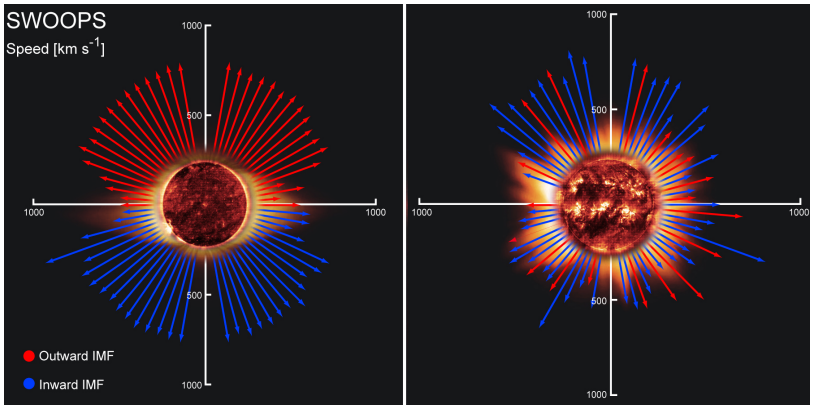

Figure 1.6: Solar wind speeds measured by the Ulysses mission during a solar minimum (left panel) and a solar maximum (right panel). `https://www.esa.int/Science_Exploration/Space_Science/Ulysses_the_science_legacy`.

and appears to originate in coronal holes. A slower flow of approximately $300\,\mathrm{km\,s^{-1}}$, called slow solar wind, is also observed, whose composition is analogous to that of the solar corona and is associated with streams in the solar equatorial belt. The slow solar wind has twice the density and greater intensity variability than the fast solar wind, as well as exhibiting a more complex structure. Figure 1.6 shows the variation of solar wind speed as a function of latitude. Near the ecliptic, both fast and slow solar winds form spiral streams due to the Sun's rotation, moving away from the star. At certain times, the fast solar wind exceeds the slow wind, generating regions of high density and magnetic fields known as Co-rotating Interaction Regions (CIRs). When these regions interact with Earth, they can trigger geomagnetic storms that manifest periodically in cycles of 27 days, corresponding to the solar rotation period. During the ascending phase of the solar cycle, near solar maximum, a decrease in the average solar wind speed is observed as coronal holes become smaller, sometimes even disappearing in many cases.

The next chapter will focus on the study of wave propagation and electromagnetic fluctuations in the solar wind, using theoretical tools that take into account the microscopic and highly dispersed nature of charged particles in space. The statistical view of the Vlasov equation will allow us to describe the electromagnetic waves present in the plasma. In interplanetary space, charged particles in the solar wind rarely collide with each other. Instead, they primarily interact through electric and magnetic fields. Therefore, the Vlasov equation is used, as a first approximation, to model these interactions without considering collisions between particles, making it suitable for describing the behavior of collisionless plasmas. Furthermore, in chapter 3, we will introduce the theoretical basis to analyze electromagnetic fluctuations, since the Vlasov formalism does not predict them, we will introduce the Fluctuation-Dissipation theorem and the theory developed in Schlickeiser and Yoon (2015) using the set of Klimontovich-Maxwell equations to further study these electromagnetic fluctuations.

Chapter 2

Plasma Waves and Electromagnetic Fluctuations

There are two ways to describe the properties and processes of plasma, the macroscopic formulation and the microscopic formulation. The former refers to a fluid or thermodynamic description, while the latter refers to a kinetic and statistical description. A statistical description is fundamental for determining macroscopic properties of the plasma and allows for the study of processes where it is necessary to describe the individual particles that constitute the plasma, such as scattering processes, radiation in plasma, and particle collisions within it. Hence, kinetic theory enables the study of processes such as wave propagation in plasmas, as well as the conditions for their stability and equilibrium. Kinetic theory, as addressed in Krall et al. (1973), provides an initial description for a microscopic many-body system, then by averaging the microscopic variables and making certain simplifications, it presents a statistical view to derive the Vlasov equation. The Vlasov equation provides a good description of the spatial evolution of non-homogeneous systems, making it the starting point for describing collisionless plasmas.

In this chapter, we will derive the Vlasov equation from the Klimontovich equation and find its solutions. As mentioned earlier, it is useful to frame the development of the Klimontovich equation since this same formalism will be used to describe electromagnetic fluctuations in magnetized plasmas according to Schlickeiser and Yoon (2015); Schlickeiser et al. (2015). Moreover, deducing the Vlasov equation from this will illustrate us the necessary approximations to understand how electromagnetic fluctuations are analyzed from the Fluctuation-Dissipation theorem formalism. Specifically, the linear Vlasov equation will be solved to find the dispersion relation for a magnetized electron-proton plasma with a background magnetic field, in the case of parallel propagation of waves to this field. Much of this chapter is based on the book Krall et al. (1973).

2.1 Microscopic Equations, Klimontovich Equation

To obtain a complete description of plasma, we need a definition of the positions and velocities of each particle at every instant of time. Let the Klimontovich distribution function be defined as

$$N_\alpha(\mathbf{x}, \mathbf{v}, t) = \sum_i \delta\left[\mathbf{x} - \mathbf{x}_i(t)\right] \, \delta\left[\mathbf{v} - \mathbf{v}_i(t)\right] \, ,$$

which specifies the microscopic system of particles of species α. If we define the phase space as $\mathbf{X} = (\mathbf{x}, \mathbf{v})$ and $d\mathbf{X} = d\mathbf{x}d\mathbf{v}$, then we may write the latter expression

as,

$$N_\alpha(\mathbf{X},t) = \sum_i \delta\left[\mathbf{X} - \mathbf{X}_i(t)\right] ,$$

where the integral of this parameter in the space defined above gives us the total number of α-type particles in the system. Taking into account the microscopic electric and magnetic fields of the particles and using the definition of $N_\alpha(\mathbf{X},t)$ in the equations of motion of the system, we obtain the *Klimontovich-Dupree equation*,

$$\frac{\partial N_\alpha(\mathbf{X},t)}{\partial t} + \mathbf{v}\cdot\frac{\partial N_\alpha(\mathbf{X},t)}{\partial \mathbf{x}} + \frac{q_\alpha}{m_\alpha}\left(\mathbf{E}^M + \frac{\mathbf{v}\times\mathbf{B}^M}{c}\right)'\cdot\frac{\partial}{\partial \mathbf{v}}\,N_\alpha(\mathbf{X},t) = 0\,,$$

where the superscript M indicates that we are using the microscopic fields, and the ()' indicates that when calculating the microscopic electromagnetic fields for the i-th particle, the field due to that particle is omitted. Here, q_α denotes the charge of the particle, m_α is the mass of the particle, $\mathbf{E}$ is the electric field, and $\mathbf{B}$ is the magnetic field. This equation essentially represents the conservation of particles in phase space ($dN_\alpha/dt = 0$). Since $N_\alpha(\mathbf{X},t)$ is not a statistical function but rather defines the position and velocity of the particles in the system, solving this system directly is inconvenient. Therefore, we require a statistical analysis, as used in the Vlasov description. The statistical description will be obtained by averaging over the microscopic equations, as mentioned earlier.

2.2 Statistical Equations for a Many-Body System

To achieve a statistical description of the system, we will consider the distribution function of the particles in system. The function describing this particle distribution

will be introduced as follows. Let

$$F_N\left(\mathbf{X}_{\alpha 1},\ldots,\mathbf{X}_{\alpha\bar{N}_\alpha};\mathbf{X}_{\nu 1},\ldots,\mathbf{X}_{\nu\bar{N}_\alpha},t\right)\; d\mathbf{X}_{\alpha 1}\cdots d\mathbf{X}_{\alpha\bar{N}_\alpha}d\mathbf{X}_{\nu 1}\cdots d\mathbf{X}_{\nu\bar{N}_\nu}\,, \tag{2.1}$$

represent the probability that at some time t, the coordinates and velocities of the particles have values $\mathbf{X}_{\alpha 1},\ldots,\mathbf{X}_{\alpha\bar{N}_\alpha},\mathbf{X}_{\nu 1},\ldots,\mathbf{X}_{\nu\bar{N}_\alpha}$ within the range $d\mathbf{X}_{\alpha 1}\cdots d\mathbf{X}_{\alpha\bar{N}_\alpha}$, $d\mathbf{X}_{\nu 1}\cdots d\mathbf{X}_{\nu\bar{N}_\nu}$, and $N=\sum_\alpha \bar{N}_\alpha$ is the total number of particles in the system. Reduced distribution functions can be obtained by integrating expression (2.1), but despite being easier to study, they provide an incomplete description of the system. Particularly, we can have the distribution of a single particle, defined as the density of particles of the same type in phase space,

$$f_\alpha\left(\mathbf{x}_{\alpha 1},\mathbf{v}_{\alpha 1},t\right)=V\int F_N\, d\mathbf{X}_{\alpha 2}\cdots d\mathbf{X}_{\alpha\bar{N}_\alpha}\prod_\nu d\mathbf{X}_{\nu i}\,,$$

where V is the volume of the system, and $\nu\in\{1,...,\bar{N}_\nu\}$. Then,

$$\frac{1}{V}\,f_\alpha\left(\mathbf{x}_{\alpha 1},\mathbf{v}_{\alpha_1},t\right)\; d\mathbf{X}\,,$$

gives us the probability of finding a particle of type α at $(\mathbf{x},\mathbf{v})$ in the volume $d\mathbf{x}\,d\mathbf{v}$. This distribution function does not account for the presence of nearby neighbors, and similarly, it is possible to continue constructing distribution functions that include interactions of three or more particles. However, this goes beyond the scope of our study, since we aim to investigate interactions mediated by the electromagnetic fields present in the plasma rather than particle-particle interactions. This is important, but to obtain the Vlasov equation, we must neglect the terms of interaction between particles. Accordingly, the statistical average of the microscopic quantities

analyzed in the Maxwell's equations for a system of particles of species α take the form,

$$\begin{aligned}
\nabla \cdot \langle \mathbf{E}^{\,M} \rangle &= 4\pi \sum_{\alpha} q_\alpha \int \langle N_\alpha(\mathbf{X}, t) \rangle \, d\mathbf{v} \,, \\
\nabla \times \langle \mathbf{B}^M \rangle &= \frac{1}{c} \frac{\partial}{\partial t} \langle \mathbf{E}^M \rangle + \frac{4\pi}{c} \sum_{\alpha} q_\alpha \int \mathbf{v} \, \langle N_\alpha(\mathbf{X}, t) \rangle \, d\mathbf{v} \,, \\
\nabla \times \langle \mathbf{E}^M \rangle &= -\frac{1}{c} \frac{\partial}{\partial t} \langle \mathbf{B}^M \rangle \,, \\
\nabla \cdot \langle \mathbf{B}^M \rangle &= 0 \,.
\end{aligned}$$

We note that the average of the microscopic fields yields the macroscopic electromagnetic fields. The macroscopic fields are an average of the microscopic fields over a volume and time interval over an ensemble; thus, these macroscopic fields describe electromagnetic fields on a large scale. If we analyze the term $\langle N_\alpha(\mathbf{X}, t) \rangle$, we notice that

$$\langle N_\alpha(\mathbf{X}, t) \rangle = \bar{n}_\alpha \, f_\alpha(\mathbf{x}, \mathbf{v}, t) \,,$$

where $\bar{n}_\alpha = \bar{N}_\alpha / V$. Similarly, if we analyze a system for two species of particles α and ν, we must take the average of the quantity $\langle N_\alpha N_\nu \rangle$. We could expect that a good approximation is

$$\langle N_\alpha(\mathbf{X}, t) N_\nu(\mathbf{X}', t) \rangle = \bar{n}_\alpha \bar{n}_\nu \, f_{\alpha\nu}(\mathbf{X}, \mathbf{X}', t) + \delta_{\alpha\nu} \bar{n}_\alpha \delta(\mathbf{X} - \mathbf{X}') f_\alpha(\mathbf{X}, t) \,,$$

where $\delta_{\alpha\nu}$ represents the Kronecker delta. At this point, it is reasonable to seek equations governing the temporal evolution of the distribution functions of different species of particles. Particularly for the distribution of a single particle, we notice

that the temporal evolution of f_α is given by,

$$\frac{\partial f_\alpha}{\partial t} + \mathbf{v}\cdot\frac{\partial f_\alpha}{\partial \mathbf{x}} + \frac{q_\alpha}{\bar{n}_\alpha m_\alpha}\left\langle \left(\mathbf{E}^M + \frac{\mathbf{v}\times\mathbf{B}^M}{c}\right)'\cdot\frac{\partial}{\partial \mathbf{v}} N_\alpha(\mathbf{X},t)\right\rangle = 0\,, \tag{2.2}$$

where we have taken the average of the Klimontovich-Dupree equation, in other words, if we consider the conservation of particles in the phase space and average that equation, we obtain Equation (2.2). This expression is not a closed equation for $f_\alpha(\mathbf{X},t)$ since it depends on the quantity $\langle N_\alpha N_\nu\rangle$, and this term has a series of expansions for various particle interactions. Therefore, we need to find the equation governing the temporal evolution of $f_{\alpha\nu}(\mathbf{X},\mathbf{X}',t)$. This procedure leads to $f_{\alpha\nu}$ still being a non-closed equation, so we need an equation for $f_{\alpha\nu\gamma}$ and so on. Hence, we must find a way to close this chain of equations so that we can find an equation describing the temporal evolution of the first distribution functions. Let us write this equation in terms of average fields and fluctuations, in this case we consider,

$$\begin{aligned} N_\alpha &= f_\alpha + \delta N_\alpha\,, \\ \mathbf{E}^M &= \mathbf{E} + \delta\mathbf{E}^M\,, \\ \mathbf{B}^M &= \mathbf{B} + \delta\mathbf{B}^M\,, \end{aligned}$$

and,

$$\begin{aligned} \mathbf{E} = \langle\mathbf{E}^M\rangle \quad &, \quad \mathbf{B} = \langle\mathbf{B}^M\rangle\,, \\ \langle\delta\mathbf{E}^M\rangle = 0 \quad &, \quad \langle\delta\mathbf{B}^M\rangle = 0\,. \end{aligned}$$

To obtain the *plasma kinetic equation*,

$$\underbrace{\frac{\partial f_\alpha}{\partial t} + \mathbf{v}\cdot\nabla f_\alpha + \frac{q_\alpha}{m_\alpha}(\mathbf{E}+\mathbf{v}\times\mathbf{B})\cdot\nabla_v f_\alpha}_{\text{collective effects at large scales}} = \underbrace{-\frac{q_\alpha}{m_\alpha}\langle\left(\delta\mathbf{E}^M + \mathbf{v}\times\delta\mathbf{B}^M\right)\cdot\nabla_v\delta N_\alpha\rangle}_{\text{collisional effects}}\,. \tag{2.3}$$

The left side of the equation takes into account for collective effects at large scale since it involves average fields, and the right side of the equation takes into account correlations and fluctuation effects in the plasma. The right side of the equation will be neglected to obtain the *Vlasov equation*.

2.2.1 BBGKY Hierarchy

The BBGKY (Bogoliubov-Born-Green-Kirkwood-Yvon) hierarchy is a set of equations used in statistical mechanics to describe the time evolution of a many-body system, particularly in the context of classical or quantum gases. It provides a systematic way to analyze the behavior of a system of interacting particles by considering correlations among subsets of particles of different sizes. It is based on the concept of particle velocity distribution functions (PVDFs). Since for multiple particles we would obtain an infinite series of equations, closure approximations are typically employed to truncate the hierarchy and make it computationally tractable. These approximations involve neglecting higher-order correlation functions or making assumptions about their behavior. A convenient way to write higher-order distribution functions is in terms of the correlation function, which are defined by the Mayer expansion,

$$
\begin{aligned}
f_{\alpha\nu}(\mathbf{X},\mathbf{X}') &= f_\alpha(\mathbf{X})f_\nu(\mathbf{X}') + g_{\alpha\nu}(\mathbf{X},\mathbf{X}',t)\,, \\
f_{\alpha\nu\gamma} &= f_\alpha(\mathbf{X})f_\nu(\mathbf{X}')f_\gamma(\mathbf{X},\mathbf{X}',\mathbf{X}'') + f_\alpha(\mathbf{X},t)g_{\nu\gamma}(\mathbf{X}',\mathbf{X}'',t) \\
&\quad + f_\nu(\mathbf{X}',t)g_{\alpha\gamma}(\mathbf{X},\mathbf{X}'',t) + f_\gamma(\mathbf{X}'',t)g_{\alpha\nu}(\mathbf{X},\mathbf{X}',t) + g_{\alpha\nu\gamma}(\mathbf{X},\mathbf{X}',\mathbf{X}'',t)\,,
\end{aligned}
$$

and so on. The statistical description has an advantage, it is possible to trun-

cate the chain of equations if a valid approximation for the higher-order correlation functions is found. This generates a hierarchy in the expressions, resulting in closed equations for the first distribution functions. Statistical equilibrium theory tells us that the correlations $g_{\alpha\nu}$ are small compared to the terms $f_\alpha f_\nu$ as long as the condition

$$\frac{1}{n\lambda_D^3} \ll 1\,,$$

is satisfied, where λ_D is the Debye length, and n is the number density of particles in the plasma. This allows for a hierarchy among the correlations. Typical values for various environments are shown in Table (2.1).

Table 2.1: Typical values of densities, electron temperatures, magnetic fields, and Debye lengths in different plasma environments.

Environment	Density (n_e m^{-3})	Electron Temperature (T K)	Magnetic Field (B T)	Debye Length (λ_D m)
Solar Core	10^{32}	10^{7}	–	10^{-11}
Tokamak	10^{20}	10^{8}	10	10^{-4}
Gas Discharge	10^{16}	10^{4}	–	10^{-4}
Ionosphere	10^{12}	10^{3}	10^{-5}	10^{-3}
Magnetosphere	10^{7}	10^{7}	10^{-8}	10^{2}
Solar Wind	10^{6}	10^{5}	10^{-9}	10
Interstellar Medium	10^{5}	10^{4}	10^{-10}	10
Intergalactic Medium	1	10^{6}	–	10^{5}

Therefore, the suggested approximation to neglect higher-order particle correlation terms is valid within the ranges of this work.

2.3 Vlasov Equation

The simplest way to approximate these terms is by ignoring the g-order terms. Physically, this corresponds to considering only *quasi-equilibrium states*, meaning we are considering states that remain in equilibrium on timescales much shorter than the particle collision time. These are the states we will consider to solve the Vlasov equation and describing steady states of the plasma under certain conditions. In this approximation, the kinetic equation for the plasma distribution function is then given by,

$$\frac{\partial f_\alpha}{\partial t} + \mathbf{v} \cdot \nabla f_\alpha + \frac{q_\alpha}{m_\alpha} \left(\mathbf{E} + \frac{\mathbf{v} \times \mathbf{B}}{c} \right) \cdot \nabla_v f_\alpha = 0 \,. \tag{2.4}$$

where

$$\nabla = \frac{\partial}{\partial \mathbf{x}} \quad , \quad \nabla_v = \frac{\partial}{\partial \mathbf{v}} \,.$$

This equation is called the *Vlasov equation*, which can be generalized to incorporate external fields. In the following sections, we will present the solution to the Vlasov equation by investigating plasma properties. Additionally, we will calculate the dispersion relation for waves propagating parallel to the background magnetic field.

2.3.1 Stationary States

The Vlasov equation has a wide variety of stationary states, meaning there are multiple states that satisfy $\partial f_{\alpha 0}/\partial t = 0$. These states are often called meta-equilibrium states since they are the only equilibrium present on a timescale smaller than the particle collision time in the plasma. Therefore, these stationary states satisfy the

following expression,

$$\left[\mathbf{v}\cdot\nabla+\frac{q_\alpha}{m_\alpha}\left(\mathbf{E}+\frac{\mathbf{v}\times\mathbf{B}}{c}\right)\cdot\nabla_v\right]f_{\alpha 0}(\mathbf{x},\mathbf{v})=0\,, \tag{2.5}$$

where any function depending on the constants of motion of a particle is also a stationary distribution. For example, considering non radiative processes, in the case of a plasma lacking background fields, the constants of motion are the energy and momentum of the particles. Therefore, any stationary distribution function depending on the velocities of the particles is a stationary state. In this example, a distribution that obeys Equation (2.5) is the Maxwell-Boltzmann distribution,

$$f_{\alpha_0}=\left(\frac{m}{2\pi k_b T}\right)^{3/2}_{\alpha}\exp\left(-\frac{m}{2k_b T}\,v^2\right)\,,$$

where m is the mass of the particles, k_B is the Boltzmann constant, T (K) is the temperature of the system, and $v\,(\mathrm{m\,s^{-1}})$ is the velocity of the particles. The choice of a distribution function depends on prior knowledge of the plasma behavior. For example, the Maxwell-Boltzmann distribution is suitable for systems where a certain collision time has passed, known as the collisional age of the plasma. These states can further be stable or unstable. Nearby states can be expressed as,

$$f_\alpha(t)=f_{\alpha 0}+\delta f_\alpha(t)\,.$$

In these cases, the amplitude of the perturbation grows over time, leading the system away from the quasi-equilibrium state $f_{\alpha 0}$, and it is called unstable. The existence of these unstable states of the distribution functions indicates that the interaction between particles alone is not sufficient for the system to evolve towards thermodynamic equilibrium. Moreover, ensuring that the plasma evolution is consistent with the Vlasov equation is not trivial. There are solutions to the Vlasov

equation that are stationary and have less entropy than the corresponding Maxwell-Boltzmann distribution, yet they are stable, for example, in the absence of collisions. This indicates that the system's evolution is not solely governed by processes of energy exchange between particles; rather, there must be other processes mediating this behavior.

2.4 Vlasov Theory for Plasma Waves

The Vlasov equation, as mentioned earlier, describes the behavior of plasma for time intervals much shorter than the collision time between particles. In addition to providing equilibrium solutions to these systems, it gives us insight into the various phenomena that exist out of equilibrium, such as the waves propagating in a plasma and their stability. This expression is also valid for describing plasmas that have evolved over several collision times, where the theory can predict other phenomena such as plasma waves or Landau damping. The Vlasov equation with a magnetic field is expressed as,

$$\frac{\partial f_\alpha}{\partial t} + \mathbf{v} \cdot \nabla f_\alpha + \frac{q_\alpha}{m_\alpha}\left(\mathbf{E} + \frac{\mathbf{v} \times \mathbf{B}}{c}\right) \cdot \nabla_v f_\alpha = 0\,. \tag{2.6}$$

This equation is obtained ignoring the collisional term of Equation (2.3). Here, the following normalization is used,

$$\bar{N}_\alpha = \bar{n}_\alpha \int f_\alpha d^3x d^3v\,,$$

where $\bar{N}_\alpha$ is the number of particles of type α in the system, and $\bar{n}_\alpha$ is the number density of particles ($\bar{N}_\alpha/V$). Here, the VDFs are normalized to unity,

$$\int f_\alpha d^3x d^3v = 1\,.$$

The associated Maxwell's equations are,

$$\nabla \cdot \mathbf{E} = 4\pi \sum_{\alpha} \bar{n}_{\alpha} q_{\alpha} \int f_{\alpha}\, d^3v + 4\pi \rho_{\text{ext}}\,,$$
$$\nabla \times \mathbf{B} = \frac{1}{c}\frac{\partial \mathbf{E}}{\partial t} + \frac{4\pi}{c} \sum_{\alpha} \bar{n}_{\alpha} q_{\alpha} \int \mathbf{v} f_{\alpha}\, d^3v + \frac{4\pi}{c}\, \mathbf{J}_{\text{ext}}\,,$$
$$\nabla \times \mathbf{E} = -\frac{1}{c}\frac{\partial \mathbf{B}}{\partial t}\,,$$

where ρ_{ext} and $\mathbf{J}_{\text{ext}}$ are the charge density and current density, respectively, defined as,

$$\rho = \sum_{\alpha} q_{\alpha} n_{\alpha} \int d^3p\, f_{\alpha}\,,$$
$$\mathbf{J} = \sum_{\alpha} q_{\alpha} n_{\alpha} \int d^3p\, \mathbf{v}\, f_{\alpha}\,.$$

where q_α and n_α are the charge and particle density of species α, and $f_\alpha = f_\alpha(\mathbf{r}, \mathbf{v}, t)$ is the single particle distribution function of each species. To describe the normal modes along the plasma, we need to solve the Vlasov equation, shown in Equation (2.6). Notice that the fields depend on the distribution function, and therefore Equation (2.6) is a nonlinear equation difficult to solve. However, it is possible to find an approximate solution of the distribution function $f_{\alpha 1}$, from an equilibrium state $f_{\alpha 0}$ using the linearized Vlasov equations. These equations are approximations of the exact equations and are simpler to solve. First, to derive these expressions, we must consider both the fields and the distribution function in terms of an equilibrium value plus a perturbation of order $\epsilon \ll 1$. That is, we

consider electromagnetic fields that fluctuate with respect to an average field,

$$\begin{aligned} f_\alpha(\mathbf{x},\mathbf{v},t) &= f_{\alpha 0}(\mathbf{x},\mathbf{v},t) + \epsilon f_{\alpha 1}(\mathbf{x},\mathbf{v},t)\,, \\ \mathbf{E}(\mathbf{x},t) &= \mathbf{E}_0(\mathbf{x},t) + \epsilon \mathbf{E}_1(\mathbf{x},t)\,, \\ \mathbf{B}(\mathbf{x},t) &= \mathbf{B}_0(\mathbf{x},t) + \epsilon \mathbf{B}_1(\mathbf{x},t)\,. \end{aligned}$$

Substituting these expressions into the Vlasov Equation (2.6) and neglecting the terms of order ϵ^2, we obtain the linearized Vlasov equations. Now, considering the expressions satisfied by the equilibrium distribution function, which is assumed known and satisfies the Vlasov equation and Maxwell's equations. By subtracting the linearized Vlasov equations from the equilibrium equations, we obtain the linearized Vlasov equations for the perturbed distribution function $f_{\alpha 1}$ and the perturbed fields $\mathbf{E}_1$ and $\mathbf{B}_1$,

$$\begin{aligned} &\frac{\partial f_{\alpha 1}}{\partial t} + \mathbf{v}\cdot\nabla f_{\alpha 1} + \frac{q_\alpha}{m_\alpha}\left(\mathbf{E}_0 + \frac{\mathbf{v}\times\mathbf{B}_0}{c}\right)\cdot\nabla_v f_{\alpha 1} \\ &\qquad = -\frac{q_\alpha}{m_\alpha}\left(\mathbf{E}_1 + \frac{\mathbf{v}\times\mathbf{B}_1}{c}\right)\cdot\nabla_v f_{\alpha 0}\,, \qquad (2.7) \\ &\nabla\cdot\mathbf{E}_1 = 4\pi\sum_\alpha \bar{n}_\alpha q_\alpha \int f_{\alpha 1}\, d^3v\,, \qquad (2.8) \\ &\nabla\times\mathbf{B}_1 = \frac{1}{c}\frac{\partial\mathbf{E}_1}{\partial t} + \frac{4\pi}{c}\sum_\alpha \bar{n}_\alpha q_\alpha \int \mathbf{v} f_{\alpha 1}\, d^3v\,, \\ &\nabla\times\mathbf{E}_1 = -\frac{1}{c}\frac{\partial\mathbf{B}_1}{\partial t}\,. \end{aligned}$$

This set of equations for the perturbed quantities can be solved by conventional methods. In this case, the distribution $f_{\alpha 0}(\mathbf{x},\mathbf{v})$ and the unperturbed fields $\mathbf{E}_0$ and $\mathbf{B}_0$ represent the steady states of the plasma, and the distribution $f_{\alpha 1}(\mathbf{x},\mathbf{v})$ represents the evolution of the initial perturbation. It is known that in plasma fluid

theory, perturbations of steady states evolve as waves propagating in them, which is why the linearized Vlasov equations are derived from perturbations in equilibrium states, as the Vlasov formalism encompasses all the results obtained in fluid theory.

2.5 Solution of the Vlasov equation for small amplitude waves propagating in a uniformly magnetized plasma.

The orbits of particles in an equilibrium plasma are complicated if a background magnetic field is included. The fact that changing the velocity distribution or the electromagnetic fields of the plasma significantly affects the behavior and type of waves propagating in them makes it impossible to implement a complete treatment, leading us to analyze equilibrium cases separately.

2.5.1 Equilibrium Conditions

Since we are considering that the system's response is mediated by perturbations from its quasi-equilibrium state, we will define the conditions necessary to consider this equilibrium. Let us consider a uniform and stationary plasma; thus, our distribution function is neither spatially nor temporally dependent. In this case, we consider the unperturbed electromagnetic fields as follows,

$$\mathbf{B}_0 = B_0\,\hat{z} \quad , \quad \mathbf{E}_0 = 0\,.$$

According to the Vlasov equation,

$$\frac{q_\alpha}{c}(\mathbf{v}\times\mathbf{B}_0)\cdot\frac{\partial f_\alpha}{\partial v} = 0\,, \tag{2.9}$$

where, by orienting our system such that $\mathbf{B}_0 = B_0\hat{z}$, we can write the particle velocity as follows,

$$v_x = v_\perp \cos\phi\,, \qquad v_y = v_\perp \sin\phi\,, \qquad v_z = v_\parallel\,,$$

where $v_\perp$ and $v_\parallel$ are the velocities perpendicular and parallel to $\mathbf{B}_0$. Then, from Equation (2.9), it follows that,

$$\frac{\partial f_\alpha}{\partial \phi} = 0\,.$$

In other words, the distribution functions in equilibrium are gyrotopic, $f_\alpha = f_\alpha(v_\perp, v_\parallel)$. In the following sections, we will discuss the choice of the distribution function and which one best models the type of plasma we want to analyze. Remember that to find the dispersion relation, we aim to find the perturbed distribution function, so we seek to solve Equation (2.7). One of the methods to solve Equation (2.7) is by integrating along the orbits of the particles in the unperturbed fields. This resolution method is called the Method of Characteristics, shown in detail in the Appendix. Using this method we obtain the solution for the perturbed distribution function,

$$f_{\alpha 1} = -\frac{q_\alpha}{m_\alpha}\int_{-\infty}^{0} d\tau \left(\bar{\mathbf{E}}_\mathbf{1} + \frac{\mathbf{v}'\times\bar{\mathbf{B}}_\mathbf{1}(\mathbf{x}',t')}{c}\right)\cdot\nabla'_v f_{\alpha 0}(\mathbf{v}')\,\exp\left(i\,\mathbf{k}\cdot\mathbf{R} - iw\tau\right)\,. \quad (2.10)$$

Where $\mathbf{R} = \mathbf{r}' - \mathbf{r}$, $\tau = t' - t$, $\mathbf{x}' = \mathbf{x}'(\tau)$, and $\mathbf{v}' = \mathbf{v}'(\tau)$. The perturbed distribution function will be studied in the case of an specific equilibrium VDF, a general form of the fields, and wave propagation parallel to the background magnetic field.

2.6 Dispersion Relation for parallel propagation

To analyze Equation (2.10), we will consider waves propagating in the $\hat{z}$ direction, i.e., we choose a wave vector of the form $\mathbf{k} = k_\parallel \hat{z}$, and electromagnetic fields of the form,

$$\begin{aligned} \bar{\mathbf{E}}_\mathbf{1} &= E_x\hat{x} + E_y\hat{y} + E_z\hat{z}\,, \\ \bar{\mathbf{B}}_\mathbf{1} &= B_x\hat{x} + B_y\hat{y} + B_z\hat{z}\,. \end{aligned}$$

We need to find the expressions for the trajectories and velocities of these particles, which is developed in the Appendix. The particle velocities in each of their components are

$$\begin{aligned} v'_x &= v_\perp \cos(\phi - \Omega_\alpha \tau)\,, \\ v'_y &= v_\perp \sin(\phi - \Omega_\alpha \tau)\,, \\ v'_z &= v_\parallel\,, \end{aligned} \tag{2.11}$$

where $\Omega_\alpha = q_\alpha B_0/m_\alpha c$ is the cyclotron frequency of species α, which is the frequency at which a particle completes a gyromotion around a magnetic field line. To find the dispersion tensor, we may write, using the Maxwell's equations, the magnetic field in terms of the electric field as,

$$\mathbf{B}_1 = \frac{ck_\parallel}{w}(E_x\hat{y} - E_y\hat{x}) \tag{2.12}$$

Substituting Equations (2.11) and (2.12) into Equation (2.10), we arrive at the result for the perturbed distribution in terms of the electric field,

$$f_{\alpha k} = -\frac{q_\alpha v_\perp}{m_\alpha}\frac{e^{i\phi}}{w_+}(iE_x + E_y)\,\mu'_{k,w} - \frac{q_\alpha v_\perp}{m_\alpha}\frac{e^{-i\phi}}{w_-}(iE_x - E_y)\,\mu'_{k,w} - \frac{2iq_\alpha v_\parallel}{m_\alpha(w - k_\parallel v_\parallel)}\frac{\partial f_0}{\partial v'^2_\parallel}E_z\,,$$

where we have defined

$$\begin{aligned} w_+ &= w - k_\parallel v_\parallel + \Omega_\alpha \,, \\ w_- &= w - k_\parallel v_\parallel - \Omega_\alpha \,, \end{aligned}$$

and,

$$\mu'_{k,w} = \left(\frac{\partial f_0}{\partial {v'_\perp}^2} + \frac{k_\parallel v'_\parallel}{w} \left[-\frac{\partial f_0}{\partial {v'_\perp}^2} + \frac{\partial f_0}{\partial {v'_\parallel}^2} \right] \right) .$$

From this, we will obtain an expression of the form $w(\mathbf{k})$, the dispersion relation, and its solutions will tell us the allowed propagation modes that exist in the plasma. To reach this, note that from the Fourier transform of Maxwell's equations we may write,

$$\hat{x} \left(k_\parallel^2 c^2 - w^2 \right) E_x + \hat{y} \left(k_\parallel^2 c^2 - w^2 \right) E_y - w^2 E_z = 4\pi i w \sum_\alpha n_\alpha q_\alpha \int_L v f_{\alpha k} \, dv^3 \,, \quad (2.13)$$

where the integral shown is performed over the Landau contour (this is explained in more detail in the following sections). In cylindrical coordinates,

$$\begin{aligned} \mathbf{v} &= v_\perp \cos\phi \, \hat{x} + v_\perp \sin\phi \, \hat{y} + v_\parallel \, \hat{z} \,, \\ dv^3 &= v_\perp dv_\perp dv_\parallel d\phi \,. \end{aligned}$$

Using the latter expressions in the current density term of the right side of Equa-

tion (2.13), we obtain,

$$
\begin{aligned}
&\left(k_{\parallel}^2 c^2 - w^2\right) E_x \\
&\qquad -\pi w \sum_{\alpha} w_{p\alpha}^2 \left(E_x \int_L v_{\perp}^3 \eta_+ \, \mu_{k,w} \, dv_{\perp} dv_{\parallel} + i \, E_y \int_L v_{\perp}^3 \eta_- \, \mu_{k,w} dv_{\perp} dv_{\parallel} \right) = 0 \\
&\left(k_{\parallel}^2 c^2 - w^2\right) E_y \\
&\qquad -\pi w \sum_{\alpha} w_{p\alpha}^2 \left(iE_x \int_L v_{\perp}^3 \eta_- \, \mu_{k,w} dv_{\perp} dv_{\parallel} - \, E_y \int_L v_{\perp}^3 \eta_+ \, \mu_{k,w} dv_{\perp} dv_{\parallel} \right) = 0 \\
&w^2 \left(1 + \frac{1}{w} \sum_{\alpha} \frac{w_{p\alpha}^2}{k_{\parallel}} \int_L \frac{\partial f_0}{\partial v_{\parallel}} \frac{v_{\parallel}}{w/k_{\parallel} - v_{\parallel}} d^3 v \right) = 0 \, ,
\end{aligned}
$$

where,

$$
\mu_{k,w} = \left(\frac{\partial f_0}{\partial {v_{\perp}}^2} \left(1 - \frac{k_{\parallel} v_{\parallel}}{w} \right) + \frac{k_{\parallel} v_{\parallel}}{w} \frac{\partial f_0}{\partial {v_{\parallel}}^2} \right) ,
$$

and,

$$
\eta_{\pm} \;\; = \;\; \frac{1}{w_+} \pm \frac{1}{w_-} ,
$$

where $w_{p\alpha}^2 = \dfrac{4\pi n_\alpha q_\alpha^2}{m_\alpha}$. It is noteworthy that the propagation mode related to the E_z component of the electric field does not depend on other components of the electric field and thus is by itself a dispersion relation. For the transverse propagating modes, we can write in matrix form,

$$
\begin{pmatrix} \phi_A(k,w) & i\phi_B(k,w) \\ -i\phi_B(k,w) & \phi_A(k,w) \end{pmatrix} \begin{pmatrix} E_x \\ E_y \end{pmatrix} = \begin{pmatrix} 0 \\ 0 \end{pmatrix} .
$$

Defining for the following sections of this chapter, the dispersion tensor

$$
\Lambda_{ij} = \begin{pmatrix} \phi_A(k,w) & i\phi_B(k,w) \\ -i\phi_B(k,w) & \phi_A(k,w) \end{pmatrix} , \tag{2.14}
$$

with,

$$\begin{aligned}\phi_A(k,w) &= \left(k_\parallel^2 c^2 - w^2\right) - \pi w \sum w_{p\alpha}^2 \int_L v_\perp^3 \eta_+ \, \mu_{k,w} dv_\perp dv_\parallel \,, \\ \phi_B(k,w) &= \pi w \sum w_{p\alpha}^2 \int_L v_\perp^3 \eta_- \mu_{k,w} dv_\perp dv_\parallel \,.\end{aligned}$$

To obtain a non-trivial solution, the determinant of the dispersion tensor must be zero. Thus, the dispersion relation for transverse modes is

$$\left(k_\parallel^2 c^2 - w^2\right) - 2\pi w \sum_\alpha w_{p\alpha}^2 \int_L \frac{v_\perp^3}{w_\pm} \left(\frac{\partial f_0}{\partial {v_\perp}^2} \left(1 - \frac{k_\parallel v_\parallel}{w}\right) + \frac{k_\parallel v_\parallel}{w} \frac{\partial f_0}{\partial {v_\parallel}^2} \right) dv_\perp dv_\parallel = 0 \,, \tag{2.15}$$

and the dispersion relation for longitudinal modes is

$$w^2 \left(1 + \frac{1}{w} \sum_\alpha \frac{w_{p\alpha}^2}{k_\parallel} \int_L \frac{\partial f_0}{\partial v_\parallel} \frac{v_\parallel}{w/k_\parallel - v_\parallel} d^3 v \right) = 0 \,. \tag{2.16}$$

In Equation (2.16) we see that the integral has a pole in $w/k_\parallel = v_\parallel$, and Equation (2.15) has a pole in $w_\pm = 0$ we will asses this in the following. Equations (2.15) and (2.16) are the dispersion relations that describe the waves propagating parallel to the background magnetic field $\mathbf{B}_0$. Note that this expression is general in terms of species, and velocity distribution function. For a bi-Maxwellian, the integral in $v_\perp$ can be done immediately, leaving the integral of $v_\parallel$ which can be written in terms of the plasma dispersion function

To analyze in more detail the dispersion relations, we need to perform the integrals along the complex plane considering the poles present in them. The integration domain for $v_\parallel$ is $[-\infty, \infty]$ in its description in cylindrical coordinates. Particularly, this is a component that, when performing the integral in the complex plane due to

the present poles, covers the entire real axis. To solve it, we must position ourselves so that the integration region remains outside the pole, which is explained in detail in the Appendix. On the other hand, the wave frequency w, can be a complex number. Thus, when choosing a particular VDF we can rewrite the above integrals by defining the *plasma dispersion function*.

2.6.1 Velocity Distribution Functions

Another topic needed to solve the dispersion relation is finding a suitable VDF to model the system. When space exploration began, scientists noticed that the way charged particles moved in space did not match the expected patterns of thermodynamic equilibrium theory. Instead of following the usual Maxwell-Boltzmann distribution, the velocities of these particles often showed sparse groups of very energetic particles at the far end of the Gaussian curve, which were better described by inverse power-law distributions. Additionally, it was common to find that the temperature in directions perpendicular to the local magnetic field was different from that in the direction parallel to the field, indicating that velocity distributions in space were often not the same in every direction, they were anisotropic. Some examples that show that the solar wind particles have anisotropic velocity distributions near Earth's orbit are discussed in Hundhausen et al. (1967a,b); Marsch et al. (1982) . Particularly, solar wind electrons present energetic tail population, and as such their VDFs should be modeled by Kappa distributions. In this work we will limit these considerations to model solar wind plasma with anisotropic VDFs, such as bi-Maxwellian distributions.

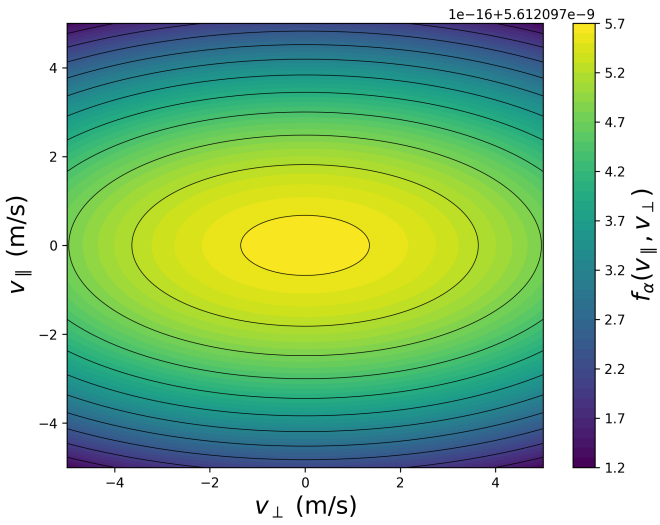

Figure 2.1: Bi-Maxwellian velocity distribution function in the velocity parameter space for $T_\perp/T_\parallel = 2$.

Consider the following definition for the equilibrium velocity distribution function,

$$f_0(v_\perp, v_\parallel) = \frac{1}{\pi^{3/2}\Theta_{\alpha,\perp}^2\Theta_{\alpha\parallel}} \exp\left[-\frac{v_\perp^2}{\Theta_{\alpha,\perp}^2} - \frac{v_\parallel^2}{\Theta_{\alpha,\parallel}^2}\right], \tag{2.17}$$

where

$$\Theta_{\alpha,\perp}^2 = \frac{2kT_{\alpha,\perp}}{m} \quad , \quad \Theta_{\alpha,\parallel}^2 = \frac{2kT_{\alpha,\parallel}}{m}.$$

In Equation (2.17) a bi-Maxwellian velocity distribution function is shown, which describes the velocity distribution of particles in a plasma. This distribution is characterized by having two populations of particles, each following a Maxwell distribution. It is used to describe plasmas that exhibit two distinct groups of particles with different temperatures. Particularly, in the solar wind, we encounter different populations of particles, such as ions and electrons from different sources. The bi-

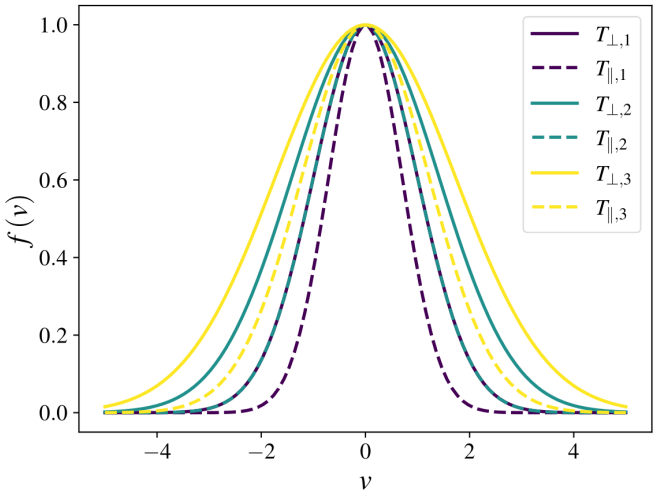

Figure 2.2: Bi-Maxwellian velocity distributions for different temperature configurations. Each curve represents a combination of perpendicular and parallel temperatures. The distributions exhibit the variation of velocity probability for particles in a plasma, highlighting the influence of temperatures in directions perpendicular and parallel to the magnetic field.

Maxwellian distribution can be useful in describing the complexity of velocities in these plasmas.

It has been shown that fluctuations in quasi-stable plasmas can be studied analytically for bi-Maxwellian distributions Gary and Lee (1994). Furthermore, *in situ* measurements of proton velocity distribution in the solar wind show that the deviations from Local thermodynamic equilibrium (LTE) can be represented by bi-Maxwellian VDFs considering different temperatures $T_\perp$ and $T_\parallel$ relative to the background magnetic field B_0 Marsch (2006). To obtain a particular dispersion relation we will include the aforementioned bi-Maxwellian VDF into Equations (2.15) and (2.16) and rewrite the integrals to define the *plasma dispersion function.*

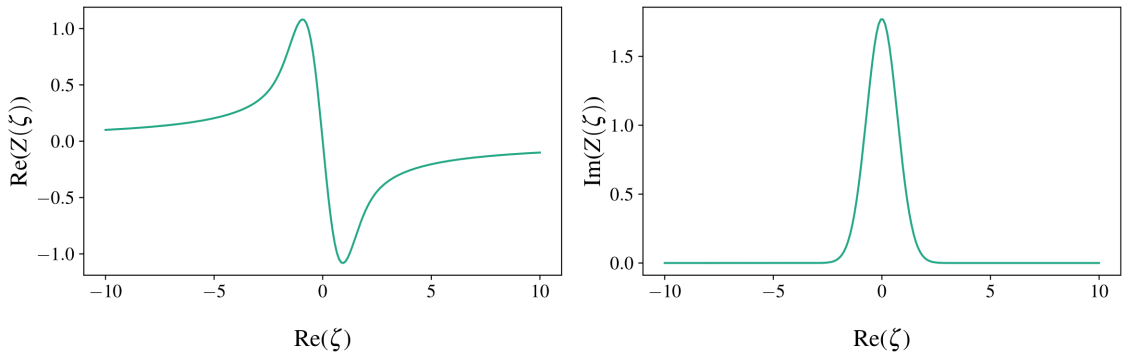

Figure 2.3: Plot of the plasma dispersion function, $Z(\zeta)$, in the complex plane. The left part shows the relationship between the real part of ζ and the real part of $Z(\zeta)$, while the right part shows the relationship between the real part of ζ and the imaginary part of $Z(\zeta)$. We only analyze the cases of $\mathrm{Re}(\zeta)$ since the imaginary parts of frequencies in the quasi-stability region are nearly zero ($\gamma < 10^{-3}$), therefore, $\mathrm{Im}(\zeta) = 0$.

Plasma Dispersion Function

We define the *plasma dispersion function* as,

$$Z_\alpha(\zeta) = \frac{1}{\sqrt{\pi}} \int_{-\infty}^{\infty} \frac{e^{-z^2}}{z - \zeta}\, dz\,, \tag{2.18}$$

where, z is defined as a complex number and ζ is defined as a real number. The derivatives of this function are,

$$Z'_\alpha(\zeta) = \frac{1}{\sqrt{\pi}} \int_{-\infty}^{\infty} \frac{(-2z)e^{-z^2}}{z - \zeta}\, dz = -2[1 + \zeta Z(\zeta)]\,,$$
$$Z''_\alpha(\zeta) = \frac{1}{\sqrt{\pi}} \int_{-\infty}^{\infty} \frac{(-2z)e^{-z^2}}{(z - \zeta)^2}\, dz = -2[Z(\zeta) - 2\zeta - 2\zeta^2 Z(\zeta)])]\,.$$

To perform the complex integrals we need to integrate around the defined Landau contour. Consider the general expression,

$$F(\zeta) = \int_{-\infty}^{\infty} du\, \frac{f(u)}{u - \zeta}\,,$$

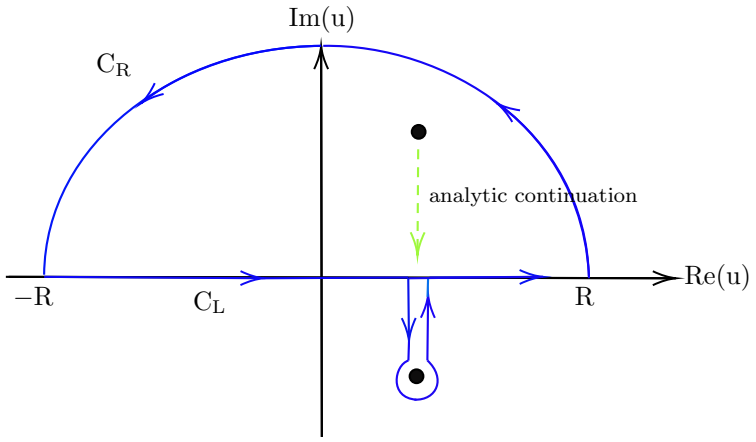

Figure 2.4: Representation of Landau's contour.

where $f(u)$ is an analytic function. It follows that the integrand has a pole at $u = \zeta$, where ζ is complex. When the complex part of ζ satisfies the condition that $\zeta > \sigma > 0$, the pole in the complex plane will lie on the integration contour, which is the real axis. We can analytically continue this expression such that ζ satisfies that $\zeta < \sigma$ by moving the pole towards the real axis. But if the pole crosses the real axis such that $\zeta < 0$, we must deform the integration contour such that the pole continues to lie on it. This deformation is called the *Landau contour* (C_L), as shown in Figure 2.4.

With this, we obtain the analytic continuation of the plasma dispersion function. The following general expression is derived in the Appendix,

$$Z(\zeta) = i\sqrt{\pi}\exp(-\zeta^2)(1 + i\,\mathrm{erfi}(\zeta))\,.$$

This expression will allow us to calculate numerically the solutions of the dispersion relation of transverse modes. In the following we solve the dispersion relations shown above.

2.6.2 Analysis of dispersion relations for parallel modes

We have expressed the VDF we will use in our system and reviewed the method to perform the complex integrals along the Landau's contour. To solve the dispersion relations of Equations (2.15) and (2.16) we substitute a particular VDF, in this case described by a bi-Maxwellian distribution written in Equation (2.17). We will continue the analysis for the dispersion relations related only to the transverse modes of the system, since these modes are directly related to fluctuations of electromagnetic fields, which is why we will focus our attention on these modes, not on the longitudinal modes. The longitudinal modes are related to fluctuations of charge densities in the plasma. In this way, substituting the aforementioned VDF and writing the complex integrals in terms of the plasma dispersion function, we obtain the dispersion relation for the transverse modes,

$$\left(k_{\parallel}^{2}c^{2}-w^{2}\right)-\sum w_{p\alpha}^{2}\left(A_{\alpha}-1+Z_{\alpha}(\zeta'_{\pm,\alpha})\left(\frac{w}{k_{\parallel}\Theta_{\alpha,\parallel}}+\left(A_{\alpha}-1\right)\zeta'_{\pm,\alpha}\right)\right)=0\,, \quad (2.19)$$

where we have defined,

$$\zeta'_{\pm,\alpha}=\frac{w\pm\Omega_{\alpha}}{k_{\parallel}\Theta_{\alpha,\parallel}} \quad , \quad z=\frac{v_{\parallel}}{\Theta_{\alpha,\parallel}},$$

and $A_{\alpha}=\Theta_{\alpha,\perp}^{2}/\Theta_{\alpha,\parallel}^{2}=T_{\alpha,\perp}/T_{\alpha,\parallel}$ is the system's thermal anisotropy for a particle of specie α. Considering the normalization,

$$x=\frac{\omega}{\Omega_{p}} \quad , \quad y=\frac{ck}{\omega_{pp}}, \quad (2.20)$$

we have, for a plasma of electron-proton species,

$$y^2 - x^2\frac{c^2}{v_{\alpha p}^2} - \left(A_p - 1 + Z(\zeta'_{\pm,p})\left(\frac{x}{y}\frac{1}{\sqrt{\beta_p}} + (A_p-1)\zeta'_{\pm,p}\right)\right) - \left(\frac{m_p}{m_e}\right)\left(A_e - 1 + Z(\zeta'_{\pm,e})\left(\frac{x}{y}\frac{1}{\sqrt{\beta_e}}\sqrt{\frac{m_e}{m_p}} + (A_e-1)\zeta'_{\pm,e}\right)\right) = 0\,.$$

Where $v_{\alpha p}^2 = B_0^2/4\pi n_\alpha m_\alpha$ is the Alfvén velocity, A_p and A_e are the proton and electron thermal anisotropy, respectively, and m_p and m_e are the proton and electron mass, respectively. Considering the cold plasma approximation for electrons, where $T_{\|e} = 0$, then $\zeta'_{\pm,e} \to \infty$, the expansion of the plasma dispersion function takes the following form,

$$Z_\alpha(x \to \infty) \sim i\sqrt{\pi}\sigma e^{-x^2} - \frac{1}{x} - \frac{1}{2x^3}\,,$$

where,

$$\sigma = \begin{cases} 0 & y > |x|^{-1}\,, \\ 1 & |y| < |x|^{-1}\,, \\ 2 & y < -|x|^{-1}\,, \end{cases}$$

therefore, using the expansion up to the second term, we finally obtain the dispersion relation for the transverse modes,

$$\Lambda_\pm = 1 - \frac{c^2}{v_\alpha^2}\frac{y^2}{x^2} + \frac{c^2}{v_\alpha^2}\frac{1}{x^2}\left(A_p - 1 \pm x + Z_\alpha(\zeta_\pm)\left(\zeta + (A_p-1)\zeta_\pm\right)\right) = 0\,, \quad (2.21)$$

where,

$$\zeta_\pm = \frac{x \pm 1}{y\sqrt{\beta_p}} \quad , \quad \zeta = \frac{x}{y\sqrt{\beta_p}}.$$

This dispersion relation will be useful to analyze the propagation modes in the plasma. Furthermore, this expression will be helpful for examining electromagnetic fluctuations in the plasma, since it is related to the final expression of the fluctuating

spectra, which will be derived in the following sections. With the final version of the dispersion relation, we may write the diagonal form of Λ_{ij} from Equation (2.14) in the circular polarization basis,

$$\Lambda_{ij} = \begin{pmatrix} \dfrac{1}{\Lambda_+} & 0 \\ 0 & \dfrac{1}{\Lambda_-} \end{pmatrix} . \tag{2.22}$$

The aforementioned dispersion relation for transverse modes was solved for various cases which are shown below. We will consider the propagation frequency of normal modes as $w = w_r + i\gamma_{\mathbf{k}}$. Where w_r represents the real part of the frequency and $\gamma_{\mathbf{k}}$ represents the imaginary part of the frequency that is also a solution of the dispersion relation. The above frequency arises from expressing oscillatory electromagnetic fields, which is analogous to describing their Fourier transform. The way we define this transform tells us how electromagnetic waves propagate, as having $\gamma_{\mathbf{k}} < 0$ gives rise to unstable normal modes which are quickly dissipated. On the other hand, modes with $\gamma_{\mathbf{k}} > 0$ define normal modes that grow in time and radically change the system's dynamics.

The normal modes found in literature for parallel propagation are firehose and ion-cyclotron instabilities. Precisely, Figure 2.5 shows an ion-cyclotron mode for $\beta_p = 0.6$ and $A_p = 1.4$ and Figure 2.6 shows a firehose mode for $\beta_p = 0.6$ and $A_p = 0.1$. Both modes can be unstable because they can involve a resonant interaction between the wave and ions or wave and background magnetic field, respectively. The resonance leads to energy exchange and amplification of perturbations for some values of beta-anisotropy, in those cases we call these modes *plasma instabilities*.

We will see below, that if we organize the solar wind observations in the beta-

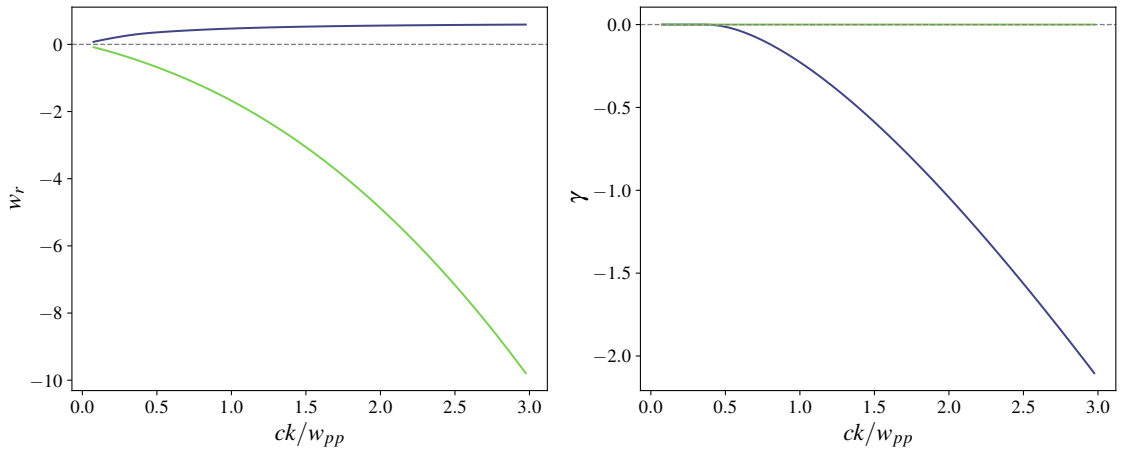

Figure 2.5: Solutions of the dispersion relation of transverse waves for $\beta_p = 0.6$ and $A_p = 1.4$.

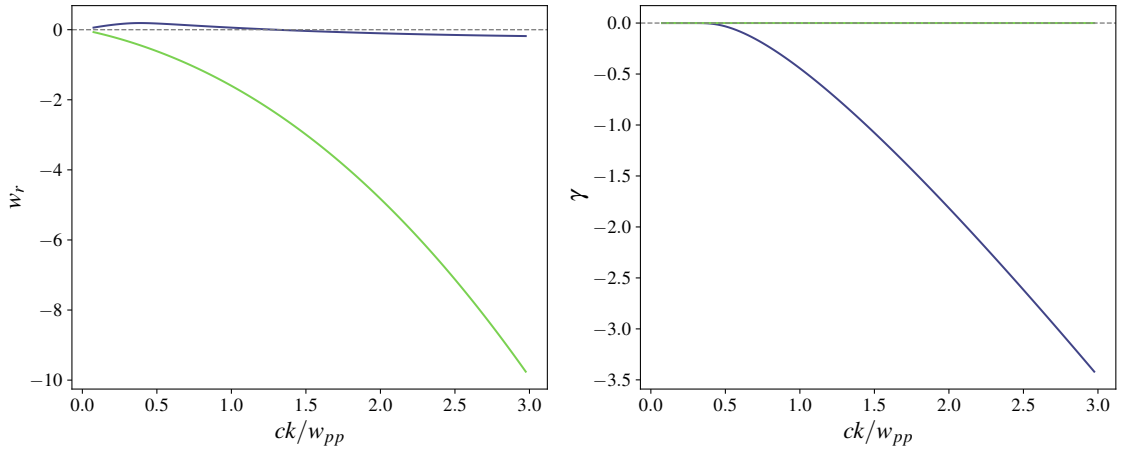

Figure 2.6: Solutions of the dispersion relation of transverse waves for $\beta_p = 0.6$ and $A_p = 0.1$.

anisotropy diagram, we observe that the data is restricted to a region, and seem to follow the contours of $\gamma \sim 10^{-3}$, which defines the quasi-stable state to which the plasma converges, staying there for a long time. In addition, we observe inside the quasi-stable region, finite levels of fluctuations, beyond what we would expect from linear kinetic theory. There are different ideas of where this fluctuations may appear such as cascading from low frequency fluid turbulence, unstable initial conditions that move to the quasi-stable region (usually can only evolve to the boundaries of the quasi-stable region), and thermally induced fluctuations. We are going to discuss *thermally induced electromagnetic fluctuations*. In the following section, we will define the theoretical basis for electromagnetic fluctuations, we will show the region of interest in the beta-anisotropy diagram, and we will explain the fundamentals for both approaches, the Fluctuation-Dissipation theorem and the system of Klimontovich-Maxwell equations.

2.7 Fluctuation Theory

Electromagnetic fluctuations in astrophysical plasmas represent a complex and dynamic phenomena that has captured the attention of the scientific community for decades. These variations in magnetic and electric fields manifest in various cosmic environments, from the solar wind, magnetosphere, to nebulae and distant galaxies. The observation and measurement of these fluctuations have been made possible thanks to technological advancements, especially through the deployment of satellites and space probes equipped with advanced instruments. Fluctuations are an inherent feature of plasmas with random particle velocities, and the quantitative determination of these is essential for understanding various processes, such as the transport of charged particles in turbulent electromagnetic fields and the formation of shock waves.

To theoretically analyze the fluctuations that naturally arise in a magnetized plasma, we use the set of Klimontovich-Maxwell equations, based on the theory developed by Schlickeiser et al. (2015) and the Fluctuation-Dissipation theorem used by Navarro et al. (2014) in the solar wind context. As mentioned earlier, the Klimontovich equation provides a microscopic description of a particle system, accounting for particle correlations and collisions. Using this approach, the Vlasov formalism is employed to derive the dispersion tensor, to latter link induced electromagnetic fluctuations to spontaneous electromagnetic fluctuations in a quasi-stable state. This is what involves the theory developed by Schlickeiser and Yoon (2015); Schlickeiser et al. (2015), as their approach with kinetic theory using the Klimontovich-Maxwell set of equations will help us understand the properties of electromagnetic fluctuations

in plasmas from a more general view.

On the other hand, we can relate the phenomenon of electromagnetic fluctuations to the Fluctuation-Dissipation Theorem, demonstrated by Callen and Welton (1951), which stipulates that the linear response of a system to an external linear perturbation is expressed in terms of the fluctuations of the system in thermal equilibrium. In this context, according to the Fluctuation-Dissipation Theorem, there is a balance between the emission and absorption of fluctuations, meaning that due to the thermal motion of the particles present in the plasma, the production of electromagnetic fluctuations is predicted. In other words, the more energy dissipation is observed, the more electromagnetic fluctuations there will be in the plasma. This is the foundation used by Navarro et al. (2014) to explain the phenomena of induced electromagnetic fluctuations in magnetized plasmas.

By developing the general expression for the spectrum of electromagnetic fluctuations, our goal is to contribute to the understanding of the fundamental properties of fluctuations in magnetized plasmas, considering various theoretical approximations and applying them to a specific case to validate and analyze the results between both proposed theories. We aim to obtain results that can be compared to *in situ* satellite measurements. Specifically, we will calculate the spectral index of thermally induced electromagnetic fluctuations for the $\beta - A$ diagram in the quasi-stability region, index which we will introduce in the following.

It has been shown in multiple articles that the magnetic spectrum shows a power-law behavior in different ranges Podesta et al. (2007, 2006); Kiyani et al. (2015); Goldstein and Roberts (1999), with the kinetic range energy spectrum often having

a power-law exponent near 3/2 Podesta et al. (2007), this range extends from 10^{-4} Hz to 10^{-2} Hz approximately, and it is the regime where kinetic theory is valid. Within this range it has been measured that the spectra exhibits a power-law similar to fluid turbulence, and strong dissipation occurs in higher frequencies as seen from the rapid fall-off of the power spectrum Goldstein and Roberts (1999). At this day, measurements are sufficient to analyze a great range since the launch of diverse spacecrafts such as *Voyager 1*, *Voyager* 2, *Wind* among others. Since then, computer simulations for turbulence Verma (2000); Müller and Biskamp (2000); Biskamp and Müller (2000) and numerical models have improved, nevertheless some theoretical groundwork is still needed. This power-law exponent is the so called spectral index of thermally induced electromagnetic fluctuations which we will calculate for the $\beta - A$ diagram, the parameter space, in the quasi-stability region. The next section is based on the fundamental concepts of fluctuations primarily based on the book written by Yoon (2019).

2.7.1 Fundamental Concepts

To describe the behavior of fluctuating physical quantities in space and time, statistical concepts will be used. That is, temporal, spatial, or ensemble averages are calculated for collections of possible states called an ensemble. Particularly, the interest is focused on how these fluctuating quantities at different instants of time or different places in space are correlated with each other. When considering the average of two physical quantities that are not correlated with each other, it should be zero; however, if we calculate the average of two physically correlated quantities, it

should have some finite value because there is a cause-and-effect relationship between these quantities. In the following, we will describe how the statistical average of the correlation of fluctuating quantities evolves. We will consider δx as a fluctuating quantity and the symbol $\langle \cdots \rangle$ will denote a statistical or ensemble average. Consider a fluctuating quantity whose average is zero, $\langle \delta f(\mathbf{r}, t) \rangle = 0$. We will refer to ensemble average to an average over phases, time, or space. Fluctuations are called *homogeneous* if the spatial dependence of the correlation between two bodies depends only on their relative distances, i.e.,

$$\langle \delta f(\mathbf{r}, t) \delta f(\mathbf{r}', t) \rangle = \langle \delta f^2 \rangle_{\mathbf{r}-\mathbf{r}', t, t'} = \langle \delta f^2 \rangle_{\mathbf{r}'-\mathbf{r}, t-t'} \, ,$$

and are called *stationary* if the correlation between two bodies depends only on their relative time difference,

$$\langle \delta f(\mathbf{r}, t) \delta f(\mathbf{r}', t) \rangle = \langle \delta f^2 \rangle_{\mathbf{r}, \mathbf{r}', t-t'} = \langle \delta f^2 \rangle_{\mathbf{r}', \mathbf{r}, t'-t} \, .$$

Therefore, for homogeneous and stationary fluctuations, the correlation between two bodies is given by,

$$\langle \delta f(\mathbf{r}, t) \delta f(\mathbf{r}', t) \rangle = \langle \delta f^2 \rangle_{\mathbf{r}-\mathbf{r}', t-t'}, \, .$$

We can represent the correlation between two bodies spectrally, transforming the variables to Fourier space; the specific definitions are found in the Appendix. It is noteworthy to mention that fluctuating quantities are defined as such in the Fourier space for both formalisms. Transforming variables to Fourier space we write,

$$\langle \delta f(\mathbf{r}, t) \delta g(\mathbf{r}, t) \rangle = \int d\mathbf{k} \int dw \langle \delta f_{\mathbf{k},w} \delta g_{\mathbf{k},w} \rangle \, .$$

When the angular frequency w satisfies the dispersion relation $w = w_{\mathbf{k}} + i\gamma_{\mathbf{k}}$, then the representation in Fourier space, for a function $f(\mathbf{r}, t)$, can be expressed as

$$f(\mathbf{r}, t) = \int d\mathbf{k} f_{\mathbf{k}} \exp(i\mathbf{k} \cdot \mathbf{r} - iw_{\mathbf{k}}t + \gamma_{\mathbf{k}}t) \,.$$

We will define the parameters that obey the dispersion relation as $()_{\mathbf{k}}$. It is important to characterize the definition of the Fourier transform in this context because it tells us how electromagnetic waves behave. According to the previous definition, if the frequency of these modes is purely real, we obtain modes that propagate and persist throughout the system's evolution. On the other hand, modes with $\gamma_{\mathbf{k}} < 0$ fail to be stable and therefore dissipate rapidly. Additionally, modes with $\gamma_{\mathbf{k}} > 0$ define modes that grow rapidly and destabilize the system. In this work, we aim to study persistent propagating modes over time, so we will consider $w = w_{\mathbf{k}}$ as a purely real quantity.

We have defined the classification of different modes present in the plasma, moreover, both formalisms need certain approximations. In this context, both of them are valid when the plasma is in a quasi-stable regime. To define a quasi-stable region in the parameter space, defined by the $\beta - A$ diagram, we obtained the maximum value of γ ($\gamma_{\text{máx}}$) for every solution of the dispersion relation, which will show us what regions in the parameter space ($\beta - A$ diagram) present plasma instabilities, this region will be shown in the following. Particularly, the parameter $\gamma_{\max}$ is a value obtained from solving the dispersion relation, in this context, it represents instabilities that are normal modes of the system. On the other hand, the fluctuations that emerge in plasma are not normal modes of the system as they appear from the thermal motion of particles, thus, we will refer to the imaginary term of the frequency

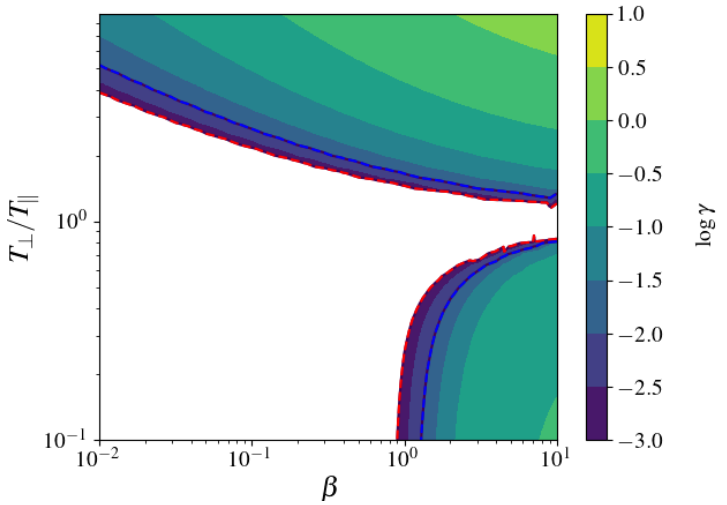

Figure 2.7: Contours of $\gamma_{\max}$, we can see the regions where instabilities are present (colored) and what regions present quasi-stability (white). The dotted red line indicates the contour for $\gamma_{\max} = 10^{-3}$ and the dotted blue line indicated the contour for $\gamma_{\max} = 10^{-2}$.

of these thermally induced electromagnetic fluctuations as γ.

Specifically, Figure 2.7 shows the regions in which the system presents quasi-stable states, or there is an absence of plasma instabilities, shown in white. The areas with values of $\gamma_{\max} > 10^{-3}$, threshold shown in dotted red line, present plasma instabilities, indicating that the system may not be marginally stable or quasi-stable. Observations of the solar wind at 1 AU exhibit a threshold value of $\gamma_{\max}$ close to this value. In other words, regions in which $\gamma_{\max} \sim 10^{-3}$ show that the system seems to evolve into a quasi-equilibrium asymptotic state without changing their β or A parameters, meaning that we encounter a dynamical equilibrium on the system. On the contrary, regions with $\gamma_{\max} > 10^{-3}$ show that the system indeed changes its β or A parameters, presumably evolving to the quasi-stable region where it stops

evolving, showing a more dynamic evolution of the system, as suggested by hybrid simulations Navarro et al. (2014).

2.7.2 Fluctuation Theories

Both proposed theories consider small fluctuations around a quasi-equilibrium state of a spatially uniform and stationary plasma. We propose that the observed fluctuations in the plasma are thermally induced electromagnetic fluctuations. It is theorized that nonlinear interactions drive the plasma towards a quasi-equilibrium state through a process often described as turbulent relaxation. However, these interactions are beyond our consideration, as we will only analyze fluctuations considering that the plasma is already in this quasi-stable state.

To analyze the aforementioned fluctuation spectrum, we will first describe the methodology shown in Navarro et al. (2014). We know that in many cases, spontaneous fluctuations can be described as a response to external linear perturbations from a stationary state, mediated by the Fluctuation-Dissipation theorem. According to this theorem, spontaneous fluctuations arise from the thermal movement of particles and are completely determined by the macroscopic properties of the plasma and the velocity distribution functions (VDFs) of the particles present in the plasma. We can relate this response to its macroscopic properties, particularly its temperature Callen and Welton (1951). To ensure that fluctuation correlations exist in different temporal states of the plasma, the Fluctuation-Dissipation theorem is only valid in the quasi-stable states of the plasma. Therefore, this theorem is applicable within the context of the present work.

On the other hand, using the formalism shown in Schlickeiser et al. (2015), we will address the spectrum of electromagnetic fluctuations from the set of Klimontovich-Maxwell equations. This derivation of the spectrum will be applicable to both non-collective fluctuations and collective modes (with dispersion relation $\omega(\mathbf{k})$) in magnetized plasmas, where the former refers to modes considering spontaneous emissions and the latter refers to modes that obey the dispersion relation, i.e., are normal modes of the system ($\Lambda_{\pm}(\omega(\mathbf{k}), \mathbf{k}) = 0$). Furthermore, the expression derived for the spectrum of electromagnetic fluctuations in Schlickeiser et al. (2015) is valid for plasmas with arbitrary composition and unspecified orientation of the wave vector with respect to a background magnetic field. We will apply this spectrum specifically to the case of a quasi-stable electron-proton plasma, using a bi-Maxwellian plasma distribution and waves propagating parallel to the background magnetic field $\mathbf{B}_0$, in conditions similar to the solar wind.

2.8 Methodology

To obtain an expression of the form $w(\mathbf{k})$ and therefore the normal modes of the system, one needs to solve the dispersion relation in Equation (2.21). Particularly, solving the dispersion relation in Equation (2.21) is solving its real and imaginary parts separately, its solutions must obey both of the following conditions,

$$\mathrm{Re}(\Lambda_{\pm}(w,\mathbf{k})) = 0 \qquad , \qquad \mathrm{Im}(\Lambda_{\pm}(w,\mathbf{k})) = 0\,.$$

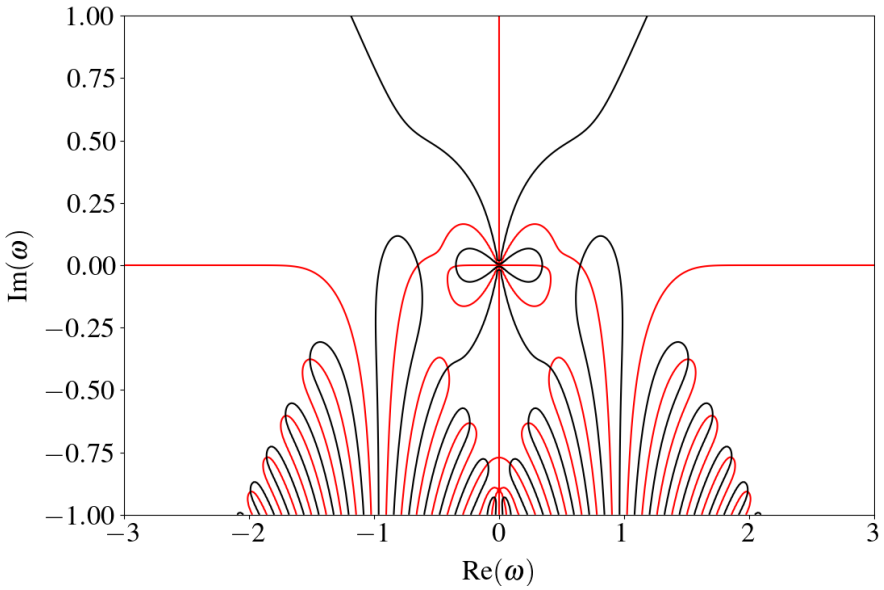

Figure 2.8: Diagram of curve levels for the real part (black) and imaginary part (red) of transversal waves $\Lambda_{-}\Lambda_{+} = 0$, using a fixed value of wavenumber $\mathbf{k} = k\hat{z}$ for an electron-proton bi-Maxwellian plasma. The solutions of the dispersion relation are the points where both curves meet.

In Figure 2.8 we show the curve levels for the real and imaginary parts of $\Lambda_{-}(k,w)\Lambda_{+}(k,w) = 0$ as function of $\mathrm{Re}(w)$ and $\mathrm{Im}(w)$ for a fixed value of wavenumber $\mathbf{k} = k\hat{z}$. To obey both conditions showed above, a solution of the dispersion

relation is the point where both curves meet. This figure is symmetric along the vertical axis $\mathrm{Re}(w) = 0$.

To obtain the normal modes we implemented a root finding method, the Secant method. This is a numerical technique to find roots of a real valued function. With this, we ensure that we will find a root of Equation (2.21). This iterative method approximates the root by successively improving the approximation through linear interpolation. The method starts with two initial guesses x_0 and x_1 such that $f(x_0)$ and $f(x_1)$ have opposite signs, indicating a root between them. At each iteration, a new approximation x_{n+1} is calculated using a linear interpolation formula. The iteration continues until either a sufficiently accurate solution is obtained or a maximum number of iterations is reached. Unlike Newton's method, the secant method does not require the computation of derivatives, making it useful when derivatives are difficult to compute, which is the case since we are calculating the roots in Equation (2.21), as seen from this expression, we are dealing with complex integrals so the Secant method is appropriate in this case. However, it may converge slower and fail to converge under certain conditions, such as functions with inflection points or poor behavior between initial guesses. In this case, initial guesses are important and since we need to calculate the entire mode of propagation, these initial guesses are used as seeds to find other roots of the dispersion relation and find the normal modes of the system completely.

As mentioned before, roots in the dispersion relation in Equation (2.21) are close together, to construct the entire normal mode, one uses a first guess and the following solution is found using the first solution as seed. With this, one searches for the next

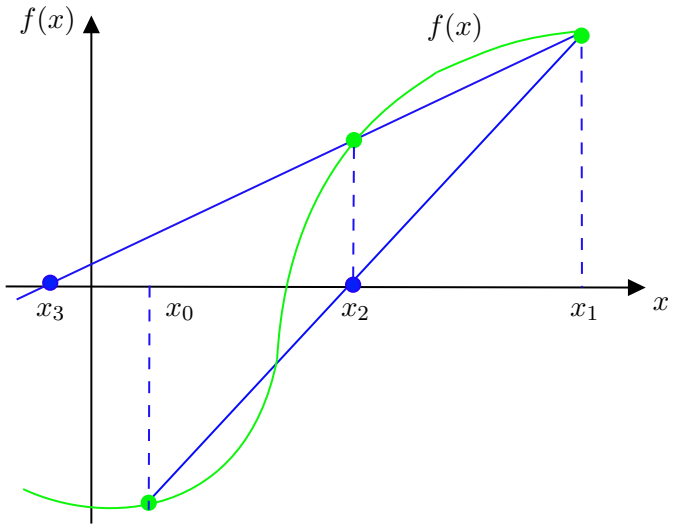

Figure 2.9: Representation of linear interpolation used in the Secant method to find a solution $f(x) = 0$. Two seeds are chosen x_0 and x_1 such that $f(x_0)$ and $f(x_1)$ have opposite signs. At each iteration, a new approximation x_{n+1} is calculated using a linear interpolation formula

solution in the nearby points of the already found seed, and continue this process until the complete mode is obtained. Indeed, we can repeat this process to find a solution $w(\mathbf{k})$ for other values of $\mathbf{k}$ and for other points where both curves meet to find every solution of the dispersion relation for every value of $\mathbf{k}$

This will allow us to obtain the solutions shown in Figures 2.5 and 2.6.

There are multiple solutions one can find, in this case, there were 500 seeds generated in a section of the complex plane, the ones with higher $\gamma_{\mathbf{k}}$ were used as seeds to find the related normal modes. As shown in Figures 2.5 and 2.6, the second panels represent the imaginary part of frequency $\gamma_{\mathbf{k}}$, which tells us if there are instabilities in the plasma if for some value of ck/w_{pp} this parameter is positive. The maximum of these values was chose to construct the contours of $\gamma_{\max}$ for every value of β and

A, as shown in Figure 2.7.

With this we have defined the region we are interested in, now we analyze the expressions derived for the magnetic spectrum of fluctuations. Here, we are interested in thermally induced electromagnetic fluctuations and not normal modes of the system, meaning we do not need a root-finding method. To calculate the spectral index that arises from the magnetic spectrum, we integrate the curves of the magnetic field fluctuations in terms of ck/w_{pp} with the adaptive Simpson method of integration. This was done for different values of w/Ω_p for every curve in terms of ck/w_{pp}, in logarithmic scale. The adaptive Simpson method is a numerical technique for approximating definite integrals with improved accuracy and efficiency. Unlike standard Simpson's rule, which divides the integration interval into equal subintervals, the adaptive Simpson's method dynamically adjusts the subinterval widths to achieve better results. It begins by applying Simpson's rule to each subinterval and estimating the error in the integral approximation as shown in Figure 2.10. If the estimated error exceeds a predefined tolerance level, the method subdivides the interval into smaller subintervals and re-applies Simpson's rule, focusing computational effort where it is most needed. The process continues until the estimated error falls below the specified tolerance level. Since these curves vary in starting and ending points of integration, an initial guess is used giving higher accuracy than non-adaptive methods.

The adaptive Simpson's method involves recursively applying Simpson's rule to

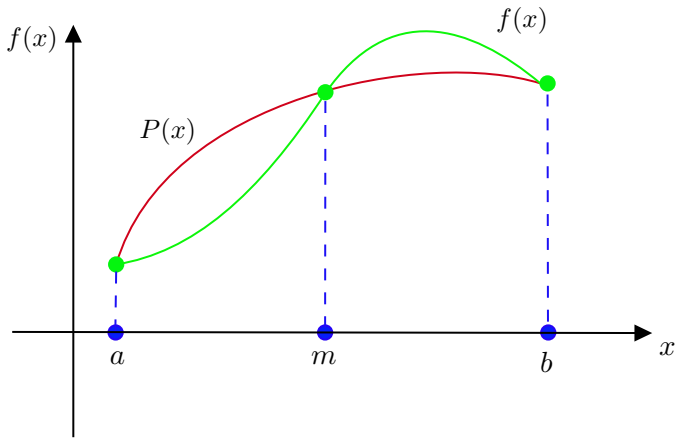

Figure 2.10: Simpson's rule derived by approximating the integrand $f(x)$ by a quadratic interpolant $P(x)$ over a subinterval $[a, b]$.

subintervals until a desired level of accuracy is achieved. Simpson's rule approximates the integral of a function $f(x)$ over a subinterval $[a, b]$ as,

$$\int_a^b f(x)\,dx \approx \frac{b-a}{6}\left[f(a) + 4f\left(\frac{a+b}{2}\right) + f(b)\right].$$

The error in this approximation can be estimated using Richardson extrapolation. This adaptive method involves comparing the error estimate with a predefined tolerance. If the error estimated is higher than the tolerance, the interval is subdivided into smaller subintervals, and Simpson's rule is re-applied recursively. Finally, the results from all subintervals are combined to obtain the final approximation of the integral.

With this, we will see that we can obtain the curves for the magnetic spectrum integrated over ck/w_{pp} in terms of w/Ω_p. These curves seem to display a power-law like behavior such that,

$$\frac{n\Omega\langle|B_\pm(w)|^2\rangle}{B_0^2} = \int_{-\infty}^{\infty} \frac{n\Omega\langle|B_\pm(w,k)|^2\rangle}{B_0^2}\,dk \sim \left(\frac{w}{\Omega_p}\right)^{-\alpha} = x^{-\alpha}. \tag{2.23}$$

We can calculate the exponent of such power-law observing the curves of both magnetic spectrums integrated over wavenumber in logarithmic scale, and performing a linear regression. This parameter α, the slope of the linear regression, is the spectral index of magnetic fluctuations. This index is related to measurements that analyze energy cascade between scales of the energy spectrum Podesta et al. (2007, 2006); Kiyani et al. (2015). We look for a power-law spectrum since it can suggest that we are dealing with a problem that presents scale invariance, meaning that, we can use the same description to explain a phenomena at different scales. Our objective is to calculate this index for every value of the $\beta - \mathrm{A}$ diagram. In what follows we will derive analytically the expressions of the spectral distribution of electromagnetic fluctuations in plasma, for both approaches mentioned before, electromagnetic fluctuation spectrum from Fluctuation-Dissipation theorem and from the Klimontovich-Maxwell set of equations.

2.9 Results

2.9.1 Electromagnetic Fluctuations from Fluctuation Dissipation Theorem

In the quasi-stability states of the solar wind there are electromagnetic fluctuations present, which are not predicted by linear kinetic theory. These fluctuations may be related to spontaneous electromagnetic fluctuations arising from discreteness and thermal motion of charged particles. These fluctuations are dynamic and can occur at different scales both spatially and temporally. To understand and model these plasma fluctuations, we can apply the Fluctuation-Dissipation theorem from statistical physics, which provides a framework for linking the thermal fluctuations in the plasma to its dissipative properties and equilibrium behavior in response to external linear perturbations. This theorem is well explained in Callen and Welton (1951). We can understand this dynamics by considering a description of a response to linear perturbations from a quasi-equilibrium state, even though LTE is not usually ensured, in most cases, we can describe the system using this approach. Meaning that, we can obtain information of the system's response to an external perturbation through the system's fluctuations or correlations, in the absence of instabilities.

We explain the procedure to obtain the general expression of the electromagnetic fluctuation spectra as it was showed in Navarro et al. (2014). The spectral distribution of electric field fluctuations in homogeneous, magnetized plasma could be written (see Sitenko (2012)) in terms of the Fluctuation-Dissipation theorem as follows,

$$\langle E_i(\mathbf{k}, w) E_j(\mathbf{k}, w) \rangle = 4\pi i \frac{k_B T}{w} \left(\Lambda_{ji}^{-1} - \Lambda_{ij}^{-1*} \right) ,$$

where T is the plasma temperature and Λ_{ij}^{-1} is the inverse of the dispersion tensor, and k_B is the Boltzmann constant. Using the Maxwell-Faraday equation, the magnetic field fluctuations can be written as,

$$\langle B_i(\mathbf{k},w)B_j^*(\mathbf{k},w)\rangle = \frac{c^2}{|w|^2}\epsilon_{iab}\epsilon_{jcd}k_a k_c \langle E_b(\mathbf{k},w)E_d^*(\mathbf{k},w)\rangle \,.$$

Therefore, the spectral distribution of transverse electromagnetic fluctuations as shown in Navarro et al. (2014) are,

$$\begin{aligned}
\langle |E_\pm|^2\rangle &= \frac{1}{w}\frac{\beta B_0^2 T_\perp}{nT_\parallel}\frac{1}{\Lambda_\pm^{(0)}}\mathrm{Im}\left(1-\frac{\Lambda_\pm^{(0)}}{\Lambda_\pm}\right) \,, \\
\frac{n\Omega}{B_0^2}\langle |B_\pm|^2\rangle &= -\beta A\,\frac{c^2k^2\Omega}{|w|^2\mathrm{Re}(w)}\mathrm{Im}\left(\frac{1}{\Lambda_\pm}\right) \,,
\end{aligned}$$

and written in terms of the normalization used to obtain the final dispersion relations, the magnetic fluctuation spectrum is,

$$\frac{n\Omega}{B_0^2}\langle |B_\pm|^2\rangle = -\beta A\,\frac{c^2}{v_{ap}^2}\frac{y^2}{|x|^2\mathrm{Re}(x)}\mathrm{Im}\left(\frac{1}{\Lambda_\pm}\right) \,.$$

The longitudinal magnetic fluctuations are identically zero for parallel propagation. This expression can be evaluated as long as $\Lambda_\pm \neq 0$ since it is singular for those values, and is valid only when wave instabilities are not present, meaning we need to situate our system in a quasi-equilibrium state. If we only analyze plasmas with stable modes that persist throughout the system's dynamics, we can consider that γ, the imaginary part of the frequency linked to instabilities in the plasma, is close to zero ($\gamma \sim 0$), therefore the expression takes the form,

$$\frac{n\Omega}{B_0^2}\langle |B_\pm|^2\rangle = -\beta A\,\frac{c^2}{v_{ap}^2}\frac{y^2}{x^3}\mathrm{Im}\left(\frac{1}{\Lambda_\pm}\right) \,. \tag{2.24}$$

This equation does not guarantee that the spectral distribution of transverse magnetic field fluctuations remains positive for every value of A, the final version is discussed in the next section, this is fixed considering that the inverse Laplace transform requires that all poles be on one side of the curve to guarantee convergence. The equation that does preserve a positive spectrum of magnetic fluctuations is,

$$\frac{n\Omega}{B_0^2}\langle|B_\pm|^2\rangle = -\beta A\,\frac{c^2}{v_{ap}^2}\,\frac{y^2}{x^2(x-x_0)}\,\mathrm{Im}\left(\frac{1}{\Lambda_\pm}\right)\,, \tag{2.25}$$

where x_0 is the value in which the imaginary term of the dispersion relation ($\mathrm{Im}(\Lambda_\pm)$) becomes zero, which can be calculated analytically. From Equation (2.25), we calculate the spectral index of electromagnetic fluctuations. The aforementioned index is analyzed to characterize the power-law that emerges from the magnetic energy spectrum.

Since a part of this work is based on the work done in Navarro et al. (2014), our first step was recreate Fig 1(a) and Fig 1(b) of the aforementioned work. In this context, in Figure 2.11 we show in logarithmic color scale Equation (2.25) for $\beta = 0.6$ and $A = T_\perp/T_\parallel = 1.4$. In Figure 2.12 we show in logarithmic color scale Equation (2.25) for $\beta = 0.6$ and $A = T_\perp/T_\parallel = 0.1$. In both figures we can observe that there is an enhancement of electromagnetic fluctuations along the normal modes of the system, furthermore in Figure 2.11 an ion-cyclotron instability is present and in Figure 2.12 a firehose instability is present. The electromagnetic fluctuations are fixed along the unstable modes. As mentioned before, electromagnetic fluctuations are present even when considering a quasi-stable plasma, and fill a relevant part

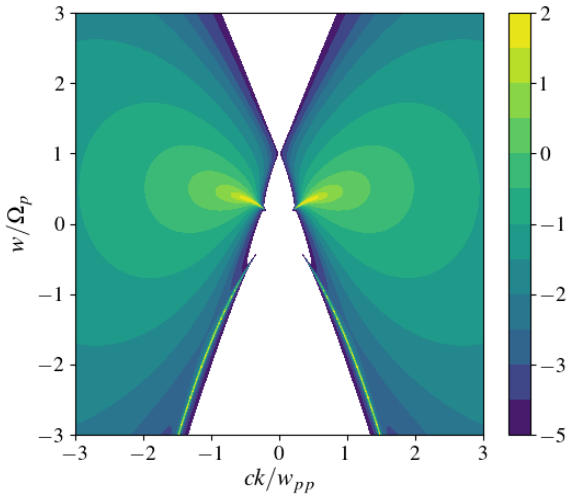

Figure 2.11: Magnetic field fluctuations $n\Omega\langle|B_-|^2\rangle/B_0^2$, in color logarithmic scale, calculated using Equation (2.25) for $v_A/c = 10^{-4}, \beta = 0.6, A = 1.4$.

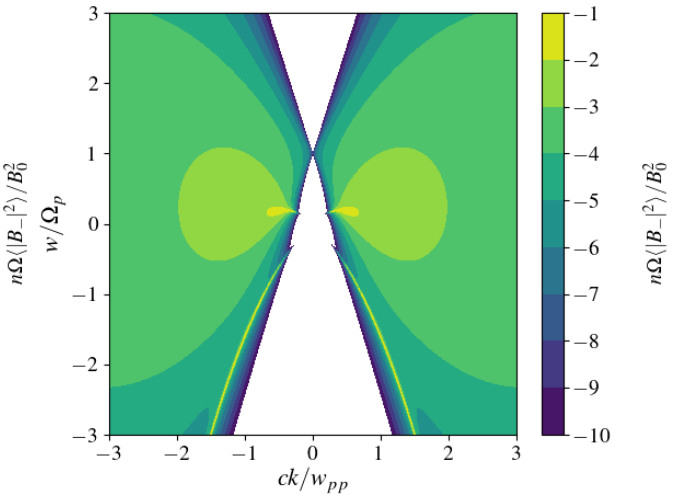

Figure 2.12: Magnetic field fluctuations $n\Omega\langle|B_-|^2\rangle/B_0^2$, in color logarithmic scale, calculated using Equation (2.25) for $v_A/c = 10^{-4}, \beta = 0.6, A = 0.1$.

of the Fourier spectrum which can be seen in 2.11 and 2.12. This results, which are an adaptation from Navarro et al. (2014), are important since they agree with the observations measured by Bale et al. (2009), where the magnitude of magnetic fluctuations are enhanced along unstable modes.

Now, to calculate the spectral index of electromagnetic fluctuations, in Figure 2.13 we plot Equation (2.25) in terms of ck/w_{pp} for negative helicity using $\beta = 0.6$ and $A = 1.4$ for some values of w/Ω_p. In Figure 2.14 we plot Equation (2.25) in terms of ck/w_{pp} for negative helicity using $\beta = 0.6$ and $A = 1.4$ for some smaller values of w/Ω_p. Note that magnetic fluctuations are greater for smaller values of w/Ω_p, this can be seen from Figure 2.11, where we plot for the same values of $\beta - A$ since magnetic

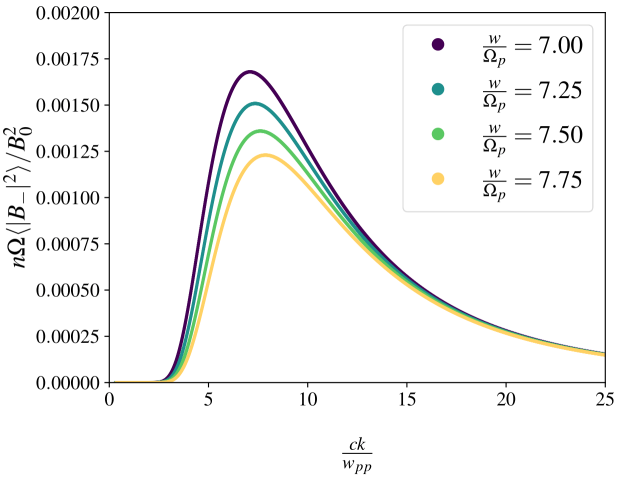

Figure 2.13: Magnetic field fluctuations $n\Omega\langle|B_-|^2\rangle/B_0^2$, in terms of ck/w_{pp}, for negative helicity, calculated using Equation (2.25) for $v_A/c = 10^{-4}, \beta = 0.6, A = 1.4$, and values of $ck/w_{pp} \sim 7$.

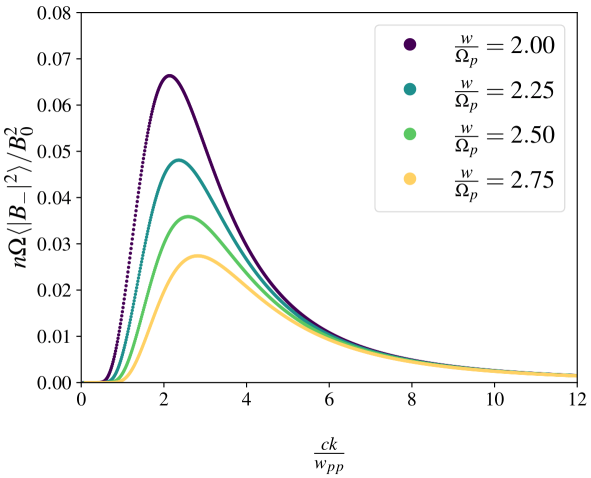

Figure 2.14: Magnetic field fluctuations $n\Omega\langle|B_-|^2\rangle/B_0^2$, in terms of ck/w_{pp}, for negative helicity, calculated using Equation (2.25) for $v_A/c = 10^{-4}, \beta = 0.6, A = 1.4$, and values of $ck/w_{pp} \sim 2$.

fluctuations are enhanced along the normal modes of the system which are closer to lower values of w/Ω_p. Moreover, note that for the plots with negative helicity, the normal modes are not shown (in this case, the ion-cyclotron instability) since we are plotting for frequency values above them. On the other hand, if we were to plot Equation (2.25) in terms of ck/w_{pp} for positive helicity we would encounter normal modes, since as mentioned before, the spectrum of electromagnetic fluctuations in Fourier space is symmetric along w/Ω_p. Although we are not interested in the role that these modes play in the spectrum of electromagnetic fluctuations, since these are normal modes of the system, therefore they do not contribute when analyzing thermally induced electromagnetic fluctuations.

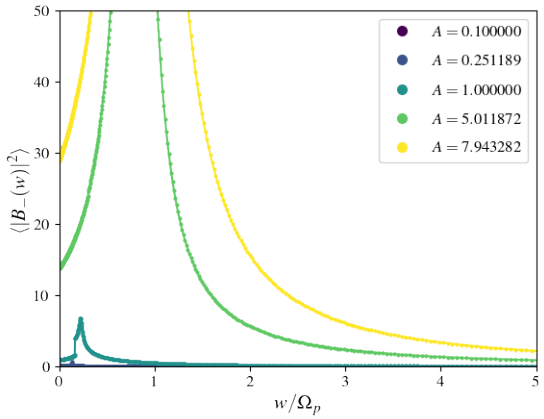

Figure 2.15: Magnetic field fluctuations $n\Omega\langle|B_-|^2\rangle/B_0^2$ integrated over ck/w_{pp}, in terms of w/Ω_p, for negative helicity, calculated using Equation (2.25) for $v_A/c = 10^{-4}, \beta = 1$.

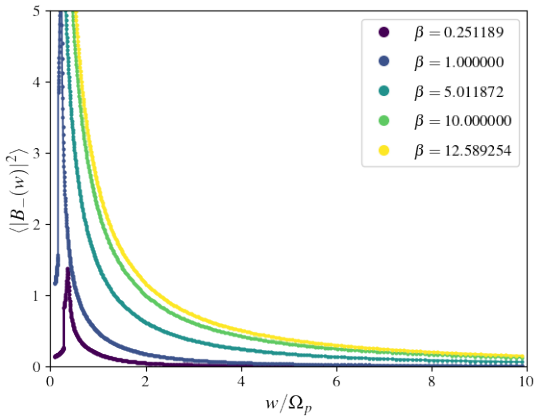

Figure 2.16: Magnetic field fluctuations $n\Omega\langle|B_-(w)|^2\rangle/B_0^2$ integrated over ck/w_{pp}, in terms of w/Ω_p, for negative helicity, calculated using Equation (2.25) for $v_A/c = 10^{-4}, A = 1$.

When integrating magnetic field fluctuations over ck/w_{pp}, for example integrating the curves shown in Figures 2.13 and 2.14 over ck/w_{pp} for every value of w/Ω_p, we obtain curves that can be represented by a power-law. Specifically, Figure 2.15 shows magnetic field fluctuations ($n\Omega\langle|B_-|^2\rangle/B_0^2$) integrated over ck/w_{pp} in terms of w/Ω_p for negative helicity from Equation (2.25) for fixed $\beta = 1$ and several values of A. On the other hand Figure 2.16 shows the same magnetic field fluctuations ($n\Omega\langle|B_-|^2\rangle/B_0^2$) integrated over ck/w_{pp} in terms of w/Ω_p for negative helicity from Equation (2.25), but now, for fixed $A = 1$ and several values of β. In this case, the right side of these curves can be represented by functions of the form $x^{-\alpha}$, to analyze this behavior, in the following we will observe this power-law like behavior in logarithmic scale.

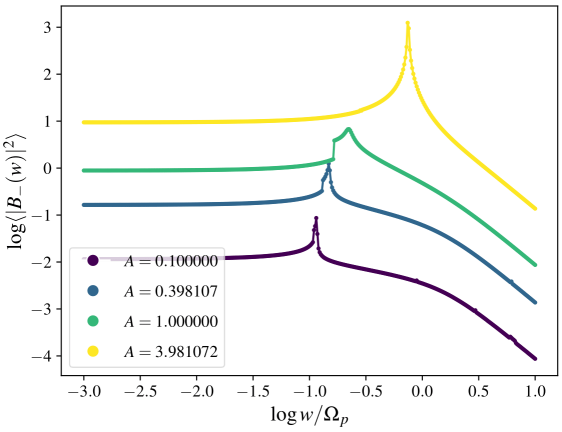

Figure 2.17: Magnetic field fluctuations $n\Omega\langle|B_-|^2\rangle/B_0^2$ integrated over ck/w_{pp}, in terms of w/Ω_p, for negative helicity, in logarithmic scale, calculated using Equation (2.25) for $v_A/c = 10^{-4}, \beta = 1$.

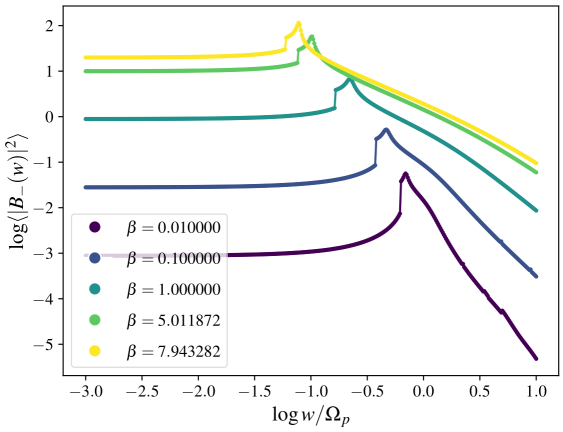

Figure 2.18: Magnetic field fluctuations $n\Omega\langle|B_-|^2\rangle/B_0^2$ integrated over ck/w_{pp}, in terms of w/Ω_p, for negative helicity, in logarithmic scale, calculated using Equation (2.25) for $v_A/c = 10^{-4}, A = 1$.

In Figures 2.17 and 2.18 we plot magnetic field fluctuations from Equation (2.25) integrated over ck/w_{pp}, in terms of w/Ω_p, for negative helicity as before, but now in logarithmic scale. In Figure 2.17 we plot for several values of A and a fixed value of $\beta = 1$, and for Figure 2.18 we plot for several values of β and a fixed value of $A = 1$. In this case, we can see the change of scale around the peaks that appear in both figures, to the right of those peaks we can see the trends of the kinetic scale or dissipation range. To calculate the index of electromagnetic fluctuations we perform a linear regression for values within the kinetic scale, from $\log w/\Omega_p = 0.5$ to $\log w/\Omega_p = 1$.

In Figure 2.19 we plot the spectral index of electromagnetic fluctuations bounded by the quasi-stability regions in the $\beta - A$ diagram using Equation (2.25) for negative

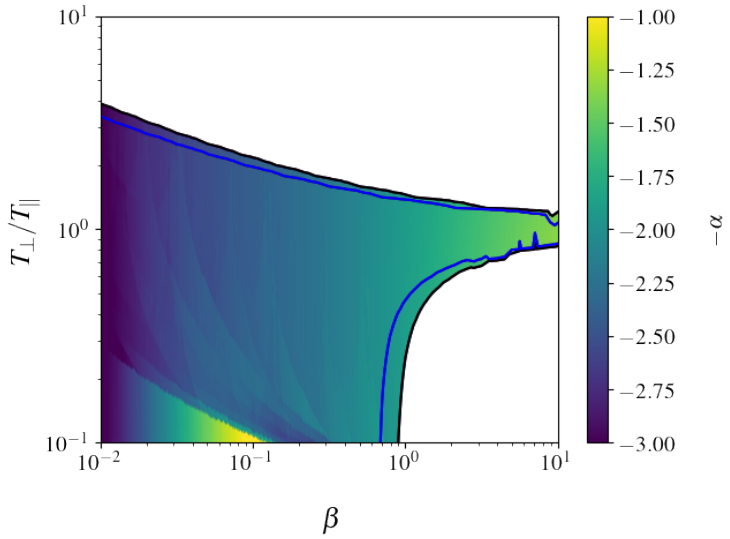

Figure 2.19: Spectral index of electromagnetic fluctuations in the quasi-stability regions in the $\beta - A$ diagram using Equation (2.25), in color logarithmic scale for negative helicity. The black lines represents the $\gamma_{\mathbf{k}}$ threshold of 10^{-3} and the blue lines represents the $\gamma_{\mathbf{k}}$ threshold of 10^{-4}.

helicity. The black lines represents the $\gamma_{\mathbf{k}}$ threshold of 10^{-3} (it is noteworthy that this parameter is the imaginary part of the frequency which is also a solution of the dispersion relation) and the blue lines represents the $\gamma_{\mathbf{k}}$ threshold of 10^{-4}. The spectral index is greater for lower values of β and does not seem to change significantly for different values of A. For each slope the coefficient of determination R^2, which for negative helicity has values of $R^2 \geq 0.9$, except for some data of lower β and A values.

In Figure 2.20, we plot the variation of the spectral index in terms of $\beta - A$ parameters. On the left panel we show the variation of the spectral index in terms of β, and we can see that this index decreases while increasing β. On the right panel we show the variation of the spectral index in terms of A, we do not observe significant changes of this index while increasing A. This can also be seen in Figure 2.19. The

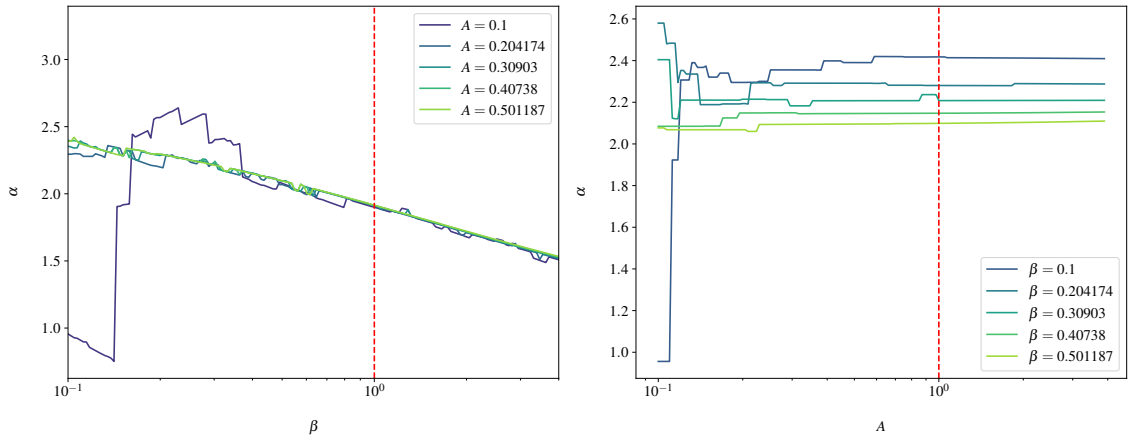

Figure 2.20: On the left panel we show the variation of the spectral index in terms of β. On the right panel we show the variation of the spectral index in terms of A. The dotted red line represents the region where for the shown values we ensure quasi-stability.

region to the left of the dotted red line represents where, for the shown values, we ensure quasi-stability approximately since we are taking the lines across $\beta = 1$ and $A = 1$, as we can see in Figure 2.20, this region belongs to the quasi-stability region but it is not the entire domain but rather cuts along the parameter space.

2.9.2 Electromagnetic Fluctuations from Klimontovich Maxwell

In this section we develop the spectrum of electromagnetic fluctuations for magnetized quasi-stable electron-proton plasma with conditions similar to the solar wind, and wave vector parallel to the background magnetic field. Using the system of the Klimontovich and Maxwell equations we derive the general fluctuation theory for magnetized plasma as developed in Schlickeiser et al. (2015). This theory expanded the results obtained for the general fluctuation theory for unmagnetized plasma by Schlickeiser and Yoon (2012). The general fluctuation spectra obtained holds for plasmas of arbitrary composition and orientation of wave vector, it also applies to both collective and non-collective modes, but we restrict ourselves to analyze the latter since we are interested in spontaneously emitted electric field fluctuations. This approach assumes small amplitude fluctuations, but it still represents a nonlinear response of the plasma. However, these nonlinear interactions could become of large amplitudes which evolve only after the system has gone through a phase of small fluctuations, and when the systems has acquired an external source of free energy. So it is primarily important to develop a small amplitude fluctuating theory first.

The fluctuating electric fields in magnetized plasma consisting of different species with gyrotropic distribution obey the wave equation,

$$\Lambda_{ij}^{+}(\mathbf{k}, w) E_j(\mathbf{k}, w) = E_i^0(\mathbf{k}, w)\,, \tag{2.26}$$

with $\Lambda_{ij}^{+}(\mathbf{k}, w)$ the Maxwell operator to be discussed in the following, and the electric field perturbations caused by uncorrelated single source particles in the plasma,

$$E_i^0(\mathbf{k}, w) = -\frac{4\pi i}{w} \sum_{\alpha} e_\alpha \int d^3p\, v_i\, N_\alpha^0(\mathbf{k}, w, \mathbf{p})\,.$$

It is supposed that any temporal variation of the electromagnetic fields is weakly adiabatic. In Schlickeiser and Yoon (2015) the Maxwell operator is defined as the dispersion tensor for oblique propagation, in this case $\Lambda_{ij}^{+}(\mathbf{k}, w)$ represents the dispersion tensor of Equation (2.22) for parallel propagation obtained in the previous Chapter. From Equation (2.26) we obtain the electric field fluctuation spectra correlated to the perturbations of the system,

$$\langle E_i(\mathbf{k}, w) E_j^*(\mathbf{k}, w)\rangle = \Lambda_{im}^{-1}(\mathbf{k}, w)\Lambda_{jn}^{*-1}(\mathbf{k}, w)\langle E_m^0(\mathbf{k}, w) E_n^{0*}(\mathbf{k}, w)\rangle \,, \tag{2.27}$$

where $\Lambda_{ij}(\mathbf{k}, w)$ is the dispersion tensor defined in Equation (2.22). The latter expression is written in terms of electric single-particle fluctuations,

$$\begin{aligned}(2\pi)^4\langle E_m^0(\mathbf{k}, w) E_n^{0*}(\mathbf{k}, w)\rangle \quad &= \quad (4\pi)^2 \mathrm{Re}\sum_a\sum_b \frac{e_a e_b}{|w|^2}\int d^3p\, d^3p'\, v_m v_n' \\ &\times \quad (2\pi)^4\langle N_a^0(\mathbf{k}, w, \mathbf{p}) N_b^{0*}(\mathbf{k}, w, \mathbf{p})\rangle \,. \end{aligned} \tag{2.28}$$

This term that comes from Maxwell's equations is the averaged correlation that comes from charge and current densities external to the system, related to the initial conditions of the system. Since applying the Fourier-Laplace transform introduces terms related to the system's initial conditions. Here

$$\begin{aligned}\langle N_a^0(\mathbf{k}, w, \mathbf{p}) N_b^{0*}(\mathbf{k}, w, \mathbf{p})\rangle \quad &= \quad \frac{1}{(2\pi)^4}\int d^3(\mathbf{x} - \mathbf{x}')\exp(-i\mathbf{k}\cdot(\mathbf{x} - \mathbf{x}') + iw\tau) \\ &\times \quad \delta_{\alpha\beta} n_\alpha f_\alpha(p_\perp, p_\parallel)\delta(\mathbf{x} - \mathbf{x}')\delta(\mathbf{v} - \mathbf{v}')\int d\tau \,, \end{aligned} \tag{2.29}$$

where $\tau = t - t'$ and the latter equation is the Fourier transform of,

$$\langle N_\alpha^0 N_\beta^{0*}\rangle = \delta_{\alpha\beta} n_\alpha f_\alpha(p_\perp, p_\parallel)\delta(\mathbf{x}(t - t') - \mathbf{x}')\delta(\mathbf{v}(t - t') - \mathbf{v}') \,. \tag{2.30}$$

This expression describes the spatio-temporal correlation of uncorrelated particles in a uniform magnetic field B_0. It defines the correlation of the Klimontovich distribution function for stationary and homogeneous fluctuations, which consider interactions of nearby uncorrelated particles. Particularly, γ must be large enough such that the Laplace transform in (2.29) can converge in the limit $\tau = (t-t') \to \infty$. Indeed, since we are considering plasmas without instabilities ($\gamma = 0$) or analogously, considering stable plasma waves, this condition cannot be satisfied. Particularly, we will consider that $w = w_r + i\epsilon$, where $\epsilon \ll 1$, and we will discuss this choice when solving the following integrals.

In the context of parallel propagation we use, $\mathbf{k}\cdot(\mathbf{x}-\mathbf{x}') = k_\parallel v_\parallel \tau$, then the spatial integral results in,

$$\langle N^0_\alpha N^{0*}_\beta \rangle = \sum_{\alpha\beta} \frac{\delta_{\alpha\beta} n_\alpha}{(2\pi)^4} \int d\tau \exp(i\tau(w - k_\parallel v_\parallel)) f_\alpha(p_\perp, p_\parallel) \delta(\mathbf{v} - \mathbf{v}') \,.$$

We may insert this equation intro Equation (2.28) to obtain the general expression for the electric single-particle fluctuation,

$$\begin{aligned} (2\pi)^4 \langle E^0_m E^{0*}_n \rangle &= (4\pi)^2 \mathrm{Re} \sum_\alpha \frac{e^2_\alpha n^2_\alpha}{|w|^2} \int d^3p \int d^3p' v_m v'_n \langle N^0_\alpha N^{0*}_\beta \rangle \,, \qquad (2.31) \\ &= 4\pi \mathrm{Re} \sum_\alpha \frac{w^2_{p\alpha} m_\alpha}{|w|^2} \int_{-\infty}^{\infty} dp_\parallel \int_0^\infty dp_\perp p_\perp f_\alpha(p_\perp, p_\parallel) I_{mn} \,, \end{aligned}$$

where we have defined,

$$I_{mn} = \int_0^\infty d\tau \int_0^{2\pi} d\phi v_m \, v_n(\tau) \exp(i\tau(w - k_\parallel v_\parallel)) \,. \qquad (2.32)$$

Here the velocities of the particles as explained in the Appendix are,

$$v_n(\tau) = \begin{pmatrix} v_\perp \cos(\phi - \Omega_\alpha \tau) \\ v_\perp \sin(\phi - \Omega_\alpha \tau) \\ v_\parallel \end{pmatrix} \,,$$

and,

$$v_m = (v_\perp \cos\phi, v_\perp \sin\phi, v_\parallel)\,.$$

From these definitions, we can obtain a general expression for parallel propagation independent of the choice of the velocity distribution function. To achieve this, we can solve the temporal integral of expression (2.32), which results in,

$$\Xi_n = \int_0^\infty d\tau v_n(\tau) \exp i(w - k_\parallel v_\parallel)\tau = \left(i\frac{v_\perp}{2}\xi_+, \frac{v_\perp}{2}\xi_-, \frac{iv_\parallel}{w - k_\parallel v_\parallel} \right)^T$$

where,

$$\xi_\pm = \frac{e^{i\phi}}{w_-} \pm \frac{e^{-i\phi}}{w_+},$$

and we used $w_\pm = w - k_\parallel v_\parallel \pm \Omega_\alpha$, as defined in the previous Chapter. Now, to completely solve the integrals shown in Equation (2.32) we must solve the angular part, considering a gyrotropic velocity distribution function we obtain

$$\begin{aligned}(2\pi)^4 \langle E_m^0(\mathbf{k}, w) E_n^{0*}(\mathbf{k}, w)\rangle &= 4\pi \mathrm{Re} \sum_\alpha \frac{w_{p\alpha}^2 m_\alpha}{|w|^2} \int_0^{2\pi} d\phi \int_{-\infty}^{\infty} dp_\parallel \\ &\quad \times \int_0^\infty dp_\perp p_\perp f_\alpha(p_\perp, p_\parallel)\, v_m \cdot \Xi_n\,, \qquad (2.33) \\ &= 4\pi \mathrm{Re} \sum_\alpha \frac{w_{p\alpha}^2 m_\alpha}{|w|^2} \int_{-\infty}^{\infty} dp_\parallel \int_0^\infty dp_\perp p_\perp f_\alpha(p_\perp, p_\parallel)\, \varsigma_{mn}\,,\end{aligned}$$

where we have defined,

$$\varsigma_{mn} = \begin{pmatrix} \frac{i\pi v_\perp^2}{2}\eta_+ & \frac{\pi v_\perp^2}{2}\eta_- & 0 \\ -\frac{\pi v_\perp^2}{2}\eta_- & \frac{i\pi v_\perp^2}{2}\eta_+ & 0 \\ 0 & 0 & \frac{2\pi i v_\parallel^2}{w - k_\parallel v_\parallel} \end{pmatrix}, \qquad (2.34)$$

and,

$$\eta_{\pm} = \frac{1}{w_+} \pm \frac{1}{w_-}.$$

Equation (2.33) is the general expression for electric single-particle fluctuations which is independent of the choice for the VDF. Notice that, due to the form of Equation (2.34), we can analyze transverse and longitudinal electromagnetic fluctuations separately. Therefore, if we aim to study transverse fluctuations, we can use the upper-left block of ς_{mn}, and if we aim to analyze longitudinal fluctuations we may use the lower-right block of ς_{mn}. Particularly, we will study transverse electromagnetic fluctuations and we will keep the notation of ς_{mn} for simplicity. We now introduce the following representation of a bi-Maxwellian velocity distribution function (VDF),

$$f_\alpha(p_\perp, p_\parallel) = \frac{1}{\pi^{3/2}\Theta'^2_{\alpha,\perp}\Theta'_{\alpha,\parallel}} \exp\left(-\frac{p_\perp^2}{\Theta'^2_{\alpha,\perp}} - \frac{p_\parallel^2}{\Theta'^2_{\alpha,\parallel}}\right), \tag{2.35}$$

in this case, α is the particle species, and

$$\Theta'^2_{\alpha,\perp} = 2k_B T_{\alpha,\perp} m_\alpha \quad , \quad \Theta'^2_{\alpha,\parallel} = 2k_B T_{\alpha,\parallel} m_\alpha \,,$$

where m is the mass of the particle, k_B the Boltzmann constant. Using the above definition of VDF in Equation (2.33) and solving the integrals over velocities. We obtain, in the circular polarization basis, for electric single-particle fluctuations,

$$\langle E^0_m(\mathbf{k}, w) E^{0*}_n(\mathbf{k}, w)\rangle \;=\; -2\pi \sum_\alpha \frac{w^2_{p\alpha} m_\alpha}{|w|^2} \left(\frac{\Theta^2_\perp}{\Theta_\parallel k_\parallel}\right) \chi_{mn} \,, \tag{2.36}$$

where

$$\chi_{mn} = \begin{pmatrix} 2\mathrm{Re}(iZ(\zeta_+)) & 0 \\ 0 & 2\mathrm{Re}(iZ(\zeta_-)) \end{pmatrix}. \tag{2.37}$$

Inserting Equation (2.36) in expression (2.27), we find that the spectrum of electric field fluctuations is,

$$\langle |E_{\pm}|^2 \rangle = 2\pi \sum_{\alpha} \frac{w_{p\alpha}^2 m_{\alpha}}{|w|^2} \left(\frac{\Theta_{\perp}^2}{\Theta_{\parallel} k_{\parallel}} \right) \frac{\mathrm{Im}(Z(\zeta_{\pm}))}{|\Lambda_{\pm}|^2}.$$

Then, using the Faraday equation we may obtain the spectrum of magnetic field fluctuations from electric field fluctuations, obtaining,

$$\langle |B_{\pm}|^2 \rangle = 4\pi \sum_{\alpha} \frac{w_{p\alpha}^2 m_{\alpha}}{|w|^4} \left(\frac{k_{\parallel} c^2 \Theta_{\perp}^2}{\Theta_{\parallel}} \right) \frac{\mathrm{Im}(Z(\zeta_{\pm}))}{|\Lambda_{\pm}|^2}.$$

Using the normalization shown in Equation (2.20), and taking the cold plasma approximation for electrons, where $\zeta_{\pm}(e) \to \infty$, then the spectrum of magnetic field fluctuations is,

$$\frac{n\Omega}{B_0^2} \langle |B_{\pm}|^2 \rangle = A\sqrt{\beta} \frac{y}{|x|^4} \frac{c^4}{v_{ap}^4} \frac{\mathrm{Im}(Z(\zeta_{\pm}))}{|\Lambda_{\pm}|^2}. \tag{2.38}$$

The longitudinal magnetic fluctuations are identically zero for parallel propagation. This expression can be evaluated as long as $\Lambda_{\pm} \neq 0$ since this expression is singular for those values, and is valid only when wave instabilities are not present, meaning we need to situate our system in a quasi-equilibrium state. If we only analyze plasmas with stable modes that persist throughout the system's dynamics, we can consider $\gamma \sim 0$. From Equation (2.38), we calculate the spectral index of electromagnetic fluctuations. Note that this Equation produces a fluctuation spectra that is not symmetric under wavenumber sign change. The aforementioned index is analyzed to characterize the power-law that emerges from the magnetic energy spectrum.

We now show the fluctuation spectra in the Fourier space to compare with the work of Navarro et al. (2014). We recreated Fig 1(a) and Fig 1(b) of the aforementioned work using Equation (2.38). In this context, in Figure 2.21 we show in logarithmic color scale Equation (2.38) for $\beta = 0.6$ and $A = T_\perp/T_\parallel = 1.4$. In Figure 2.22 we show in logarithmic color scale Equation (2.38), but now for $\beta = 0.6$ and $A = T_\perp/T_\parallel = 0.1$. There is an enhancement of electromagnetic fluctuations along the normal modes of the system, furthermore in Figure 2.21 an ion-cyclotron instability is present and in Figure 2.22 a firehose instability is present. The electromagnetic fluctuations are fixed along the unstable modes. As mentioned before, electromagnetic fluctuations are present even when considering a quasi-stable plasma, and fill a relevant part of the Fourier spectrum, which can be seen in Figures 2.21 and 2.22. These results, which are an adaptation from Navarro et al. (2014), are important since they agree with the observations measured by Bale et al. (2009), where the magnitude of magnetic fluctuations are enhanced along instability modes.

In Figure 2.23 we plot Equation (2.38) in terms of ck/w_{pp} for negative helicity using $\beta = 0.6$ and $A = 1.4$ for some values of w/Ω_p. In Figure 2.24 we plot Equation (2.38) in terms of ck/w_{pp} for negative helicity using $\beta = 0.6$ and $A = 1.4$, but now for some smaller values of w/Ω_p. Note that magnetic fluctuations are greater for smaller values of w/Ω_p, this can be seen from Figure 2.21, where we plot for the same values of $\beta - A$, since magnetic fluctuations are enhanced along the normal modes of the system which are closer to lower values of w/Ω_p. Moreover, for the negative helicity plots the normal modes do not appear since we are plotting for frequency values above

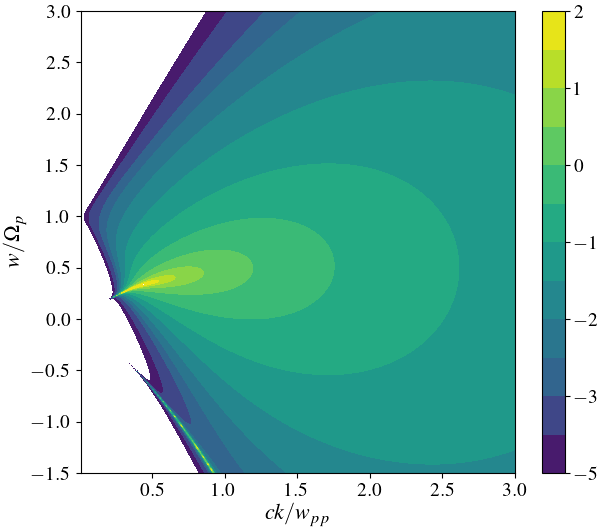

Figure 2.21: Magnetic field fluctuations $n\Omega\langle|B_-|^2\rangle/B_0^2$, in color logarithmic scale, for negative helicity, calculated using Equation (2.38) for $v_A/c = 10^{-4}, \beta = 0.6, A = 1.4$.

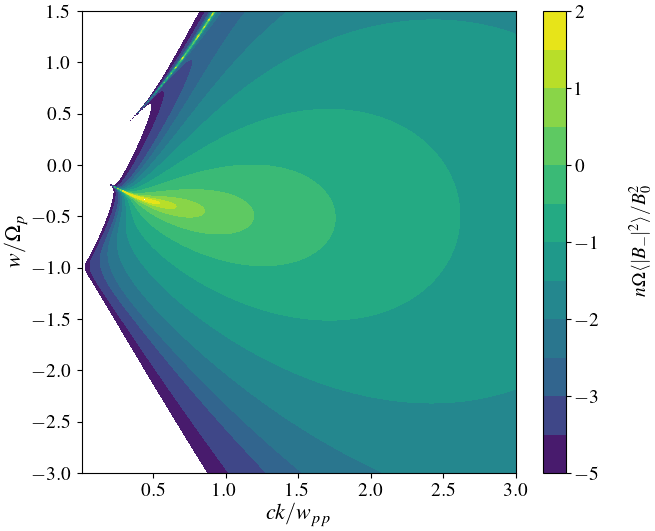

Figure 2.22: Magnetic field fluctuations $n\Omega\langle|B_+|^2\rangle/B_0^2$, in color logarithmic scale, for positive helicity, calculated using Equation (2.38) for $v_A/c = 10^{-4}, \beta = 0.6, A = 1.4$.

them. On the other hand, if we were to plot Equation (2.38) in terms of ck/w_{pp} for positive helicity we will encounter normal modes, although we are not interested in the role these modes play in the spectrum of electromagnetic fluctuations, since we are interested in spontaneously emitted electromagnetic fluctuations.

When integrating magnetic field fluctuations over ck/w_{pp}, for example integrating the curves shown in Figures 2.23 and 2.24 over ck/w_{pp} for every value of w, we obtain curves that can be represented by a power-law. In this sense, Figure 2.25 shows magnetic fluctuations ($n\Omega\langle|B_-|^2\rangle/B_0^2$) integrated over ck/w_{pp} in terms of w/Ω_p for negative helicity from Equation (2.38) for $\beta = 1$ and several values of A. In Figure

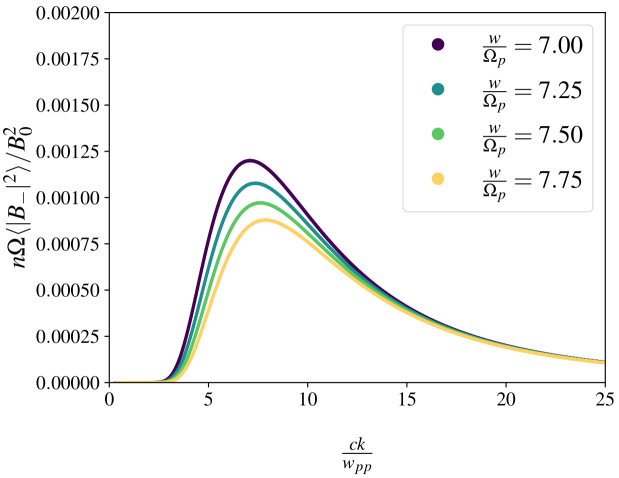

Figure 2.23: Magnetic field fluctuations $n\Omega\langle|B_-|^2\rangle/B_0^2$, in terms of ck/w_{pp}, for negative helicity, calculated using Equation (2.38) for $v_A/c = 10^{-4}$, $\beta = 0.6$, $A = 1.4$, and values of $ck/w_{pp} \sim 7$.

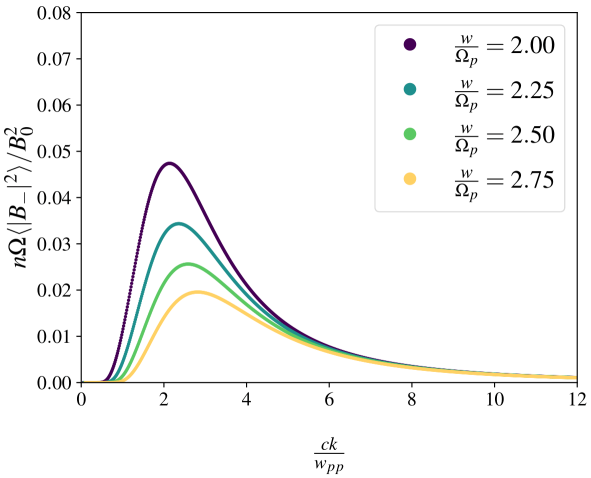

Figure 2.24: Magnetic field fluctuations $n\Omega\langle|B_-|^2\rangle/B_0^2$, in terms of ck/w_{pp}, for negative helicity, calculated using Equation (2.38) for $v_A/c = 10^{-4}$, $\beta = 0.6$, $A = 1.4$, and values of $ck/w_{pp} \sim 2$.

2.26 we show the same magnetic fluctuations ($n\Omega\langle|B_-|^2\rangle/B_0^2$) integrated over ck/w_{pp} in terms of w/Ω_p for negative helicity from Equation (2.38) but now for $A = 1$ and several values of β. In this case, the right side of these curves can be fitted by functions of the form $x^{-\alpha}$, to analyze this behavior, in the following we will observe this power-law like behavior in logarithmic scale.

In Figures 2.27 and, 2.28 we plot magnetic field fluctuations from Equation (2.38) integrated over ck/w_{pp} in terms of w/Ω_p for negative helicity as before, but now in logarithmic scale. In Figure 2.27 we plot for several values of anisotropy for a

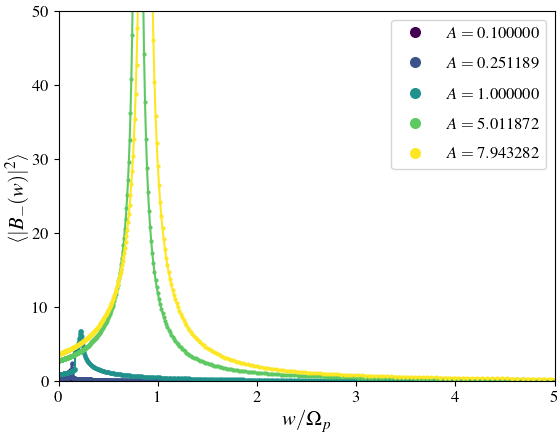

Figure 2.25: Magnetic field fluctuations $n\Omega\langle|B_-|^2\rangle/B_0^2$ integrated over ck/w_{pp}, in terms of w/Ω_p, for negative helicity, calculated using Equation (2.38) for $v_A/c = 10^{-4}, \beta = 1$.

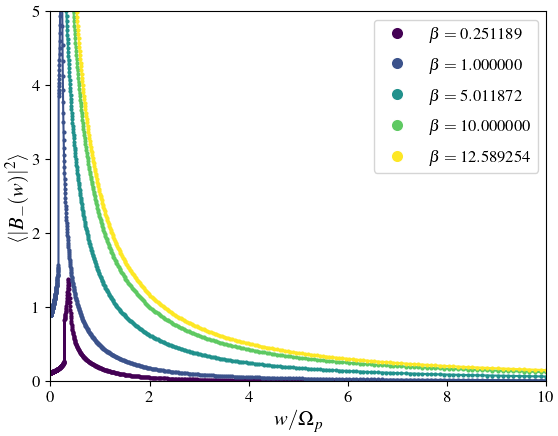

Figure 2.26: Magnetic field fluctuations $n\Omega\langle|B_-|^2\rangle/B_0^2$ integrated over ck/w_{pp}, in terms of w/Ω_p, for negative helicity, calculated using Equation (2.38) for $v_A/c = 10^{-4}, A = 1$.

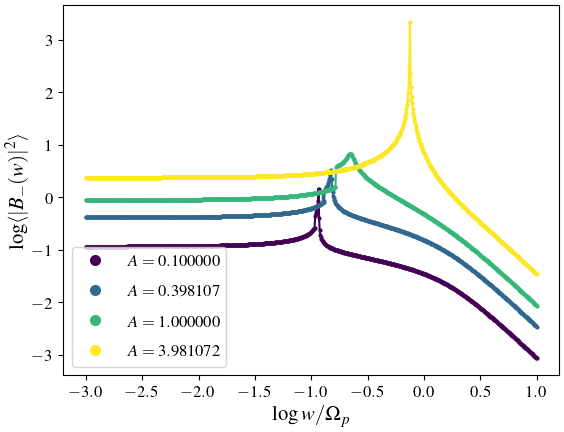

Figure 2.27: Magnetic field fluctuations $n\Omega\langle|B_-|^2\rangle/B_0^2$ integrated over ck/w_{pp}, in terms of w/Ω_p, for negative helicity, in logarithmic scale, calculated using Equation (2.38) for $v_A/c = 10^{-4}, \beta = 1$.

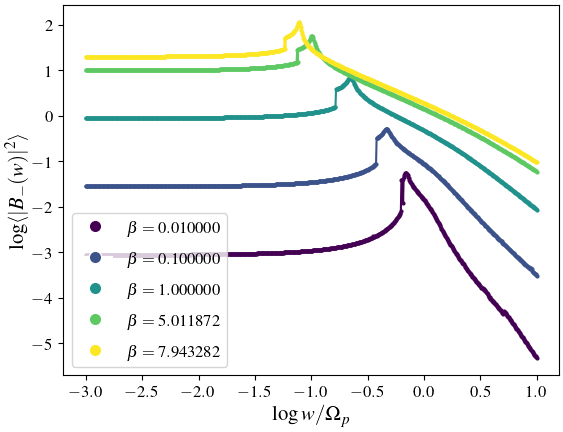

Figure 2.28: Magnetic field fluctuations $n\Omega\langle|B_-|^2\rangle/B_0^2$ integrated over ck/w_{pp}, in terms of w/Ω_p, for negative helicity, in logarithmic scale, calculated using Equation (2.38) for $v_A/c = 10^{-4}, A = 1$.

fixed value of $\beta = 1$. In Figure 2.28 we plot for several values of β for a fixed value of $A = 1$. The slope of these curves $(-\alpha)$ does not change substantially for fixed values of β while varying A, on the contrary, one may see a more significant change when fixing A and varying β, where for smaller values of β we observe higher values of α. The role of anisotropy seems to just be related to the magnitude of magnetic fluctuations, as seen in Figure 2.27. Different values of A do not change the behavior while increasing w/Ω_p. To obtain the index of electromagnetic fluctuations we perform a linear regression for these curves for values within the kinetic scale, from $\log w/\Omega_p = 0.5$ to $\log w/\Omega_p = 1$.

In Figure 2.29 we plot the spectral index of electromagnetic fluctuations bounded by the quasi-stability regions in the $\beta - A$ diagram using Equation (2.38) for negative helicity. The black lines represents the $\gamma_{\mathbf{k}}$ threshold of 10^{-3} and the blue lines represents the $\gamma_{\mathbf{k}}$ threshold of 10^{-4}. We observe that the spectral index is greater for lower values of β and does not seem to change significantly for different values of A. For each slope the coefficient of determination R^2, which for positive and negative helicity has values of $R^2 \geq 0.9$.

In Figure 2.30, we plot the variation of the spectral index in terms of $\beta - A$ parameters. On the left panel we show the variation of the spectral index in terms of β, and we can see that this index decreases while increasing β. On the right panel we show the variation of the spectral index in terms of A, we do not observe changes of this index while increasing A. This can also be seen in Figure 2.29. The region to the left of the dotted red line represents where, for the shown values, we ensure

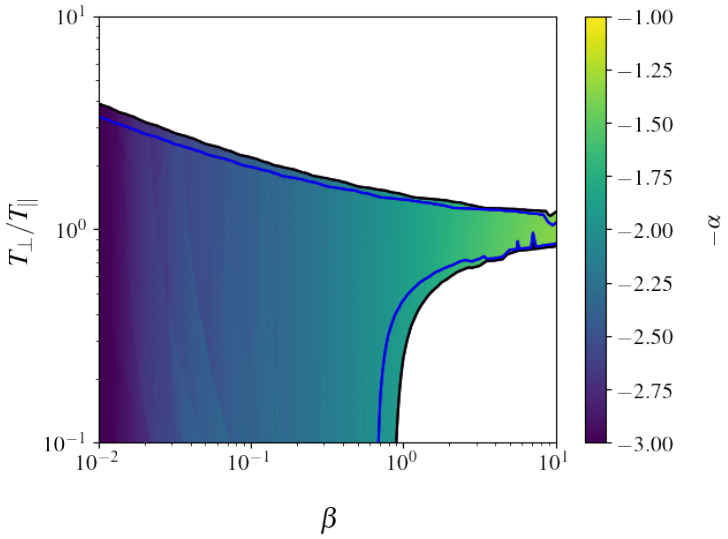

Figure 2.29: Spectral index of electromagnetic fluctuations in the quasi-stability regions in the $\beta - A$ diagram using Equation (2.38), in color logarithmic scale for negative helicity. The black lines represents the $\gamma_{\mathbf{k}}$ threshold of 10^{-3} and the blue lines represents the $\gamma_{\mathbf{k}}$ threshold of 10^{-4}.

quasi-stability approximately since we are taking the lines across $\beta = 1$ and $A = 1$, as we can see in Figure 2.29, this region belongs to the quasi-stability region but it is not the entire domain but rather cuts along the parameter space.

In the following we will discuss the implications of these results. Particularly we will analyze the theoretical differences of both approaches, from Navarro et al. (2014) and Schlickeiser et al. (2015) to elucidate the contributions between different processes in plasma to electromagnetic fluctuations. One of the main differences between both approaches will be assessed both theoretically and analytically in what follows.

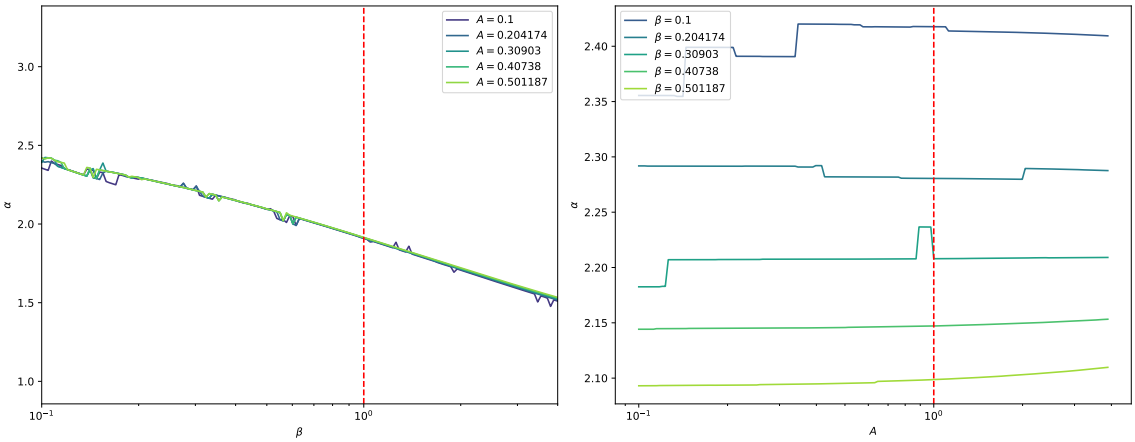

Figure 2.30: On the left panel we show the variation of the spectral index in terms of β. On the right panel we show the variation of the spectral index in terms of A. The region to the left of the dotted line is where for the shown values we ensure quasi-stability.

2.9.3 Analysis and comparison between formalisms

Studying closely the analytical expressions derived for the spectrum of magnetic fluctuations, consider the following definitions of both. For the Fluctuation-Dissipation methodology, we have

$$\frac{n\Omega}{B_0^2}\langle|B_\pm|^2\rangle_{\text{F-D}} = \beta\frac{T_\perp}{T_\parallel}\frac{c^2}{v_{ap}^2}\frac{y^2}{x^3}\frac{\text{Im}(\Lambda_\pm)}{|\Lambda_\pm|^2} \tag{2.39}$$

and for the Klimontovich-Maxwell methodology, we have

$$\frac{n\Omega}{B_0^2}\langle|B_\pm|^2\rangle_{\text{K-M}} = \sqrt{\beta}\frac{T_\perp}{T_\parallel}\frac{c^4}{v_{ap}^4}\frac{y}{x^4}\frac{\text{Im}(Z(\xi_\pm))}{|\Lambda_\pm|^2}. \tag{2.40}$$

When expanding the dispersion relation of Equation (2.39), we obtain an expression where the equation derived from the Klimontovich-Maxwell methodology is included in the equation derived from the Fluctuation-Dissipation theorem. Thus,

we may write,

$$\frac{n\Omega}{B_0^2}\langle|B_\pm|^2\rangle_{\text{F-D}} = \frac{n\Omega}{B_0^2}\langle|B_\pm|^2\rangle_{\text{K-M}} + \frac{n\Omega}{B_0^2}\langle|B_\pm|^2\rangle_{\text{ext}}\,, \tag{2.41}$$

where,

$$\frac{n\Omega}{B_0^2}\langle|B_\pm|^2\rangle_{\text{ext}} = \sqrt{\beta}\,\frac{T_\perp}{T_\parallel}\left(\frac{T_\perp}{T_\parallel}-1\right)\frac{c^4}{v_{ap}^4}\,\frac{y(x\pm 1)}{x^3}\,\frac{\text{Im}(Z(\zeta_\pm))}{|\Lambda_\pm|^2}\,. \tag{2.42}$$

According to the fluctuating spectra, the magnitude of electromagnetic fluctuations is greater for the expression derived from the Klimontovich-Maxwell (K-M) formalism when $A < 1$, since the term $n\Omega\,\langle|B_\pm|^2\rangle_{\text{ext}}/B_0^2$ in Equation (2.41) contributes to this spectra when $A \neq 1$. Note that, when $T_\perp = T_\parallel$ both spectrum describe the same spectral index, as can be seen from evaluating this consideration on Equation (2.42), and depicted in Figure 2.31, where we show the spectral index α in terms of β for $A = 1$.

Particularly, using the Fluctuation-Dissipation (F-D) methodology, in Figure 2.32 we plot the Fourier power spectrum from Equation (2.25) for $\beta = 0.6$ and $A = 1.4$ for negative helicity in the Fourier spectrum. Using the Klimontovich-Maxwell (K-M) methodology, In Figure 2.33 we plot the Fourier power spectrum from Equation (2.38) for $\beta = 0.6$ and $A = 1.4$ for negative helicity. In both figures, using both approaches, electromagnetic fluctuations are enhanced along unstable modes.

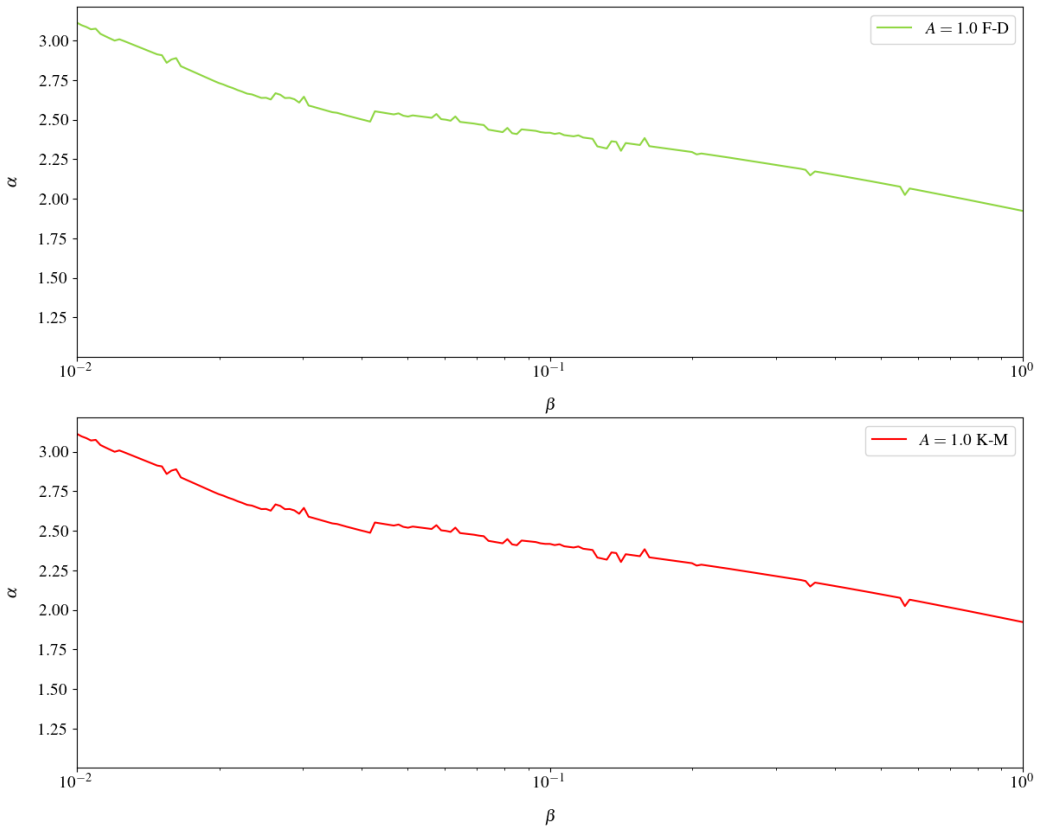

Figure 2.31: Spectral index of electromagnetic fluctuations in terms of β and $A = 1$, on the top panel we show the curve obtained using the F-D formalism and the bottom panel shows the curve obtained using the K-M formalism.

In Figure 2.34 we plot Equation (2.25) using the F-D approach for $\beta = 0.6$ and $A = 1.4$ for positive helicity in the Fourier power spectrum. In Figure 2.35 we plot Equation (2.38) using the K-M approach for $\beta = 0.6$ and $A = 1.4$ for negative helicity in the Fourier power spectrum. In both figures electromagnetic fluctuations are enhanced along the firehose instability. Note that negative helicity and positive helicity look inverted between each other, and therefore the analysis of the spectral index of electromagnetic fluctuations is analogue if we consider positive values of

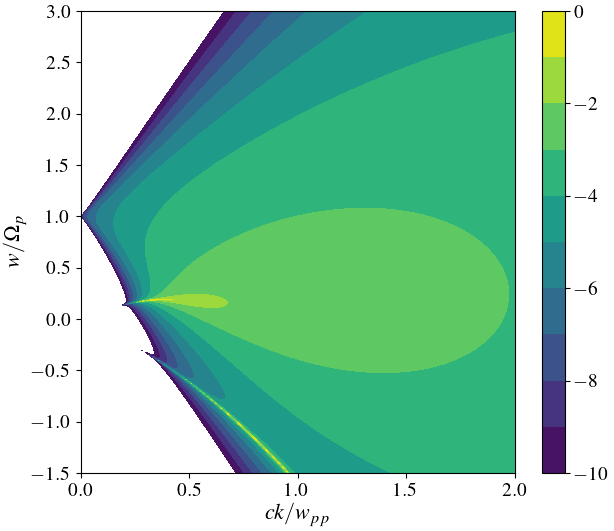

Figure 2.32: Magnetic field fluctuations $n\Omega\langle|B_-|^2\rangle/B_0^2$, in color logarithmic scale, for negative helicity, calculated using Equation (2.25) derived from Fluctuation Dissipation formalism for $v_A/c = 10^{-4}, \beta = 0.6, A = 0.1$.

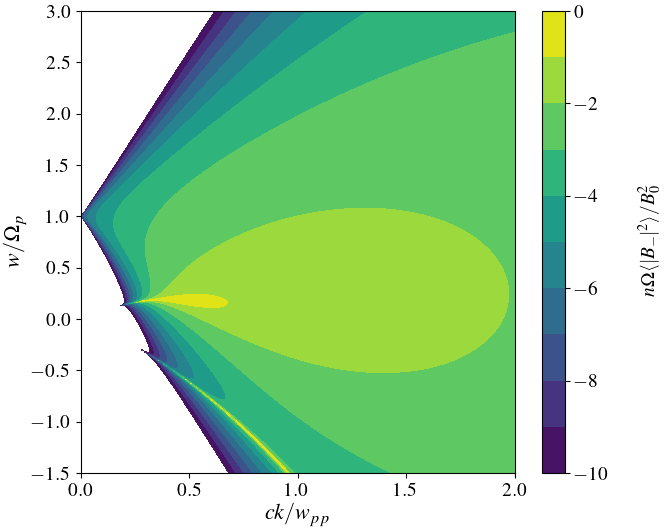

Figure 2.33: Magnetic field fluctuations $n\Omega\langle|B_-|^2\rangle/B_0^2$, in color logarithmic scale, for negative helicity, calculated using Equation (2.38) derived from Klimontovich-Maxwell formalism for $v_A/c = 10^{-4}, \beta = 0.6, A = 0.1$.

w/Ω_p for both helicities (which was done in this work) or if we consider positive and negative values of w/Ω_p for one of the helicities. Qualitatively, both spectrum show the same behavior along instabilities, the main difference between both methodologies is the magnitude of electromagnetic fluctuation spectra, as already mentioned and observed from the analytical derivation of Equation (2.41).

As described above, the expression derived from the F-D theorem can be reformulated to incorporate the fluctuating spectra derived from the set of K-M equations. This indicates that the phenomena and processes in the plasma are considered dif-

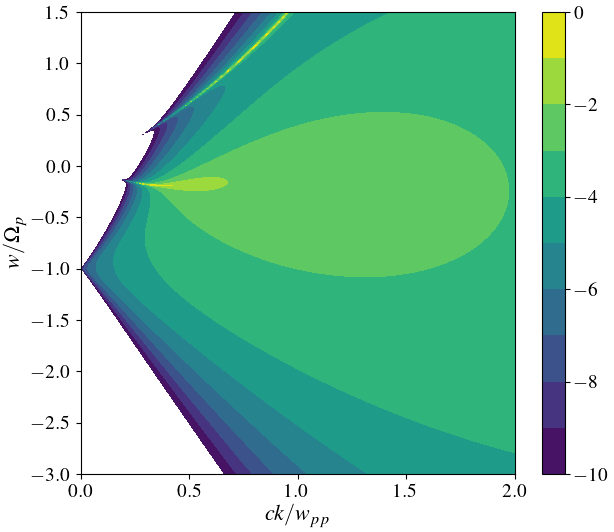

Figure 2.34: Magnetic field fluctuations $n\Omega\langle|B_+|^2\rangle/B_0^2$, in color logarithmic scale, for positive helicity, calculated using Equation (2.25) derived from Fluctuation Dissipation formalism for $v_A/c = 10^{-4}, \beta = 0.6, A = 0.1$.

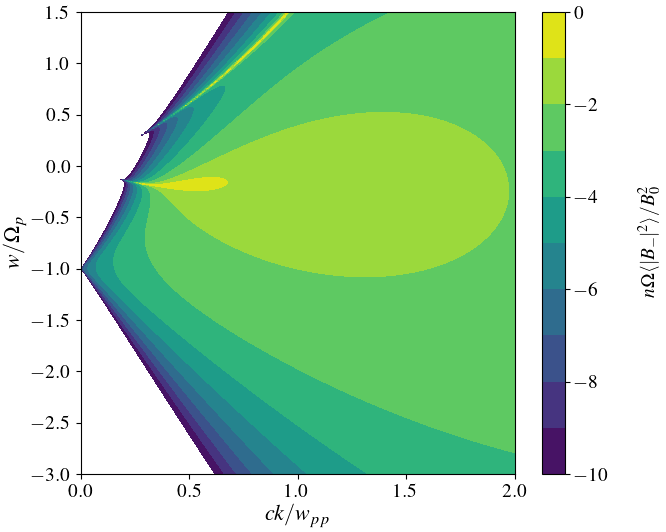

Figure 2.35: Magnetic field fluctuations $n\Omega\langle|B_+|^2\rangle/B_0^2$, in color logarithmic scale, for positive helicity, calculated using Equation (2.38) derived from Klimontovich-Maxwell formalism for $v_A/c = 10^{-4}, \beta = 0.6, A = 0.1$.

ferently in both methodologies.

Both approaches employ the dispersion tensor obtained from the Vlasov formalism and the small fluctuation approximation to derive the electromagnetic fluctuation spectra of the plasma in a quasi-equilibrium state. They both establish a general connection between the correlation function of fluctuating quantities in the plasma and the resulting thermally induced electromagnetic fluctuations. However, neither methodology accounts for larger amplitude fluctuations, which may be significant for turbulence, instabilities, and particle acceleration. These large amplitude phenomena could play a crucial role in damping instabilities in the Solar Wind. Notably, the

F-D approach examines the system's response to a linear perturbation and explains fluctuations due to the thermal motion of the particles in the plasma. In contrast, the K-M approach begins with an exact microscopic description of the system via the Klimontovich equation.

Another potential source of the magnitude difference between the formalisms is that the F-D formalism considers the system's response to a linear perturbation as inducing a change in the velocity distribution function (VDF). This approach describes an equilibrium VDF and its perturbation due to the thermal energy change of the VDF. This aspect is less clear in the K-M formalism. Although it uses the Klimontovich distribution function, which encompasses the distribution of particles and their evolution in the system, it does not explicitly include a perturbation due to changes in the VDF, as evident in Equation (2.30).

2.9.4 Discussion

The final expression obtained for the F-D formalism, Equation (2.24), does not ensure that electromagnetic fluctuations are positive in the whole spectrum. In fact, because of the construction of this equations, fluctuations should be purely positive, but Equation (2.19) becomes zero when $\mathrm{Im}(\Lambda_{\pm}) = 0$. This term can be written as,

$$Z_{\alpha}\left(\frac{x \pm 1}{y\sqrt{\beta_p}}\right)\left(\frac{x}{y\sqrt{\beta_p}} + (A-1)\frac{x \pm 1}{y\sqrt{\beta_p}}\right) = 0\,. \tag{2.43}$$

This leads us to conclude that there is a certain value for x where this expression for the spectrum of electromagnetic fluctuations becomes zero, this value can be obtained analytically,

$$x_{0\pm} = \frac{w}{w_p} = \mp\frac{A-1}{A}\,. \tag{2.44}$$

Where the sub-index $\pm$ is used to identify between using positive of negative helicity. Indeed this is a removable indetermination, since Equation (2.19) can be written including this consideration, rewriting the expression as,

$$\frac{n\Omega}{B_0}\langle|B_{\pm}|^2\rangle = -\beta A\,\frac{c^2}{v_{ap}^2}\,\frac{y^2}{x^2(x-x_0)}\,\mathrm{Im}\left(\frac{1}{\Lambda_{\pm}}\right)\,. \tag{2.45}$$

For the results in Chapter 2, we used the latter expression, this ensures that fluctuations are positive in the whole spectrum. Both spectrum for the non-fixed and fixed final expression are shown in Figures 2.36 and 2.37 for negative helicity, using $A = 1.4$ and $\beta = 0.6$. Figures 2.38, and 2.39 show the spectrum of electromagnetic fluctuations for positive helicity, using $A = 1.4$ and $\beta = 0.6$, both for the non-fixed and fixed final expression, respectively.

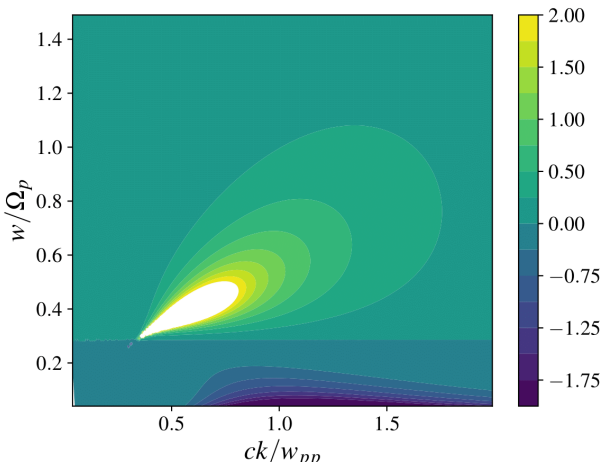

Figure 2.36: Spectrum of electromagnetic fluctuations in the Fourier space for $A = 1.4$ and $\beta = 0.6$ for negative helicity using Equation (2.24).

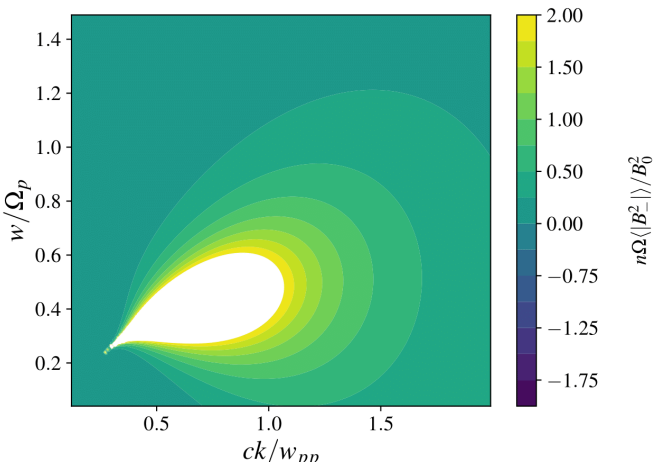

Figure 2.37: Spectrum of electromagnetic fluctuations in the Fourier space for $A = 1.4$ and $\beta = 0.6$ for negative helicity using Equation (2.25).

Note that, for the spectra shown in Figure 2.36 we obtain negative values for $A = 1.4$ exactly in $w/\Omega_p = 0.28$, which is the value calculated analytically when $\mathrm{Im}(\Lambda_\pm^{-1}) = 0$, which is then fixed as shown in Figure 2.37 incorporating this value into the expression for the magnetic spectra. On the other hand we would not observe negative fluctuations in the positive region of the Fourier spectrum if we consider $A > 1$ which is this particular case. For positive helicity as shown in Figure 2.38 the value where we would encounter negative electromagnetic fluctuations is $w/\Omega_p = -0.28$, which is then fixed as shown in Figure 2.39 incorporating this value into the expression for the magnetic spectra. Using expression (2.45) completely removes the issue of negative magnitude of the fluctuating spectra as shown in Figures 2.37 and 2.39.

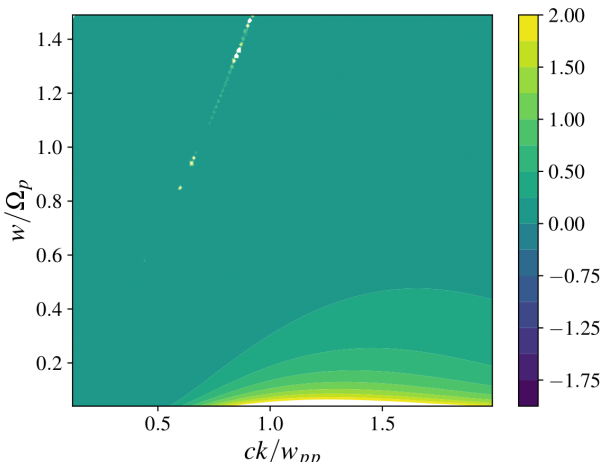

Figure 2.38: Spectrum of electromagnetic fluctuations in the Fourier space for $A = 1.4$ and $\beta = 0.6$ for positive helicity using Equation (2.24).

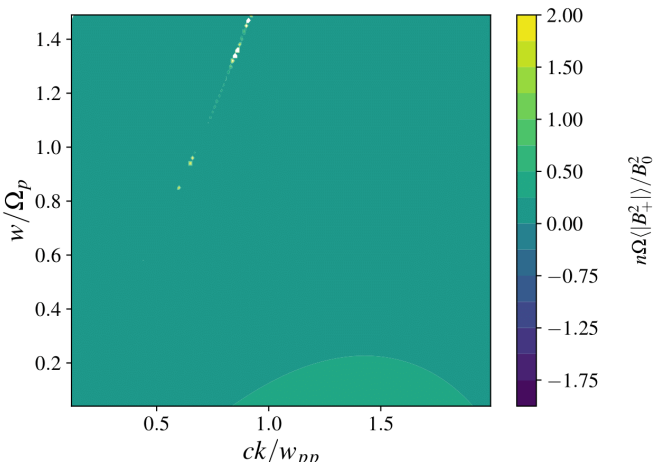

Figure 2.39: Spectrum of electromagnetic fluctuations in the Fourier space for $A = 1.4$ and $\beta = 0.6$ for positive helicity using Equation (2.25).

In terms of results, to calculate the spectral index of electromagnetic fluctuations, the magnitude of these fluctuations is slightly changed. For instance, for certain values of frequencies, the magnitude is affected. To calculate the spectral index of electromagnetic fluctuations, using Equation (2.24) or Equation (2.25) will only change the place where we perform the linear regression of the curve, so the results do not have a substantial change.

2.10 Conclusion

In this thesis we obtained the spectral index of electromagnetic fluctuations using two different approaches, the Fluctuation-Dissipation (F-D) theorem using the expression for the spectra of magnetic fluctuations as obtained in Navarro et al. (2014) and the set of Klimontovich-Maxwell (K-M) equations using the theory of small amplitude fluctuations for magnetized plasmas developed in Schlickeiser et al. (2015), first developed for unmagnetized plasma in Schlickeiser and Yoon (2012). Using the Klimontovich-Maxwell formalism we obtained the expression for the spectra of magnetic fluctuations as shown in Schlickeiser et al. (2015). Both expressions are specific for an electron-proton quasi-stable bi-Maxwellian plasma.

The methodology used in Navarro et al. (2014) using the F-D approach is in agreement with observations made by Bale et al. (2009). As shown in Figures 2.11 and 2.12 electromagnetic fluctuations are enhanced along unstable modes. The methodology using the K-M approach is also in agreement with observations made by Bale et al. (2009), as shown in Figures 2.21 and 2.22 electromagnetic fluctuations are also enhanced along unstable modes. This can be seen in Figure 1.3, where the magnitude of magnetic fluctuations is shown and it is enhanced along firehose and ion-cyclotron instabilities. The Fluctuation-Dissipation (F-D) theorem focuses on linear perturbations over the system and explains fluctuations due to thermal motion of the plasma particles. It connects the correlation functions of fluctuating quantities of the plasma and the resulting induced electromagnetic fluctuations. Surely, according to Figures 2.32 and 2.33 we observe that the main difference is the magnitude of the magnetic fluctuating spectra when $A \neq 1$. Both methods rely on the Vlasov formalism and its

solutions of the dispersion relation but omit large amplitude effects that may affect turbulence and instabilities, that may be crucial for understanding solar wind mechanisms. One reason of the difference in magnitude between the formalisms could be that the F-D formalism considers the system's response to a linear perturbation as inducing a change in the velocity distribution function (VDF).

This formalism describes both an equilibrium VDF and a perturbation due to the change in thermal energy of it. In contrast, this aspect is less clear in the K-M formalism. Although the K-M formalism employs the Klimontovich distribution function, which encompasses the distribution of particles and their evolution within the system, it does not explicitly account for a perturbation due to those changes in the velocity distribution function. Thus, the difference between both formalisms is that F-D considers a change of the VDF due to the free thermal energy, affecting the magnitude of electromagnetic fluctuations in plasmas, but they both consider the fluctuating energy generated by spontaneous and induced electromagnetic fluctuations.

This work is useful to elucidate the theoretical differences of the contribution of electromagnetic fluctuations from different formalisms. As well, it can be used to compare the spectral index of electromagnetic fluctuations in the parameter space ($\beta - A$ diagram) obtained using two theoretical formalisms with solar wind data obtained from satellites. Many measurements for power spectra have been made in different ranges Podesta et al. (2006), Podesta et al. (2007), Kiyani et al. (2015), Alexandrova et al. (2008), and Sorriso-Valvo et al. (2007) just to name a few, therefore it may be relevant to obtain a complete description for the spectral index in

fluctuating plasmas. Indeed, solar wind processes are complex and dynamic, in this work we used fluctuating theory to explain these phenomena, but this could go even further analyzing these processes using large amplitude theories since they could play an important role in regulating the quasi-stable states of the plasma. Simultaneously, there is evidence that shows that this problem should be approached from a 2-dimensional perspective, using oblique propagating waves to the background magnetic field. Somewhat of an advance was made towards this direction and it will hopefully help us to explain further the existence of electromagnetic fluctuations in the solar wind.

Chapter 3

Appendix

3.1 Fourier Space

The definition of the spatial Fourier transformation and its inverse transformation is given by,

$$f_{\mathbf{k}} = \frac{1}{(2\pi)^3} \int d\mathbf{r}\, f(\mathbf{r})\, e^{-i\mathbf{k}\cdot\mathbf{r}} \quad , \quad f(\mathbf{r}) = \int d\mathbf{k}\, f(\mathbf{k})\, e^{i\mathbf{k}\cdot\mathbf{r}}\,.$$

The Fourier transformation of a function $f(\mathbf{r},t)$ in space and time is defined such that,

$$\begin{aligned} f_{\mathbf{k},w} &= \frac{1}{(2\pi)^4} \int d\mathbf{r} \int dt f(\mathbf{r},t)\, e^{-i\mathbf{k}\cdot\mathbf{r}+iwt}\,, \\ f(\mathbf{r},t) &= \int d\mathbf{k} \int dw f_{\mathbf{k},w}\, e^{i\mathbf{k}\cdot\mathbf{r}-iwt}\,. \end{aligned}$$

When the angular frequency w satisfies the dispersion relation $w = w_{\mathbf{k}} + i\gamma_{\mathbf{k}}$ which is a function of $\mathbf{k}$, then the representation of the function $f(\mathbf{r},t)$ can be expressed such that,

$$f(\mathbf{r},t) = \int d\mathbf{k} f_{\mathbf{k}}\, \exp(i\mathbf{k}\cdot\mathbf{r} - iw_{\mathbf{k}}t + \gamma_{\mathbf{k}}t)\,.$$

If $f(\mathbf{r},t)$ is real, then $f^*(\mathbf{r},t) = f(\mathbf{r},t)$, where the asterisk $()^*$ represents the

complex conjugate. It follows that,

$$\int d\mathbf{k} f_{\mathbf{k}}^{*} \exp(-i\mathbf{k}\cdot\mathbf{r} + iw_{\mathbf{k}}t) = \int d\mathbf{k} f_{\mathbf{k}} \exp(i\mathbf{k}\cdot\mathbf{r} - iw_{\mathbf{k}}t)\,,$$

and the following symmetry relations hold,

$$f_{\mathbf{k}}^{*} = f_{-\mathbf{k}}\,, \qquad w_{-\mathbf{k}} = -w_{\mathbf{k}}\,, \qquad \gamma_{-\mathbf{k}} = \gamma_{\mathbf{k}}\,.$$

3.2 Trajectories and Velocities

Consider a zero electric field magnitude ($E_0 = 0$) and a non-zero magnetic field magnitude ($B_0 \neq 0$), the equation of motion of the particles in the system is,

$$\frac{d\mathbf{v}}{dt} = \frac{q}{m}\frac{\mathbf{v}\times\mathbf{B_0}}{c}\,, \tag{3.1}$$

if we solve this equation considering $\mathbf{B} = B_0\hat{z}$, and particle velocities as $\mathbf{v} = [v_\perp\cos\phi, v_\perp\sin\phi, v_\parallel]$. The position of a charged particle in a magnetic field as a function of time is,

$$\mathbf{r}(t) = a_c\left(\sin(\Omega_\alpha t-\phi)\,\hat{x} + \cos(\Omega_\alpha t-\phi)\,\hat{y} + \Omega_\alpha\frac{v_\parallel}{v_\perp}t\,\hat{z}\right)\,, \tag{3.2}$$

where $v_\perp = a_c\Omega_\alpha$. Thus, the velocity of a charged particle in a magnetic field is,

$$\mathbf{v}(t) = v_\perp\left(\cos(\phi-\Omega_\alpha t)\,\hat{x} + \sin(\phi-\Omega_\alpha t)\,\hat{y} + v_\parallel\,\hat{z}\right)\,. \tag{3.3}$$

3.3 Method of Characteristics

The method of characteristics consists of finding curves along which the partial differential equation to be solved becomes an ordinary differential equation. We need

to solve an equation of the form,

$$\frac{\partial f_{\alpha 1}}{\partial t} + \mathbf{v} \cdot \nabla f_{\alpha 1} + \mathbf{a}(\mathbf{x}, \mathbf{v}, t) \cdot \nabla_v f_{\alpha 1} = g(\mathbf{x}, \mathbf{v}, t)\,,$$

with $\mathbf{a}(\mathbf{x}, \mathbf{v}, t)$, the acceleration described by,

$$\mathbf{a}(\mathbf{x}, \mathbf{v}, t) = \frac{q_\alpha}{m_\alpha}\left(\frac{\mathbf{v} \times \mathbf{B}_0}{c}\right).$$

We will define the curve going from t to $t' = t + dt$ as the characteristic curve. The equations of motion that are satisfied are,

$$\frac{d\mathbf{x}'}{dt'} = \mathbf{v}' \quad , \quad \frac{d\mathbf{v}'}{dt} = \frac{q_\alpha}{m_\alpha}\left(\frac{\mathbf{v} \times \mathbf{B_0}(x', t')}{c}\right),$$

and consider the boundary conditions,

$$\mathbf{x}'(t' = t) = \mathbf{x}\,,$$

$$\mathbf{v}'(t' = t) = \mathbf{v}\,.$$

If we calculate the total derivative of the distribution function at t', $f_{\alpha 1} = [\mathbf{x}'(t'), \mathbf{v}'(t'), t']$,

$$\frac{df_{\alpha 1}}{dt} = \frac{\partial f_{\alpha 1}}{\partial t'} + \frac{\partial f_{\alpha 1}}{\partial \mathbf{v}'}\frac{d\mathbf{v}'}{dt} + \frac{\partial f_{\alpha 1}}{\partial \mathbf{x}'}\frac{d\mathbf{x}'}{dt}\,.$$

Using the equations of motion in this expression, we notice that we arrive at an expression that satisfies Equation (2.7),

$$\frac{df_{\alpha 1}}{dt} = -\frac{q_\alpha}{m_\alpha}\left(\mathbf{E_1}(x', t') + \frac{\mathbf{v}' \times \mathbf{B_1}(x', t')}{c}\right) \cdot \nabla'_v f_{\alpha 0}(\mathbf{x}', \mathbf{v}')\,.$$

since the left side of Equation (2.7) is the total derivative of the perturbed distribution. We can integrate this expression since it is an exact differential so that,

$$f_{\alpha 1} = -\frac{q_\alpha}{m_\alpha}\int_{-\infty}^{t} dt' \left(\mathbf{E_1}(x', t') + \frac{\mathbf{v}' \times \mathbf{B_1}(x', t')}{c}\right) \cdot \nabla'_v f_{\alpha 0}(\mathbf{x}', \mathbf{v}')\,.$$

Considering solutions of the form,

$$\mathbf{E_1}(\mathbf{x},t) = \bar{\mathbf{E}}_\mathbf{1}\, \exp\left(i\,\mathbf{k}\cdot\mathbf{r} - iwt\right) \quad , \quad \mathbf{B_1}(x,t) = \bar{\mathbf{B}}_\mathbf{1}\, \exp\left(i\,\mathbf{k}\cdot\mathbf{r} - iwt\right) ,$$

and using the change of variables $\mathbf{R} = \mathbf{r}' - \mathbf{r}$ and $\tau = t' - t$, we must solve the integral

$$f_{\alpha k} = -\frac{q_\alpha}{m_\alpha}\int_{-\infty}^{0} d\tau \left(\bar{\mathbf{E}}_\mathbf{1} + \frac{\mathbf{v}'\times\bar{\mathbf{B}}_\mathbf{1}(\mathbf{x}',t')}{c}\right)\cdot\nabla'_v f_{\alpha 0}(\mathbf{v}')\, \exp\left(i\,\mathbf{k}\cdot\mathbf{R} - iw\tau\right) . \quad (3.4)$$

The expression (2.10) will be useful to obtain the dispersion relation for parallel propagation.

3.4 Plasma Dispersion Function

Its general definition is given by,

$$Z(\zeta) = \frac{1}{\sqrt{\pi}}\int du\, \frac{e^{-u^2}}{u-\zeta},$$

which is not continuous in the complex plane. On the other hand, the first derivative of this expression yields,

$$Z'(\zeta) = -\frac{1}{\sqrt{\pi}}\int du\, e^{-u^2}\,\partial_\zeta\,\frac{1}{u-\zeta} = -\frac{2}{\sqrt{\pi}}\int du\frac{ue^{-u^2}}{u-\zeta} = -2[1+\zeta Z(\zeta)]\,.$$

Let's consider this identity as a differential equation,

$$e^{\zeta^2}Z(\zeta) = -2\int_0^\zeta dt e^{t^2} + Z(0)\,. \quad (3.5)$$

From the boundary condition at $\zeta = 0$, for real ζ,

$$\frac{1}{\sqrt{\pi}}\int du\, \frac{e^{-u^2}}{u-\zeta} = i\sqrt{\pi}e^{-\zeta^2}\,,$$

thus, $Z(0) = i\sqrt{\pi}$, plugging this into Equation (3.5), and changing the integration variable to $t = -ix$,

$$Z(\zeta) = e^{-\zeta^2}\left(i\sqrt{\pi} + 2i\int_0^{i\zeta} dx\, e^{-x^2}\right) = 2ie^{-\zeta^2}\int_{-\infty}^{i\zeta} dx\, e^{-x^2}\,.$$

Finally, we have,

$$Z(\zeta) = i\sqrt{\pi}\exp(-\zeta^2)(1 + i\,\mathrm{erfi}(\zeta))\,,$$

that we use in our calculations, since it is continuous in the complex plane.

3.5 Bessel Functions

Bessel functions are the solutions to the following differential equation,

$$z^2y''(z) + zy'(z) + (z^2 - n^2)y(z) = 0\,.$$

Here, n is an integer for cases where the problem exhibits cylindrical symmetry or in cases where spherical symmetry is present, this value can be a semi-integer. These functions arise when computing the dispersion relation of a plasma in a background magnetic field considering wave propagation oblique to it.

For integer index n, Bessel functions $J_n(x)$ correspond to the coefficients in the Laurent series expansion around $s = 0$ of a *generating function*,

$$\exp\left(\frac{z}{2}\left(s - \frac{1}{s}\right)\right) = \sum_{n=-\infty}^{\infty} J_n(z)s^n\,.$$

Taking the variable change $s = e^{i\phi}$, we obtain the relation,

$$e^{iz\sin\phi} = \sum_{n=-\infty}^{\infty} J_n(z)e^{in\phi}\,. \tag{3.6}$$

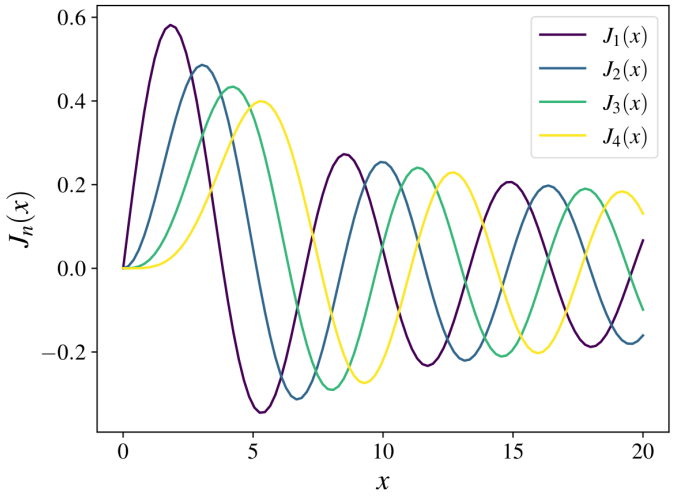

Figure 3.1: Bessel functions of the first kind with different zeros. Each curve corresponds to the Bessel function associated with one of its characteristic zeros.

Bessel functions satisfy the following recurrence relations,

$$\begin{aligned} J_{l-1}(\mu) - J_{l+1}(\mu) &= 2J_l'(\mu)\,, \\ J_{l-1}(\mu) + J_{l+1}(\mu) &= \frac{2l}{\mu} J_l(\mu)\,. \end{aligned}$$

These can also be written as,

$$\sum_{m=-\infty}^{\infty} J_m(b) \int_0^{2\pi} d\phi \exp(i(m-n)(\phi-\psi)) \begin{pmatrix} \cos\phi \\ \sin\phi \\ 1 \end{pmatrix}$$

$$= 2\pi \begin{pmatrix} nJ_n(b)\cos\psi/b + iJ_n'(b)\sin\psi \\ nJ_n(b)\sin\psi/b - iJ_n'(b)\cos\psi \\ J_n(b) \end{pmatrix}$$

and other useful expressions are,

$$\begin{aligned}
\sum_n J_n(\mu)\int_0^{2\pi} d\phi\cos\phi\,\exp(i\phi(n-l)) &= 2\pi\frac{lJ_l(\mu)}{\mu},\\
\sum_n J_n(\mu)\int_0^{2\pi} d\phi\sin\phi\,\exp(i\phi(n-l)) &= -2\pi i J_l'(\mu)\,,\\
\sum_n J_n(\mu)\int_0^{2\pi} d\phi\,\exp(i\phi(n-l)) &= 2\pi J_l(\mu)\,.
\end{aligned}$$

Considering other identities of Bessel functions,

$$\exp\left[i\mu\sin(\phi-\Omega_\alpha\tau)\right] = \sum_{n=-\infty}^{\infty} J_n\left(\mu\right)\exp(in(\phi-\Omega_\alpha\tau))\,, \tag{3.7}$$

where $\mu=\dfrac{k_\perp v_\perp}{\Omega_\alpha}$, particularly we also have,

$$\exp\left[i\mu\sin(\phi)\right] = \sum_{n=-\infty}^{\infty} J_n\left(\mu\right)\exp(in(\phi))\,, \tag{3.8}$$

3.6 Solution of integrals for oblique case dispersion relation

Using identities (3.7) and (3.8), expressed according to Equation (3.6) in Equation (3.13), we have to solve integrals of the following form

$$\begin{aligned}
\vartheta_1 &= \sum_{n=-\infty}^{\infty} J_n(\mu)\exp(i\phi(n-l))\sum_{l=-\infty}^{\infty} J_l(\mu)\int_{-\infty}^{0} d\tau\exp\left(-i(-k_\parallel v_\parallel + w - l\Omega_\alpha)\tau\right),\\
\vartheta_2 &= \sum_{n=-\infty}^{\infty} J_n(\mu)\exp(in\phi)\int_{-\infty}^{0} d\tau\cos(\phi-\Omega_\alpha\tau)\exp\left(-i\mu\sin(\phi-\Omega_\alpha\tau)+i(k_\parallel v_\parallel - w)\tau\right),\\
\vartheta_3 &= \sum_{n=-\infty}^{\infty} J_n(\mu)\exp(in\phi)\int_{-\infty}^{0} d\tau\sin(\phi-\Omega_\alpha\tau)\exp\left(-i\mu\sin(\phi-\Omega_\alpha\tau)+i(k_\parallel v_\parallel - w)\tau\right).
\end{aligned}$$

Integrating these expressions,

$$\vartheta_1 = \sum_{n,l=-\infty}^{\infty} J_n(\mu)\, J_l(\mu) \exp(i\phi(n-l))\ \frac{i}{w - l\Omega_\alpha - k_\parallel v_\parallel},$$

$$\vartheta_2 = \sum_{n=-\infty}^{\infty} J_n(\mu) \exp(in(\phi)) \int_{-\infty}^{0} d\tau\ \cos(\phi - \Omega_\alpha\tau) \exp\left(-i\mu \sin(\phi - \Omega_\alpha\tau) + i(k_\parallel v_\parallel - w)\tau\right)\ ,$$

$$\vartheta_3 = \sum_{n=-\infty}^{\infty} J_n(\mu) \exp(in(\phi)) \int_{-\infty}^{0} d\tau\ \sin(\phi - \Omega_\alpha\tau) \exp\left(-i\mu \sin(\phi - \Omega_\alpha\tau) + i(k_\parallel v_\parallel - w)\tau\right)\ .$$

Let's see the first derivative of the expression with Bessel functions with respect to μ and with respect to $(\phi - \Omega_\alpha\tau)$, we may rewrite those as the following,

$$\sin(\phi - \Omega_\alpha\tau) \exp\left[-i\mu \sin(\phi - \Omega_\alpha\tau)\right] = -i \sum_{n=-\infty}^{\infty} J_n'(\mu) \exp(-in(\phi - \Omega_\alpha\tau)),$$

$$\cos(\phi - \Omega_\alpha\tau) \exp\left[-i\mu \sin(\phi - \Omega_\alpha\tau)\right] = \sum_{n=-\infty}^{\infty} \frac{n}{\mu} J_n(\mu) \exp(-in(\phi - \Omega_\alpha\tau))\,,$$

from this, we may write

$$\sin(\phi - \Omega_\alpha\tau) \exp\left[-i\mu \sin(\phi - \Omega_\alpha\tau)\right] = \frac{i}{2} \sum_{n=-\infty}^{\infty} (J_{n-1} - J_{n+1}) \exp(-in(\phi - \Omega_\alpha\tau)),$$

$$\cos(\phi - \Omega_\alpha\tau) \exp\left[-i\mu \sin(\phi - \Omega_\alpha\tau)\right] = \frac{1}{2} \sum_{n=-\infty}^{\infty} (J_{n-1} + J_{n+1}) \exp(-in(\phi - \Omega_\alpha\tau))\,.$$

Using the latter expressions, we can replace the expressions in the integrals, and solve them as follows

$$\vartheta_1 = \sum_{n,l=-\infty}^{\infty} J_n(\mu) J_l(\mu) \exp(i\phi(n-l)) \frac{i}{w - l\Omega_\alpha - k_\parallel v_\parallel}, \tag{3.9}$$

$$\vartheta_2 = \frac{1}{2} \sum_{n,l=-\infty}^{\infty} J_n(\mu) \exp(i(n-l)\phi)(J_{l-1} + J_{l+1}) \frac{i}{w - l\Omega_\alpha - k_\parallel v_\parallel}, \tag{3.10}$$

$$\vartheta_3 = \frac{i}{2} \sum_{n,l=-\infty}^{\infty} J_n(\mu) \exp(i(n-l)\phi)(J_{l-1} - J_{l+1}) \frac{i}{w - l\Omega_\alpha - k_\parallel v_\parallel}\,, \tag{3.11}$$

On the other hand, we must write the magnetic field in terms of the electric field to assemble the current matrix, that is,

$$\mathbf{B} = -k_{\parallel} E_y \hat{x} + (E_x k_{\parallel} - E_z k_{\perp})\hat{y} + E_y k_{\perp} \hat{z}\,.$$

Using the above in the velocity distribution function we obtain,

$$\begin{aligned} f_{\alpha k} &= \frac{q_\alpha}{m_\alpha}\frac{\partial f_0}{\partial v_\perp^2} v_\perp \sum_{n,l=-\infty}^{\infty} \frac{J_n(\mu)\exp(i(n-l)\phi)}{i(w - l\Omega_\alpha - k_{\parallel} v_{\parallel})}\left(E_x\ (J_{l+1} + J_{l-1})\ + iE_y\ (J_{l-1} - J_{l+1})\right) \\ &+ \frac{2q_\alpha}{m_\alpha} v_{\parallel} E_z \frac{\partial f_0}{\partial v_{\parallel}^2} \sum_{n,l=-\infty}^{\infty} J_n(\mu)\, J_l(\mu) \exp(i\phi(n-l))\, \frac{1}{i(w - l\Omega_\alpha - k_{\parallel} v_{\parallel})}\,, \\ &+ \frac{q_\alpha}{m_\alpha}\frac{v_{\parallel} v_\perp}{w}\Big[-\frac{\partial f_0}{\partial v_\perp^2} + \frac{\partial f_0}{\partial v_{\parallel}^2}\Big] \sum_{n,l=-\infty}^{\infty} \frac{J_n(\mu)\exp(i(n-l)\phi)}{i(w - l\Omega_\alpha - k_{\parallel} v_{\parallel})}((E_x k_{\parallel} - E_z k_{\perp})(J_{l-1} + J_{l+1}) \\ &+ ik_{\parallel} E_y (J_{l-1} - J_{l+1}))\,. \end{aligned}$$

3.7 Dispersion Relation for oblique propagation

In this case, the treatment of the problem is the same, but we must include a component of propagation perpendicular to the background magnetic field, thus

$$\mathbf{k} = k_{\perp}\hat{x} + k_{\parallel}\hat{z}\,. \tag{3.12}$$

Taking into consideration Equation (3.12), the electromagnetic fields and the particle velocities considered in the case of parallel propagation in Equation (2.10), the perturbed distribution function is written as,

$$\begin{aligned} f_{\alpha k} &= -\frac{2q_\alpha}{m_\alpha}\frac{\partial f_0}{\partial v_\perp'^{\,2}} v_\perp \int_{-\infty}^{0} d\tau \Big((E_x\cos(\phi - \Omega_\alpha\tau) + E_y \sin(\phi - \Omega_\alpha\tau))\exp(\alpha_-) \\ &- \frac{2q_\alpha}{m_\alpha}\frac{v_{\parallel} v_\perp}{c}\Big[\frac{\partial f_0}{\partial v_{\parallel}'^{\,2}} - \frac{\partial f_0}{\partial v_\perp'^{\,2}}\Big] \int_{-\infty}^{0} d\tau (B_y\cos(\phi - \Omega_\alpha\tau) - B_x\sin(\phi - \Omega_\alpha\tau))\ \exp(\alpha_-) \\ &- \frac{2q_\alpha}{m_\alpha} v_{\parallel} E_z \frac{\partial f_0}{\partial v_{\parallel}^2} \int_{-\infty}^{0} d\tau\ \exp(\alpha_+)\,, \end{aligned} \tag{3.13}$$

where,

$$\alpha_{\pm} = \left(\pm i \frac{k_{\perp} v_{\perp}}{\Omega_{\alpha}} (\sin\phi + \sin(\phi - \Omega_{\alpha}\tau)) + i(k_{\parallel} v_{\parallel} - w)\tau \right) .$$

The integrals to be solved differ from those found in the case of parallel propagation; in this case, we must consider an expansion of the exponential terms in terms of Bessel functions.

Using identities (3.7) and (3.8) in Equation (3.13) (this is solved in more detailed in the previous section of the Appendix) and solving these integrals, we find the general form of the velocity distribution function,

$$f_{\alpha k} = \frac{q_{\alpha}}{m_{\alpha}} \sum_{n,l} \frac{J_n(\mu)\exp(i\phi(n-l))}{i(w - l\Omega_{\alpha} - k_{\parallel} v_{\parallel})} \left(X v_{\perp}(J_{l-1} + J_{l+1}) + iY v_{\perp}(J_{l-1} - J_{l+1}) + 2 v_{\parallel} Z J_l \right) ,$$

where we define

$$\begin{aligned} X &= E_x \frac{\partial f_0}{\partial v_{\perp}^2} + \frac{v_{\parallel}}{w}(E_x k_{\parallel} - E_z k_{\perp}) \left[\frac{\partial f_0}{\partial v_{\parallel}^2} - \frac{\partial f_0}{\partial v_{\perp}^2} \right] , \\ Y &= E_y \frac{\partial f_0}{\partial v_{\perp}^2} + E_y \frac{v_{\parallel} k_{\parallel}}{w} \left[\frac{\partial f_0}{\partial v_{\parallel}^2} - \frac{\partial f_0}{\partial v_{\perp}^2} \right] , \\ Z &= E_z \frac{\partial f_0}{\partial v_{\parallel}^2} , \end{aligned}$$

With this, from the Maxwell equations, we can write the expression that defines the dispersion relation,

$$k_{\parallel}(k_{\parallel}E_x - k_{\perp}E_z)\hat{x} + E_y(k_{\perp}^2 + k_{\parallel}^2)\hat{y} - k_{\perp}(k_{\parallel}E_x - k_{\perp}E_z)\hat{z} = \frac{w^2}{c^2}E_1 + \frac{iw}{c^2} 4\pi \sum_{\alpha} n_{\alpha} q_{\alpha} \int_L v f_{\alpha k} dv^3 .$$

separating the equations by components,

$$\begin{aligned}
k_\parallel c^2(k_\parallel E_x - k_\perp E_z) &= w^2 E_x + 4\pi i w \sum_\alpha n_\alpha q_\alpha \int_L v_\perp^2 \cos\phi\, f_{\alpha k} dv_\perp dv_\parallel d\phi\,, \\
E_y c^2(k_\perp^2 + k_\parallel^2) &= w^2 E_y + 4\pi i w \sum_\alpha n_\alpha q_\alpha \int_L v_\perp^2 \sin\phi\, f_{\alpha k} dv_\perp dv_\parallel d\phi\,, \\
-k_\perp c^2(k_\parallel E_x - k_\perp E_z) &= w^2 E_z + 4\pi i w \sum_\alpha n_\alpha q_\alpha \int_L v_\perp v_\parallel\, f_{\alpha k} dv_\perp dv_\parallel\,,
\end{aligned}$$

thus, we obtain the set of equations that will give origin to the components of the dispersion tensor for oblique propagation, for instance we have,

$$\begin{aligned}
&E_x \left\{ 1 - \frac{k_\parallel^2 c^2}{w^2} - \frac{2\pi}{w} \sum \left(\frac{w_{p\alpha}^2}{w_c} \right) \int_{-\infty}^{\infty} dv_\parallel \int_0^\infty \varphi_{v_\perp, v_\parallel} \left(\frac{l^2 \Omega_\alpha^3}{k_\perp^2} J_l^2(\mu) \chi_\alpha \right) dv_\perp \right\} \\
&+ E_y \left\{ -\frac{2\pi i}{w} \sum \left(\frac{w_{p\alpha}^2}{w_c} \right) \int_{-\infty}^{\infty} dv_\parallel \int_0^\infty \varphi_{v_\perp, v_\parallel} \left(\frac{l \Omega_\alpha^2 v_\perp}{k_\perp} J_l(\mu) J_l'(\mu) \chi_\alpha \right) dv_\perp \right\} \\
&+ E_z \left\{ \frac{k_\parallel k_\perp c^2}{w^2} - \frac{2\pi}{w} \sum \left(\frac{w_{p\alpha}^2}{w_c} \right) \int_{-\infty}^{\infty} dv_\parallel \int_0^\infty \varphi_{v_\perp, v_\parallel} \left(\frac{l \Omega_\alpha^2 v_\parallel J_l^2(\mu)}{k_\perp} \Lambda_\alpha \right) dv_\perp \right\} = 0\,.
\end{aligned}$$

the second equation is,

$$\begin{aligned}
&E_x \left\{ \frac{2\pi i}{w} \sum \left(\frac{w_{p\alpha}^2}{\Omega_\alpha} \right) \int_{-\infty}^{\infty} dv_\parallel \int_0^\infty \varphi_{v_\perp, v_\parallel} \left(\frac{l \Omega_\alpha^2 v_\perp}{k_\perp} J_l(\mu) J_l'(\mu)\, \chi_\alpha \right) dv_\perp \right\} \\
&+ E_y \left\{ 1 - \frac{c^2}{w^2}(k_\perp^2 + k_\parallel^2) - \frac{2\pi}{w} \sum \left(\frac{w_{p\alpha}^2}{\Omega_\alpha} \right) \int_{-\infty}^{\infty} dv_\parallel \int_0^\infty \varphi_{v_\perp, v_\parallel} \left(w_c J_l'^{\,2}(\mu) v_\perp^2 \chi_\alpha \right) dv_\perp \right\} \\
&+ E_z \left\{ \frac{2\pi i}{w} \sum \left(\frac{w_{p\alpha}^2}{\Omega_\alpha} \right) \int_{-\infty}^{\infty} dv_\parallel \int_0^\infty \varphi_{v_\perp, v_\parallel} \left(v_\perp v_\parallel \Omega_\alpha J_l(\mu) J_l'(\mu) \Lambda_\alpha \right) dv_\perp \right\} = 0\,.
\end{aligned}$$

the last equation is,

$$E_x \left\{ \frac{k_\parallel k_\perp c^2}{w^2} - \frac{2\pi}{w} \sum \left(\frac{w_{p\alpha}^2}{\Omega_\alpha} \right) \int_{-\infty}^{\infty} dv_\parallel \int_0^{\infty} \varphi_{v_\perp, v_\parallel} \left(\frac{l\Omega_\alpha^2}{k_\perp} J_l^2(\mu) v_\parallel \chi_\alpha \right) dv_\perp \right\}$$
$$+E_y \left\{ -\frac{2\pi i}{w} \sum \left(\frac{w_{p\alpha}^2}{\Omega_\alpha} \right) \int_{-\infty}^{\infty} dv_\parallel \int_0^{\infty} \varphi_{v_\perp, v_\parallel} \left(J_l(\mu) J_l'(\mu) \Omega_\alpha v_\parallel v_\perp \chi_\alpha \right) dv_\perp \right\}$$
$$+E_z \left\{ 1 - \frac{k_\perp^2 c^2}{w^2} - \frac{2\pi}{w} \sum \left(\frac{w_{p\alpha}^2}{\Omega_\alpha} \right) \int_{-\infty}^{\infty} \int_0^{\infty} \varphi_{v_\perp, v_\parallel} dv_\parallel \left(v_\parallel^2 \Omega_\alpha J_l^2(\mu) \Lambda_\alpha \right) \, dv_\perp \right\} = 0 \,,$$

where,

$$\varphi_{v_\perp, v_\parallel} = \frac{2 v_\perp}{k_\parallel v_\parallel + l\Omega_\alpha - w} \,.$$

This are the same components as obtained in Krall et al. (1973). Where we defined,

$$\chi_\alpha = \left(\frac{\partial f_0}{\partial v_\perp^2} + \frac{v_\parallel k_\parallel}{w} \left[\frac{\partial f_0}{\partial v_\parallel^2} - \frac{\partial f_0}{\partial v_\perp^2} \right] \right) \,,$$
$$\Lambda_\alpha = \frac{\partial f_0}{\partial v_\parallel^2} - \frac{l\Omega_\alpha}{w} \left(\frac{\partial f_0}{\partial v_\parallel^2} - \frac{\partial f_0}{\partial v_\perp^2} \right) \,.$$

Similarly, as in the previous section, this dispersion relation will give us a way to analyze the propagation modes in the plasma, and likewise, this expression will be useful to examine the electromagnetic fluctuations in the plasma.

Bibliography

H. M. Mott-Smith, "History of "plasmas"," *Nature*, vol. 233, no. 5316, pp. 219–219, 1971.

H. Alfvén, "Plasma universe," *Physica Scripta*, vol. 1987, no. T18, p. 20, 1987.

J. A. Van Allen and L. A. Frank, "Radiation around the earth to a radial distance of 107,400 km," *Nature*, vol. 183, 1959.

H. Alfvén, "Existence of electromagnetic-hydrodynamic waves," *Nature*, vol. 150, no. 3805, pp. 405–406, 1942.

S. Bale, J. Kasper, G. Howes, E. Quataert, C. Salem, and D. Sundkvist, "Magnetic fluctuation power near proton temperature anisotropy instability thresholds in the solar wind," *Physical review letters*, vol. 103, no. 21, p. 211101, 2009.

C.-Y. Tu and E. Marsch, "A model of solar wind fluctuations with two components: Alfvén waves and convective structures," *Journal of Geophysical Research: Space Physics*, vol. 98, no. A2, pp. 1257–1276, 1993.

E. Marsch and C.-Y. Tu, "Spectral and spatial evolution of compressible turbulence

in the inner solar wind," *Journal of Geophysical Research: Space Physics*, vol. 95, no. A8, pp. 11 945–11 956, 1990.

R. Schlickeiser, M. Michno, D. Ibscher, M. Lazar, and T. Skoda, "Modified temperature-anisotropy instability thresholds in the solar wind," *Physical Review Letters*, vol. 107, no. 20, p. 201102, 2011.

J. C. Kasper, A. J. Lazarus, and S. P. Gary, "Wind/swe observations of firehose constraint on solar wind proton temperature anisotropy," *Geophysical research letters*, vol. 29, no. 17, pp. 20–1, 2002.

P. Hellinger, P. Trávníček, J. C. Kasper, and A. J. Lazarus, "Solar wind proton temperature anisotropy: Linear theory and wind/swe observations," *Geophysical research letters*, vol. 33, no. 9, 2006.

R. Navarro, P. Moya, V. Muñoz, J. Araneda, J. Valdivia *et al.*, "Solar wind thermally induced magnetic fluctuations," *Physical Review Letters*, vol. 112, no. 24, p. 245001, 2014.

A. F. Vinas, P. S. Moya, R. Navarro, and J. A. Araneda, "The role of higher-order modes on the electromagnetic whistler-cyclotron wave fluctuations of thermal and non-thermal plasmas," *Physics of Plasmas*, vol. 21, no. 1, 2014.

A. F. Viñas, P. S. Moya, R. E. Navarro, J. A. Valdivia, J. A. Araneda, and V. Muñoz, "Electromagnetic fluctuations of the whistler-cyclotron and firehose instabilities in a maxwellian and tsallis-kappa-like plasma," *Journal of Geophysical Research: Space Physics*, vol. 120, no. 5, pp. 3307–3317, 2015.

J. Araneda, H. Astudillo, and E. Marsch, "Interactions of alfvén-cyclotron waves with ions in the solar wind," *Space science reviews*, vol. 172, pp. 361–372, 2012.

E. S. Weibel, "Spontaneously growing transverse waves in a plasma due to an anisotropic velocity distribution," *Phys. Rev. Lett.*, vol. 2, pp. 83–84, 1959. [Online]. Available: https://link.aps.org/doi/10.1103/PhysRevLett.2.83

R. Schlickeiser and P. Yoon, "Spontaneous electromagnetic fluctuations in unmagnetized plasmas i: General theory and nonrelativistic limit," *Physics of Plasmas*, vol. 19, no. 2, p. 022105, 2012.

R. Schlickeiser, A. Ganz, U. Kolberg, and P. Yoon, "Electromagnetic fluctuations in magnetized plasmas ii: Extension of the theory for parallel wave vectors," *Physics of Plasmas*, vol. 22, no. 10, p. 102111, 2015.

R. Kubo, "The fluctuation-dissipation theorem," *Reports on progress in physics*, vol. 29, no. 1, p. 255, 1966.

H. B. Callen and T. A. Welton, "Irreversibility and generalized noise," *Physical Review*, vol. 83, no. 1, p. 34, 1951.

R. Schlickeiser and P. Yoon, "Electromagnetic fluctuations in magnetized plasmas. i. the rigorous relativistic kinetic theory," *Physics of Plasmas*, vol. 22, no. 7, p. 072108, 2015.

N. Krall, A. Trivelpiece, and J. Kempton, *Principles of Plasma Physics*, ser. International series in pure and applied physics. McGraw-Hill, 1973. [Online]. Available: https://books.google.cl/books?id=b0BRAAAAMAAJ

A. Hundhausen, S. Bame, and N. Ness, "Solar wind thermal anisotropies: Vela 3 and imp 3," *Journal of Geophysical Research*, vol. 72, no. 21, pp. 5265–5274, 1967.

A. Hundhausen, J. Asbridge, S. Bame, H. Gilbert, and I. Strong, "Vela 3 satellite observations of solar wind ions: A preliminary report," *Journal of Geophysical Research*, vol. 72, no. 1, pp. 87–100, 1967.

E. Marsch, K.-H. Mühlhäuser, R. Schwenn, H. Rosenbauer, W. Pilipp, and F. Neubauer, "Solar wind protons: Three-dimensional velocity distributions and derived plasma parameters measured between 0.3 and 1 au," *Journal of Geophysical Research: Space Physics*, vol. 87, no. A1, pp. 52–72, 1982.

S. P. Gary and M. A. Lee, "The ion cyclotron anisotropy instability and the inverse correlation between proton anisotropy and proton beta," *Journal of Geophysical Research: Space Physics*, vol. 99, no. A6, pp. 11 297–11 301, 1994.

E. Marsch, "Kinetic physics of the solar corona and solar wind," *Living Reviews in Solar Physics*, vol. 3, pp. 1–100, 2006.

J. Podesta, D. Roberts, and M. Goldstein, "Spectral exponents of kinetic and magnetic energy spectra in solar wind turbulence," *The Astrophysical Journal*, vol. 664, no. 1, p. 543, 2007.

——, "Power spectrum of small-scale turbulent velocity fluctuations in the solar wind," *Journal of Geophysical Research: Space Physics*, vol. 111, no. A10, 2006.

K. H. Kiyani, K. T. Osman, and S. C. Chapman, "Dissipation and heating in solar wind turbulence: from the macro to the micro and back again," p. 20140155, 2015.

M. L. Goldstein and D. A. Roberts, "Magnetohydrodynamic turbulence in the solar wind," *Physics of Plasmas*, vol. 6, no. 11, pp. 4154–4160, 1999.

M. K. Verma, "Intermittency exponents and energy spectrum of the burgers and kpz equations with correlated noise," *Physica A: Statistical Mechanics and its Applications*, vol. 277, no. 3-4, pp. 359–388, 2000.

W.-C. Müller and D. Biskamp, "Scaling properties of three-dimensional magnetohydrodynamic turbulence," *Physical Review Letters*, vol. 84, no. 3, p. 475, 2000.

D. Biskamp and W.-C. Müller, "Scaling properties of three-dimensional isotropic magnetohydrodynamic turbulence," *Physics of Plasmas*, vol. 7, no. 12, pp. 4889–4900, 2000.

P. H. Yoon, *Classical Kinetic Theory of Weakly Turbulent Nonlinear Plasma Processes*. Cambridge University Press, 2019.

A. Sitenko, *Electromagnetic fluctuations in plasma*. Elsevier, 2012.

O. Alexandrova, V. Carbone, P. Veltri, and L. Sorriso-Valvo, "Small-scale energy cascade of the solar wind turbulence," *The Astrophysical Journal*, vol. 674, no. 2, p. 1153, 2008.

L. Sorriso-Valvo, R. Marino, V. Carbone, A. Noullez, F. Lepreti, P. Veltri, R. Bruno, B. Bavassano, and E. Pietropaolo, "Observation of inertial energy cascade in interplanetary space plasma," *Physical review letters*, vol. 99, no. 11, p. 115001, 2007.